



UNIVERSIDADE ESTADUAL DE CAMPINAS
FACULDADE DE ENGENHARIA MECÂNICA
E INSTITUTO DE GEOCIÊNCIAS

YURLEY KARINA ANAYA JAIMES

**FLOW ASSURANCE OF WAXY CRUDE OIL:
PHYSICAL AND CHEMICAL CHARACTERIZATION,
CRITICAL TEMPERATURES AND RHEOLOGICAL
BEHAVIOR FOR THE RESTART PROBLEM-
EXPERIMENTAL STUDY**

***GARANTIA DE ESCOAMENTO DE ÓLEOS
PARAFÍNICOS: CARACTERIZAÇÃO FÍSICO-QUÍMICA,
TEMPERATURAS CRÍTICAS E COMPORTAMENTO
REOLÓGICO EM PROBLEMAS DE REPARTIDA-
ESTUDO EXPERIMENTAL***

CAMPINAS

2016

YURLEY KARINA ANAYA JAIMES

**FLOW ASSURANCE OF WAXY CRUDE OIL: PHYSICAL
AND CHEMICAL CHARACTERIZATION, CRITICAL
TEMPERATURES AND RHEOLOGICAL BEHAVIOR FOR
THE RESTART PROBLEM-EXPERIMENTAL STUDY**

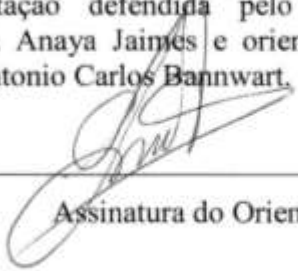
***GARANTIA DE ESCOAMENTO DE ÓLEOS PARAFÍNICOS:
CARACTERIZAÇÃO FÍSICO-QUÍMICA, TEMPERATURAS
CRÍTICAS E COMPORAMENTO REOLÓGICO EM
PROBLEMAS DE REPARTIDA-ESTUDO EXPERIMENTAL***

Dissertation presented to the Mechanical Engineering Faculty and Geosciences Institute of the University of Campinas in partial fulfillment of the requirements for the degree of Master in Petroleum Sciences and Engineering in the area of Exploitation.

Dissertação de Mestrado apresentada à Faculdade de Engenharia Mecânica e Instituto de Geociências da Universidade Estadual de Campinas como parte dos requisitos exigidos para obtenção do título de Mestre em Ciências e Engenharia de Petróleo, na área de Exploração.

Orientador: Prof. Dr. Antonio Carlos Bannwart
Coorientador: Dra. Vanessa Cristina Bizotto Guersoni

Este exemplar corresponde à versão final da Dissertação defendida pelo aluno Yurley Karina Anaya Jaimes e orientada pelo Prof. Dr. Antonio Carlos Bannwart.



Assinatura do Orientador

CAMPINAS

2016

Agência(s) de fomento e nº(s) de processo(s): CAPES, 33003017

Ficha catalográfica
Universidade Estadual de Campinas
Biblioteca da Área de Engenharia e Arquitetura
Luciana Pietrosanto Milla - CRB 8/8129

An18f Anaya Jaimes, Yurley Karina, 1988-
Flow assurance of waxy crude oil: physical and chemical characterization, critical temperatures and rheological behavior for the restart problem - experimental study / Yurley Karina Anaya Jaimes. – Campinas, SP : [s.n.], 2016.

Orientador: Antonio Carlos Bannwart.
Coorientador: Vanessa Cristina Bizotto Guersoni.
Dissertação (mestrado) – Universidade Estadual de Campinas, Faculdade de Engenharia Mecânica e Instituto de Geociências.

1. Óleo. 2. Escoamento. 3. Reologia. 4. Parafinas. I. Bannwart, Antonio Carlos, 1955-. II. Guersoni, Vanessa Cristina Bizzoto, 1979-. III. Universidade Estadual de Campinas. Faculdade de Engenharia Mecânica. IV. Título.

Informações para Biblioteca Digital

Título em outro idioma: Garantia de escoamento de óleos parafínicos: caracterização físico-química, temperaturas críticas e comportamento reológico em problemas de repartida - estudo experimental

Palavras-chave em inglês:

Oil

Flow

Rheology

Paraffins

Área de concentração: Exploração

Titulação: Mestra em Ciências e Engenharia de Petróleo

Banca examinadora:

Antonio Carlos Bannwart [Orientador]

Marcos Akira Davila

Monica Feijo Naccache

Data de defesa: 22-02-2016

Programa de Pós-Graduação: Ciências e Engenharia de Petróleo


UNIVERSIDADE ESTADUAL DE CAMPINAS
FACULDADE DE ENGENHARIA MECÂNICA
E INSTITUTO DE GEOCIÊNCIAS

DISSERTAÇÃO DE MESTRADO ACADÊMICO


**FLOW ASSURANCE OF WAXY CRUDE OIL:
PHYSICAL AND CHEMICAL CHARACTERIZATION,
CRITICAL TEMPERATURES AND RHEOLOGICAL
BEHAVIOR FOR THE RESTART PROBLEM-
EXPERIMENTAL STUDY**

Autor: Yurley Karina Anaya Jaimes
Orientador: Prof. Dr. Antonio Carlos Bannwart
Coorientador: Dra. Vanessa Cristina BizottoGuersoni.

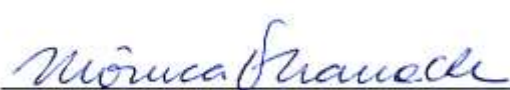
A Banca Examinadora composta pelos membros abaixo aprovou esta Dissertação:



Prof. Dr. Antonio Carlos Bannwart, Presidente
FEM / DEP / UNICAMP



Prof. Dr. Marcos Akira Davila
FEM / DEMM / UNICAMP



Profa. Dra. Monica Feijo Naccache
DEM / PUC RIO

Campinas, 22 de fevereiro de 2016.

A Ata da Defesa, assinada pelos membros da Comissão Examinadora, consta no processo de vida acadêmica do aluno.

DEDICATION

To my beloved parents

ACKNOWLEDGEMENTS

Firstly, I would like to thank my parents for all their love and support through my life. My sister and brother deserve my heartfelt thanks as well.

I would like to express my sincere gratitude to my advisor, Professor PhD Antonio Carlos Bannwart and PhD Vanessa Cristina Bizzoto, for their guidance and support through this study.

I would like to send a special thank you to teachers, researchers and technicians of DEP and CEPETRO for their support and assistance during this work.

To Repsol-Sinopec Brazil by investment and technical support provided on this years.

To Capes for the financial support.

To all my friends for their constant support and belief in me and my dreams.

Thank you to everyone who made these past two years such an incredible time.

ABSTRACT

The physicochemical characteristics of a Brazilian waxy crude oil were determined using ASTM Standard Methods for every feature evaluated. This characterization is important because heavier oil compounds like wax, asphaltenes and resins are widely associated to the solid deposit formation due to their high molecular weight. Besides, the content of resins is large enough to stabilize the asphaltenes in the crude oil. Thus, flow assurance problems in offshore production system of the oil studied; correspond to wax precipitation and gelation.

Water content in the waxy crude oil was also determined in order to ensure that no emulsion would form during the rheological and restart pipeline test. The percentage of water in the waxy crude oil was found to be small and represents no risk either in the development of experiments or the reproducibility of their results.

Critical temperatures related to the gelation process of waxy crude oils such as the Wax Appearance Temperature (WAT), the gelation temperature and the pour point temperature were identified for the oil under study. Determination of these temperatures was made based on analytical technique (DSC), rheological tests and ASTM standard method, respectively.

Rheological tests were performed with the purpose to characterize the waxy oil behavior under static and dynamic conditions, through the cooling process and seabed conditions (around 4°C). The fluid showed a complex behavior at temperatures below the gelation temperatures, exhibiting a yield stress-like behavior.

Start-up experiments were performed in laboratory model in order to determine the pressure required to break the gel formed. Results of these experiments confirmed the yield stress-like behavior of the waxy crude oil.

Based on the results obtained by rheological measurements and by the start-up experiments, it was calculated the minimum differential pressure required to restart the flow in a line blocked with gelled waxy crude oil.

Key Words: Waxy crude oil, Flow Assurance, Yield Stress, Restart, Rheology

RESUMO

Neste estudo foram determinadas as características físico-químicas de um óleo parafínico do Brasil, usando normas técnicas ASTM (*American Society for Testing and Materials*) para cada característica avaliada. A caracterização físico-química é importante já que os compostos mais pesados, como parafinas, resinas e asfaltenos estão associados com a formação de depósitos sólidos devido ao seu elevado peso molecular. Não obstante o conteúdo de resinas foi suficientemente grande para estabilizar os asfaltenos no óleo. Assim o problema de garantia de escoamento do óleo estudado, em sistemas de produção offshore corresponde à precipitação e gelificação de parafinas causando problemas de repartida de linhas gelificadas.

O conteúdo de água foi determinado de modo a assegurar que nenhuma emulsão pode se formar durante os ensaios reológicos e de repartida de linhas gelificadas. Assim verificou-se uma percentagem mínima de água no óleo parafínico, que representa ausência de risco no desenvolvimento de ensaios e na reprodutibilidade dos seus resultados.

As temperaturas críticas relacionadas como o processo de gelificação de óleos parafínicos foram identificados para o óleo estudado, a Temperatura Inicial de Aparecimento dos cristais (TIAC), a temperatura de gelificação e o ponto de fluidez. A determinação destas temperaturas foi feita com base na técnica analítica de Calorimetria Diferencial de Varredura (DSC), testes reológicos e norma técnica ASTM D5853-11, respectivamente.

Ensaio reológico foram realizados com a finalidade de caracterizar o comportamento do óleo parafínico sob condições estáticas e dinâmicas, no processo de resfriamento até a temperatura do leito marinho (cerca de 5°C). O fluido mostrou um comportamento complexo a temperaturas abaixo da temperatura de gelificação.

Experimentos de repartida foram realizados no laboratório em uma linha horizontal, a fim de determinar a pressão necessária para quebrar o gel formado e reiniciar o escoamento dentro da linha. Os resultados dos experimentos em escala piloto confirmaram a existência de uma tensão limite de escoamento do óleo parafínico.

Com base nos resultados obtidos por medições reológicas e nos experimentos de repartida, calculou-se a pressão mínima necessária para reiniciar o escoamento na linha bloqueada como óleo parafínico gelificado.

Palavras-Chave: Óleo Parafínico, Garantia de Escoamento, tensão mínima de escoamento, repartida, reologia.

LIST OF FIGURES

Figure 1. Structures of hydrocarbon involved in wax deposition.....	24
Figure 2. Possible hysteresis loop responses (Mewis et al. 2009).....	39
Figure 3. Response of the thixotropic material with a complex shear history to the stepwise experiments (Mewis et al. 2009).	40
Figure 4. Waxy crude oil sealed barrel of 50L provided by Repsol Sinopec Brazil.	45
Figure 5. 100 mL bottle of waxy crude oil.	46
Figure 6. Karl Fisher equipment: T50 Titrator – Mettler Toledo.....	47
Figure 7. GC 2010 Shimadzu Plus used in the characterization of paraffinic fractions.....	48
Figure 8. Test jar carrying apparatus in a thermostatic bath at 21 °C for pour point determination.	50
Figure 9. Density meter DMA 4500 (Anton Paar).	51
Figure 10. TA Instruments Q2000 equipment for DSC experiments.....	51
Figure 11. Rheoscope modulus of controlled-stress rheometer - Thermo Scientific, Haake Mars III.	53
Figure 12. Cone-plate geometry with cone size of 60 mm.....	54
Figure 13. Controlled-stress rheometer - Thermo Scientific, Haake Mars II.....	54
Figure 14. Schematic diagram of apparatus for the restart experiments (Geest, 2015).	57
Figure 15. Inner tank of horizontal flow loop.	58
Figure 16. Test section in the water bath.....	58
Figure 17. External tank of horizontal flow loop.	59
Figure 18. Pressurization system for restart experiments.....	59
Figure 19. Labview panel for monitoring the restart experiments.	59
Figure 20. Chromatogram analysis for waxy crude oil.	63
Figure 21. Boiling point versus recovered mass of waxy crude oil.	63
Figure 22. HSTD analysis for waxy crude oil.	64
Figure 23. Density versus temperature of waxy crude oil.....	66
Figure 24. DSC thermograms of waxy crude oil for a cooling rate of 1 °C/min (a) and 3 °C/min (b).	67
Figure 25. Wax precipitation curve determined by DSC thermogram at cooling rate of 3 °C/min.	68

Figure 26. Rheological measurements for waxy crude oil at shear rate of 1 s^{-1} and cooling rates of 0.5, 1.0 and $3.0 \text{ }^{\circ}\text{C}/\text{min}$. Scale bar = $10 \text{ }\mu\text{m}$	72
Figure 27. Flow curve of waxy crude oil at different temperatures.	74
Figure 28. Flow curves adjusted to the rheological models: Newtonian behavior (a) and non-Newtonian behavior (b).	75
Figure 29. Flow curves adjusted to the rheological models for non-Newtonian behavior: 4 and $5 \text{ }^{\circ}\text{C}$ (a), 10, 15 and $20 \text{ }^{\circ}\text{C}$ (b).	78
Figure 30. Viscosity versus shear rate at constant temperatures.	79
Figure 31. Viscosity of waxy crude oil under different shear rates.	79
Figure 32. Oscillatory test for waxy oil at 5°C under 0.5 and 1.0 Hz without aging.	80
Figure 33. Typical behavior of G' and G'' versus temperature for determination of gelation temperature obtained at cooling rate of $0.5 \text{ }^{\circ}\text{C}/\text{min}$	82
Figure 34. Typical behavior of G' and G'' versus temperature for determination of gelation temperature obtained at cooling rate of $1.0 \text{ }^{\circ}\text{C}/\text{min}$	82
Figure 35. Typical behavior of G' and G'' versus temperature for determination of gelation temperature obtained at cooling rate of $3^{\circ}\text{C}/\text{min}$	83
Figure 36. Gel behavior at $5 \text{ }^{\circ}\text{C}$ under stress amplitude of 1 Pa for the different aging time: 0-100 Hz (a) and zoom of 0 to 6 Hz (b).	84
Figure 37. Oscillatory measurements for yield stress determination without aging times.	86
Figure 38. Oscillatory measurements for yield stress determination with aging time of 1 hour.	86
Figure 39. Oscillatory measurements for yield stress determination with aging time of 5 hours.	87
Figure 40. Oscillatory measurements for yield stress determination with aging time of 24 hours.	87
Figure 41. Yield stress determination by strain rate-controlled measurement without aging time.	88
Figure 42. Yield stress determination by strain rate-controlled measurement for aging time of 1 hour.	89
Figure 43. Yield stress determination by strain rate-controlled measurement for aging time of 5 hours.	89
Figure 44. Yield stress determination by strain rate-controlled measurement for aging time of 24 hours.	90

Figure 45. Yield stress determination by strain rate-controlled measurement under 0.1 s^{-1} (a) and 0.1 s^{-1} zoom (b).....	91
Figure 46. Yield stress determination by strain rate-controlled measurement under 1 s^{-1} (a) and 1 s^{-1} zoom (b).....	92
Figure 47. Hysteresis loop for 0 to 100 s^{-1} and 0 to 1000 s^{-1} : Shear stress versus shear rate (a) and viscosity versus shear rate (b).	95
Figure 48. Shear stress versus time for three consecutive loops from 0 to 100 s^{-1}	96
Figure 49. Hysteresis loop between 0 and 1000 s^{-1} applied at different duration times. Shear stress versus shear rate (a) and viscosity versus shear rate (b).	97
Figure 50. All variables measured in the restart experiments for the first test with aging time of 1 hour.	100
Figure 51. Detail of the pressure and level of inner tank for the first test with aging time of 1 hour.	101
Figure 52. Temperature recorded for the restart experiment with aging time of 1 hour.	102
Figure 53. Detail of the pressure and level of inner tank for the second test with aging time of 1 hour.	102
Figure 54. Detail of the pressure and level of inner tank for the third test with aging time of 1 hour.	103
Figure 55. Comparison between results for experiment with aging time of 1 hour.	103
Figure 56. All variables measured in the restart experiments for the first test with aging time of 5 hours.	104
Figure 57. Detail of the pressure and level of inner tank for the first test with aging time of 5 hours.	105
Figure 58. Detail of the pressure and level of inner tank for the second test with aging time of 5 hours.	105
Figure 59. Comparison between results for experiment with aging time of 5 hour.	106
Figure 60. All variables measured in the restart experiments for the first test with aging time of 24 hour.	107
Figure 61. Detail of the pressure and level of inner tank for the first test with aging time of 24 hours.	107
Figure 62. Detail of the pressure and level of inner tank for the second test with aging time of 24 hours.	108
Figure 63. Comparison between results for experiment with aging time of 24 hours.	108
Figure 64. Restart pressure for the different aging times evaluated.	109

LIST OF TABLES

Table 1. Overview of laboratory pipeline shut-in and restart experiments (Paso, 2014).	41
Table 2. Asphaltenes and resins content for the waxy crude oil.	60
Table 3. Water content of the waxy crude oil.....	61
Table 4. Total Acid Number (TAN) content of the waxy crude oil.	61
Table 5. Mass percentage for some carbon atoms of the n-paraffin of the waxy crude oil.....	62
Table 6. Pour point temperature of waxy crude oil.	64
Table 7. Density of waxy crude oil.	65
Table 8. Values from DSC characterization of waxy crude oil.....	66
Table 9. Effect of cooling rate on the WAT and microstructure of the first wax crystals obtained by rheo-optical experiments. Scale bar = 10 μm	69
Table 10. Micrographs of waxy crude oils at different temperatures and cooling rates of 0.5, 1.0 and 3.0 $^{\circ}\text{C}/\text{min}$. Scale bar = 10 μm	70
Table 11. Micrographs of Waxy Crude Oil at different temperatures with a cooling rate of 1 $^{\circ}\text{C}/\text{min}$ and aging time of 0h, 1h and 5h. Scale bar = 10 μm	71
Table 12. Crystallization temperature of waxy crude oil at different cooling rates.	73
Table 13. Fitted parameters for the flow curves with Newtonian behavior.	76
Table 14. Parameters of the Cross model for the waxy crude oil.....	76
Table 15. Dynamic yield stress values by Cross model fitted.....	76
Table 16. Parameters of the Herschel–Bulkley model for the waxy crude oil.....	77
Table 17. Gelation temperature of the waxy crude oils at different cooling by oscillatory test.	81
Table 18. Yield stress for different aging time measured by oscillatory test.	85
Table 19. Yield stress (overshoot stress) for different aging time by strain-controlled measurements.	93
Table 20. Stress overshoot from the hysteresis loop at different test time.....	98
Table 21. Hysteresis loop areas as a measure of thixotropy of waxy crude oil.....	98
Table 22. Inlet line pressure and ΔP total for the restart experiments with an aging time of 1 hour.....	104
Table 23. Inlet line pressure and ΔP total for the restart experiments with an aging time of 5 hours.	106

Table 24. Inlet line pressure and ΔP total for the restart experiments with an aging time of 24 hours.	109
Table 25. Comparison between restart pressures obtained by rheological measurements and by flow line measurements.	111

LIST OF ACRONYMS

WAT	Wax Appearance Temperature
CPT	Cloud Point Temperature
T _g	Gelation Temperature
PPT	Pour Point Temperature
ASTM	American Society for Testing and Materials
DSC	Differential Scanning Calorimetry
GC	Gas Chromatography

LIST O F SYMBOLS

σ	Shear stress (Pa)
σ_0	Yield stress (Pa)
η	Viscosity (Pa s)
$\dot{\eta}$	Shear rate (1/s)
K	Consistency index in the Herschel-Bulkley model
n	Flow behavior index in the Herschel–Bulkley model
η_a	Apparent viscosity in the Cross and Carreau models (Pa s)
$\dot{\gamma}_b$	Consistency index of dilatant region in the Cross model (1/s)
n	Dimensionless exponent in the Cross model
λ_c	Constant related to relaxation times in the Carreau model (1/s)
N	Dimensionless exponent in the Carreau model
η_0	Zero shear rate viscosity (Pa s)
η_∞	Viscosity at high shear rate (Pa s)
G'	Storage modulus (Pa)
G''	Loss modulus (Pa)
λ	Structural parameter
T	Characteristic aging time for buildup of the microstructure (sec)
α	Rate at which the microstructure is broken down under shear
β and n	Parameters designating how strongly the microstructure influences the viscosity
τ_w	Shear stress at the pipe wall (Pa)
L	Length of the pipe (m)
D	Diameter of the pipe (m)
ΔP	Pressure differential (Pa)
c_w	Concentration of precipitated paraffin (% w/w)
T_w	Given temperature at which c_w is measured (°C)
Q	Total thermal effect of paraffin precipitation (J/g)

TABLE OF CONTENTS

1. INTRODUCTION	19
1.1 MOTIVATION	20
1.2 RESEARCH OBJECTIVES	21
1.3 THESIS OVERVIEW	22
2. LITERATURE REVIEW	23
2.1 WAXY CRUDE OIL	23
2.2 STRUCTURE OF WAX.....	23
2.3 STRUCTURE AND STRENGTH OF THE GEL	24
2.4 CRITICAL TEMPERATURES IN THE FLOW ASSURANCE OF WAXY CRUDE OILS.....	25
2.4.1 WAX APPEARANCE TEMPERATURE (WAT) OR CLOUD POINT TEMPERATURE	25
2.4.2 POUR POINT TEMPERATURE (PPT)	27
2.4.3 GELATION TEMPERATURE OR GEL POINT	27
2.5 RHEOLOGY	29
2.5.1 RHEOLOGY OF WAXY CRUDE OILS	30
2.5.2 YIELD STRESS	30
2.5.3 TIME-DEPENDENT FLUIDS.....	37
2.6 RESTART PROBLEM: PIPE FLOW EXPERIMENTS	41
3. MATERIALS AND METHOD	45
3.1 MATERIALS	45
3.1.1 SAMPLING OF WAXY CRUDE OIL	45
3.1.2 PRETREATMENT OF WAXY CRUDE OIL BEFORE ANY TEST	46

3.2 EXPERIMENTAL SECTION	46
3.2.1 CHARACTERIZATION OF THE CRUDE OIL.....	46
3.2.2 RHEOLOGICAL MEASUREMENTS	53
3.2.3 RESTART EXPERIMENT IN THE HORIZONTAL LOOP	56
4. RESULTS AND DISCUSSION.....	60
4.1 CHARACTERIZATION OF THE CRUDE OIL.....	60
4.1.1 ASPHALTEN AND RESIN CONTENTS.....	60
4.1.2 WATER CONTENT – KARL FISHER.....	61
4.1.3 TOTAL ACID NUMBER (TAN) CONTENT.....	61
4.1.4 CHARACTERIZATION OF n-PARAFFINS FRACTION BY GAS CHROMATOGRAPHY (GC).....	62
4.1.5 CHARACTERIZATION OF n-PARAFFINS FRACTION BY HIGH TEMPERATURE SIMULATED DISTILLATION (HSTD)	63
4.1.6 POUR POINT TEMPERATURE.....	64
4.1.7 DENSITY	65
4.1.8 DIFFERENTIAL SCANNING CALORIMETRY (DSC)	66
4.1.9 WAX SOLUBILITY CURVE.....	68
4.1.10 RHE-OPTICAL MEASUREMENTS	69
4.2 RHEOLOGICAL CHARACTERIZATION MEASUREMENTS.....	72
4.2.1 VISCOSITY AND FLOW CURVES.....	72
4.2.2 OSCILLATORY TESTS.....	80
4.2.3 GELATION TEMPERATURE.....	81
4.2.4 GEL BEHAVIOR BY OSCILLATORY TESTS.....	83
4.2.5 YIELD STRESS	84
4.2.6 THIXOTROPY.....	93
4.3 RESTART EXPERIMENTS IN THE HORIZONTAL FLOW LOOP ...	99

4.3.1	AGING TIME OF ONE HOUR (1h)	99
4.3.2	AGING TIME OF FIVE HOURS (5h)	104
4.3.3	AGING TIME OF TWENTY-FOUR HOURS (24h)	106
4.3.4	COMPARISON BETWEEN DIFFERENT AGING TIMES.....	109
4.4	COMPARISON BETWEEN MODEL PIPELIN AND CONTROLLED STRESS RHEOMETER.....	110
5	CONCLUSIONS.....	112
6	SUGGESTIONS FOR FUTURE STUDIES	115
7	REFERENCES	116

1. INTRODUCTION

Physicochemical and rheological characterization of the waxy crude oil plays an important role in the flow assurance of petroleum industry in specific applications like production, transportation and storage in deep-water.

When the waxy crude oil is in reservoir conditions, at temperatures between 70 °C and 150 °C, and pressures in the range of 50 MPa and 100 MPa (Venkatesan, 2005), the fluid presents a Newtonian behavior. However, when the oil leaves the reservoir rock, it is led by the production lines at the subsea bed with temperatures around 4°C, the minerals solubilized in the oil begins to precipitate due to the cooler environment (marine environment, deep water, ultra-deep water). These precipitated solids make the oil behaves as a complex non-Newtonian fluid.

The most common minerals encountered in waxy crude oils are waxes, hydrates and asphaltenes (J. G. Speight, 2007 and S. Betancourt, 2007).

Along the process of cooling the pipeline in the seabed, the fluid reaches the Wax Appearance Temperature (WAT). Once the waxy crude oil is cooled below its WAT, it forms a viscoelastic gel inside the lines. On the other hand, in offshore oil production there are some planned or unexpected shutdown, where the oil is continuously cooled within the pipeline, forming a solid deposit (Kok et al., 1996). At temperature below the pour point, the precipitated solids agglomerated to form a network with certain quantity of oil trapped in it. This wax crystal network takes a gel like characteristics, increasing its viscosity with the decrease of the temperature (Kunal Karan 2000).

The formation of the network with paraffin and oil, as well as its aging, present serious complications for the restart process, because the pumping pressure becomes greater than normal operating pressure (Davidson et al., 2004). In order to solve these kind of problems and ensure that the oil going to keep flowing into production lines, there is a research area called Flow Assurance.

The gelled waxy crude oil exhibits a complex rheological behavior similar to yield stress fluid, which is related to the gel strength of the wax crystal network. In order to restart the gelled pipeline to make the crude oil flows inside the pipeline, it is necessary to apply a high pressure to exceed a certain minimum value called yield stress.

There are many techniques to deal with the problem of paraffin deposition and hence avoid the formation of wax crystal network. These techniques use mechanical, thermal

and chemical methods. Nevertheless, the design, application and schedule of any preventive and/or remediation technique requires the knowledge of the gel strength of these yield stress like fluids (Venkatesan, 2005). Constitutive rheological models can be used to describe the behavior of waxy crude oil, and how their properties are affected by precipitate formation at low temperatures. On this account, it is necessary to determine the rheological characteristics of the fluid to adjust its behavior to an appropriate constitutive model that enables the implementation of an efficient and less costly strategy control of wax deposition.

1.1 MOTIVATION

Wax deposition in pipelines results from the precipitation of n-alkanes with carbon number higher than 18 from the waxy crude oil under a cold environment. This deposit grows in thickness forming a wax crystal network, which blocks the flowline, avoiding the flow of the oil inside it.

Some cases of unsuccessful management of the wax deposition problem took place in the Gulf of Mexico, where at least 17 pipelines were plugged in 1994 and the production had to be stopped in order to replace the plugged portion of the lines, and since then this number has been increasing. The cost of this operation was about \$40,000,000 per incident as reported by Elf Aquitaine (Venkatesan, 2002).

A oil field in the United Kingdom operated by Lasso Company was abandoned because of recurring paraffin plugging problems at a cost of over \$100 million USD according to the U.S. Department of Energy (DOE). The remediation of pipelines blockages in water depths of about 400 m can cost \$1 million/mile USD (Venkatesan, 2002).

There are waxy crude oil fields around the world. Regions like Alaska, Mexico, Brazil, the north of Africa, the Middle East, United Kingdom, among others have large reserve of waxy crude oil. In the specific case of Brazil, there are some waxy crude oil from fields in Campos Basin in Rio de Janeiro and from Recôncavo Basin in Bahia (Santos, 2012). In 2011 Brazil produced 100,000 barrels per day of oil from its deep-water pre-salt fields, but it is targeting a tenfold increase to 1 million barrels oil per day by 2017.

Forecasts anticipate that in 2017, oil production from deep-sea areas will exceed 8 million barrels oil per day around the world, three times higher than the deep-sea production recorded in 2002 that was 2.4 million barrels oil per day (Moristis, 2002).

Exploration and production activities in offshore petroleum industry have huge engineering challenges related to the flow assurance. Thus, some flowline designs for oils wells as far as 160 miles away from the shore have been developed because at greater distances from the shore major risks of severe and extensive wax precipitation, deposition and finally gelification problems (Nguyen,2004).

Considering that 20% of the world petroleum reserves corresponds to waxy crude oils (Vinay, 2007), it is important to have a complete knowledge of these complex fluids. The understanding of their behavior allows achieving the adjustment to a constitutive model that describes faithfully the behavior of waxy crude oils. This adjustment can be made based on the physicochemical and rheological characterization.

1.2 RESEARCH OBJECTIVES

The objectives of this research are to understand the wax deposition problem, its relationship with the physicochemical features, and its rheological behavior in order to identify the basic principles of the yielding process, its gel strength, and the yield stress-like behavior.

To define regions in the yielding process of waxy crude oil based on the determination of the critical temperatures from the physicochemical and rheological characterization. These regions of risk are a very useful tool for the application of prevent, remediate and remove strategies in the wax crystal gelification and the restart problem.

The establishment of physicochemical and rheological characteristics on a solid experimental basis with a Brazilian waxy crude oil allows determining the variables that influence the wax crystal structure and the restart problems.

The study is focused in the rheological characterization and experimental validation by horizontal flow line experiments, in order to determine the minimum pressure to restart the flow inside the gelled line.

The definition of some variables in the restart test of a gelled line, such as the magnitude of applied pressure and the duration of this pressure application over the gelled system allow finding an optimal and efficient point in engineering and economic terms, in order to ensure the flow of waxy crude oil through subsea pipelines.

1.3 THESIS OVERVIEW

This dissertation is organized as follows:

Chapter 1: This chapter shows an overview of the restart problem in gelled lines of waxy crude oil production, the motivation to conduct this study and the proposed objectives.

Chapter 2: This chapter presents an overview and background of waxy crude oils, the yielding process of gelled lines, their main rheological characteristics, and the restart problem.

Chapter 3: This chapter provides the detailed procedures followed in each experiment of physicochemical and rheological characterization. Moreover, the experimental procedure to determine the pressure required to restart the flow within a gelled pipeline is presented.

Chapter 4: This chapter presents the results obtained from the physicochemical and rheological characterization test, as well as the results obtained from laboratory model tests are presented. Discussion of this research was made based on the main findings for the waxy crude oil under study.

Chapter 5: Conclusions are drawn from the experimental findings presented in the preceding chapter.

2. LITERATURE REVIEW

2.1 WAXY CRUDE OIL

Waxy crude oils are fluids with a high amount of wax in their composition. Crude oils usually have an important fraction of branched and cyclic paraffins. This fraction of wax remains soluble in the fluid, until it reaches its solubility limit, which is a function of the temperature. A regular waxy crude oil contains other heavy organic components such as asphaltenes and resins. These components can interact with the waxes and influence the deposition process (Rønningsen and Bjørndal, 1991; Venkatesan et al., 2003; Yi and Zhang, 2011).

Waxy crude oil causes many problems in its production, transportation and storage. These fluids present a complex behavior when reach its solubility limit, below its crystallization temperature. This complex behavior has been studied using rheological measurements and scaled to laboratory model conditions, confirming its time dependence and yield stress-like behavior (Liu Gang, 2015; Guo, L. 2013; Zhao, Yansong, 2013, Zhao, Yansong, 2012).

2.2 STRUCTURE OF WAX

The large component of most solids deposits from crude oil is wax. The waxes present in crude oils are divided in two categories. The first group is the macro crystalline paraffin or distillate waxes, composed of mainly straight-chain paraffins (n-alkanes) between C18 and C50; and the second group correspond to the microcrystalline or amorphous waxes, which contain larger amounts of isoparaffins (branched chain alkanes) and naphthenes (cyclic alkanes). Naphthenes present a considerably greater carbon number, between C18 and C36 (Kok and Lettoffe, 1999). These microcrystalline waxes (C18 to C36) correspond to the naphthenic hydrocarbons, which also deposit as a wax (Garcia, 1998).

Samples of wax deposits from pipelines have been analyzed, finding fractions of n-paraffins, iso-paraffins and cyclic compounds. These components represent the major constituent fraction of the crude oil. Researches indicate that increasing iso-paraffin fraction contribute to form microcrystalline or amorphous wax solids (Rønningen, 1991). Figure 1 shows some molecular structures of hydrocarbon in order to understand the type of chemical structures involved in the wax deposition problem.

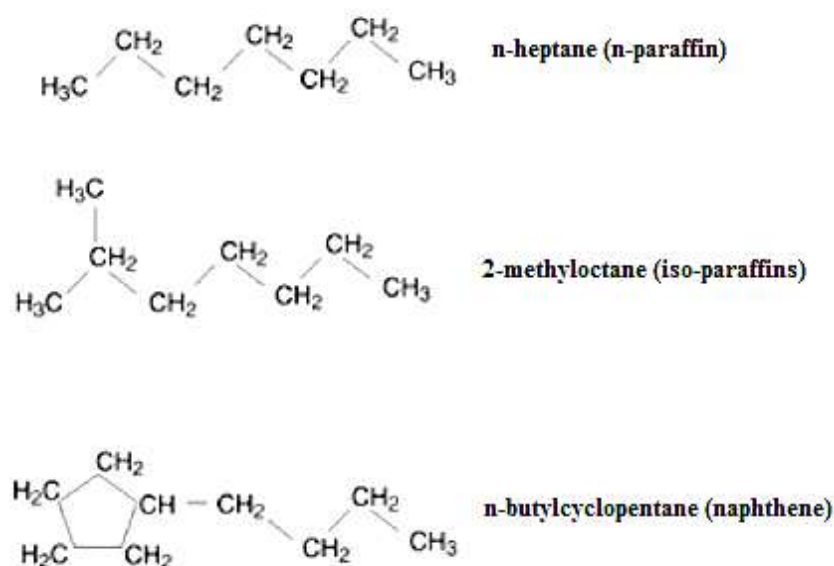


Figure 1. Structures of hydrocarbon involved in wax deposition.

The differences in the compositional characteristics of the oils; represent an additional effort in studying the specific behavior of each oil, determining its physicochemical and rheological characteristics.

2.3 STRUCTURE AND STRENGTH OF THE GEL

The gel structure formed when the oil is cooled below the point of solubility limit of the paraffinic components in the waxy crude oil, depends on the types of wax crystals, their shear and thermal histories. Morphology and structure of the wax crystals play an important role in the rheological behavior of waxy crude oils (Peng Gao, 2006). Process of crystals formation and aggregation in the gel is favored by lower temperatures and longer times i.e. low cooling rates (Visintin, 2005).

Microstructure and morphology of wax crystals have influence on the rheological properties, mainly when the surrounding temperature is below the temperature at which the first wax crystals start to form (Wax Appearance Temperature, WAT). The relationship between wax crystal morphology and structure, the precipitated wax, and composition of waxy crude oil has been widely studied and discussed in the last years in order to clarify the influence of each variable on the rheological behavior. Nevertheless, it has not been possible to establish a pattern that links the tendency of the variables mentioned above, due to the complexity and irregularity of the wax crystal morphology (Zhang and Liu, 2008).

Gel strength is an important parameter concerning the restart process of gelled lines. In the case of planned or unexpected shut down situations, where the gel is formed under quiescent conditions, the gel strength can be measured through the yield stress, which is the minimum shear stress needed to break the gel formed and restart the flow inside pipeline. Thus, the restart of gelled lines is associated to the gel strength, and thereby the yield stress.

In order to understand the gel characteristics, its structure and its strength, it is important to verify the three main stages of the phase transformation process that leads to gelation of the wax crystal network inside the pipeline. The first stage is the wax precipitation, followed by wax deposition and finally wax gelation (A. Japper-Jaafar, 2015).

The wax gelation process is a complex process that has been described in some research works (Kane, 2003 and Singh, 2000). The authors proposed three stages:

1. Formation of lamellar sub-crystals
2. Aggregation of sub-crystals, forming a large space filling network
3. Overlapping and interlocking of the aggregation

2.4 CRITICAL TEMPERATURES IN THE FLOW ASSURANCE OF WAXY CRUDE OILS

There are some critical temperatures related to the gel formation process of waxy crude oil, the Wax Appearance Temperature (WAT) or Cloud Point Temperature (CPT), the Gelation Temperature (T_g) or Gel Point Temperature, and the Pour Point Temperature (PPT), which are keys points in the study of rheological behavior of waxy crude oils.

2.4.1 WAX APPEARANCE TEMPERATURE (WAT) OR CLOUD POINT TEMPERATURE

WAT is one of the most important flow assurance variables that need to be determined for a waxy crude oil. This temperature corresponds to the value where the visible crystallization occurs. WAT depends on the concentration and molecular weight of the waxes and the other components presents in the hydrocarbon matrix (Kok, 1996). When the wax solubility limit is reached during the cooling process of waxy crude oil, the wax begins to precipitate in the form of solid crystals.

There are two methods to determine the WAT: thermodynamically and experimentally. The thermodynamics WAT represents the true solid-liquid phase boundary temperature, the temperature where solid and liquid phases are in equilibrium at a given

pressure. The experimental WAT is the temperature where the first crystal is detected. Hence, the accuracy of this value depends on the measurement technique used. Typically, at a fixed pressure the experimental WAT is higher than the thermodynamic WAT (Karan and Raatulowsky, 2000).

The following techniques are commonly used to determine the WAT:

- Determination based on visual methods of the *American Society for Testing and Materials (ASTM)*, where the oil sample is placed in a glass jar and then immersed in a cooling bath. The WAT is registered when cloudiness is first observed in the sample.
- The WAT can be determined using a cold finger, where a temperature-controlled rod is inserted in a slowly heated oil sample. The temperature at which wax begins to adhere to the rod determines the value of WAT.
- Some viscometric techniques that detect a change in the rheological behavior as a result of the wax precipitation in the oil sample. For instance, the break in the curve of viscosity versus temperature is taken as the WAT.
- Differential Scanning Calorimetry (DSC) detects the latent heat of fusion liberated during the wax crystallization process. This technique has been widely used for WAT determination. The DSC technique gives information about heat capacities and heats of fusion or transition associated with liquid-solid and solid-liquid phase transitions.
- Visual techniques like cross-polarized microscopy are also used in WAT determination. A microscope provided of a controlled temperature device is employed to monitor the formation of wax crystals in the oil sample during the cooling process using polarized light and polarized objectives on the microscope.
- PVT cells with a light source and a light power are used to determine the WAT. Light transmittance property is evaluated. Thus when the wax crystals precipitate in the oil sample, the amount of light transmitted is reduced, and the WAT can be recorded from the curve of light power received versus temperature. This technique allows the use of high pressures, and it is possible to analyze live oil samples.
- The use of ultrasonic signal passing through the oil sample and then received at a transducer is also used. The velocity of the ultrasonic wave depends on the density of the oil sample, so the change in the transient time for the wave occurs in the WAT point.

2.4.2 POUR POINT TEMPERATURE (PPT)

The pour point of a waxy crude oil is the temperature at which it loses its flow characteristic during a cooling process under quiescently conditions below the WAT.

The continuous wax precipitation during the cooling process results in an increase in the amount and magnitude of wax crystals. This arrangement of precipitated crystals develops a 3D network formed by oil trapped and wax crystals, which has gel-like features. The wax crystal network is bonded to the cooled wall pipeline, which leads to the increase in the gel viscosity and the modification of the flow properties (Karan and Ratulowsky, 2000; Venkatesan, 2002).

The pour point temperature can be used as an approximate indicator of the temperature at which the oil will develop a yield stress. At temperatures below the PPT, waxy crude oils present time-dependent flow characteristics (Rønningsen 1992).

The pour point is determined according to the ASTM D5853-11 standard test method. This method consists in heating the sample to a temperature that ensures that the wax crystals are dissolved in the oil. After that, the sample is cooled, and its movement must be verified in intervals of 3 °C until the sample shows no movement when the test tube is held in a horizontal position for 5 seconds. Thus, the pour point is the temperature at which no movement was observed in the oil sample.

The pour point is an important variable in the restart problem, where the waxy-oil gel is formed under quiescent conditions, i.e. with no applied shear stress or shear rate (Venkatesan, 2002).

2.4.3 GELATION TEMPERATURE OR GEL POINT

The gel point or gelation temperature is the point where the solid behavior of the sample is predominant over its liquid behavior. These solid and liquid behaviors are rheologically defined through the evaluation of the storage (G') and loss moduli (G''). Thus, gelation temperature represents the change from the liquid-like behavior of the sample to the solid-like behavior during the cooling process. However, some liquid behavior remain and allows it to move until reach the no flow condition at the pour point temperature. Consequently, the gel point is higher than the pour point.

The test begins with the cooling at the temperature above Wax Appearance Temperature (WAT), where the oil sample behaves as Newtonian. In this region, the loss modulus is higher than the storage modulus. Just below the WAT, where the wax crystal began

to precipitate, the storage modulus increases faster than the loss modulus during the cooling process until they reach the same value, in this point it is obtained the gelation temperature or gel point (Venkatesan, 2002).

Gelation temperature determination is based on the oscillatory test as proposed by several authors (Webber 2001; Venkatesan et al., 2003; Lopes-da-Silva and Coutinho, 2004, 2007; Kané et al., 2004; Visintin et al. 2005; Magda et al. 2009; Tinsley et al., 2009; Phillips et al. 2011). Oscillatory shearing uses a low amplitude and low frequency in order to assess the storage (G') and loss (G'') moduli through the viscous-elastic response during the cooling process. When the viscous behavior is dominant, the storage modulus is smaller than the loss modulus, and the storage modulus is larger than the loss modulus when the elastic behavior is more pronounced in the oil sample. Thus, at higher temperatures, the material behaves as a viscous liquid, (G'' is larger than G'). In a first stage of the cooling process, both moduli G' and G'' increment their values. In a second stage G' begins to increase faster than G'' until a certain temperature where the crossover between G' and G'' takes place, this temperature is called gelation temperature. When G' exceeds G'' at temperatures below the crossover temperature, the solid elastic behavior of the material is predominant over the liquid viscous behavior (Andrade, 2015).

The results of oscillatory tests depend directly on the cooling rate and the shear stress applied during the cooling. This dependence condition makes the difference between the pour point and gel point determination, because the pour point is determined under zero shear stress, i.e. quiescent or static condition and the gel point varies with the conditions of the test.

Some studies have been carried out in order to search tendencies related to the influence of variables on the gelation temperature.

- Visintin et al. (2005) concluded that higher cooling rates lead to lower gelation temperature values.
- Smith and Ramsden (1987) identified a critical initial cooling temperature that provides the highest gelation temperature value when a constant cooling rate is imposed over the sample under quiescent conditions. Thus, if the initial cooling rate is lower or higher than this critical value, the gelation temperature will be smaller.
- Rønningsen et al. (1991) studied 17 samples of crude oils at two different initial cooling temperatures, and only the gelation temperature of one oil sample was not affected by the initial cooling rate. The general tendency showed that the initial cooling temperature reduces the gelation temperature.

- Marchesini et al. (2012) also showed the existence of a critical initial cooling temperature that produce the largest viscosity and the largest gelation temperature.

2.5 RHEOLOGY

Bingham introduced the term “Rheology” to designate the study of the deformation and flow of materials. The American Society of Rheology (Barnes, 1989) officially accepted this definition in 1992. Materials in solid, liquid and intermediate states present deformation as a consequence of any stress or load application. This response is different for each material and/or fluid, and rheological models should describe their behavior.

Deformation is the change of the size and the shape of any material due to external or internal forces application. The irreversibility of the deformation depends on the material capability to return to the original state after the stress or load is removed.

Generally, the fluids are classified in two types: Newtonian and non-Newtonian.

Newtonian fluids present a constant viscosity, independent of the shear stress applied and time, under isobaric and isothermal conditions, i.e. the relation between shear stress and shear rate is linear.

Non-Newtonian fluids exhibit a viscosity dependence on the shear rate and/or shear rate history, thus the relation between the shear stress and the shear rate is non-linear. These fluids can be classified in three categories:

1. Time-Independent fluids are those that do not depend on time and shear rate or strain; the rheological behavior is a function only of the shear stress applied, i.e. dilatant and pseudoplastic fluids.
2. Time-Dependent fluids are characterized by the dependence of the shear stress history applied on the fluid and time, i.e. thixotropic and rheopectic fluids.
3. Viscoelastic fluids exhibit both viscous and elastic features when they are subjected to a deformation and they show time-dependence strain, i.e. Kelvin–Voigt and Maxwell materials.

2.5.1 RHEOLOGY OF WAXY CRUDE OILS

Below the gelation temperature, the waxy crude oil exhibits a complex rheological behavior. Once the pour point temperature is reached, a 3D network structure formed completes the transition of crude oil from solid to colloidal gel (Visintin et al, 2005; Zhu et al, 2007).

The complexity of these fluids is related to viscoelastic behavior, the yield stress and thixotropic characteristics (Zhang and Liu, 2008; Magda et al, 2007). These complexity features represent a problem during the restart of gelled lines after shut-in. Waxy crude oil flowing in the pipeline presents a thermal and shear history, which have great influence on their rheological behavior and their critical temperatures. For instance, Zhang and Liu (2008) found that the gel point tends to reduce when the wax is precipitating from the oil in shearing, because of disturbance of porous wax crystal structure. Hou (2007) corroborated this finding, he also encountered that viscoelastic parameters, like storage modulus, loss modulus, loss angle and gelation temperature measured by oscillatory tests, are affected by the thermal and shear history.

The key variable in the study of restart problem in paraffinic oils is to determine the pressure required to restart the flow into the pipeline. This pressure is directly related to the yield stress.

2.5.2 YIELD STRESS

Yield stress is a critical stress amplitude value, below which the fluid does not flow, but deform plastically such as solid. After a finite deformation, the structure is recovered when the stress is removed (Nguyen and Boger, 1992). When the yield stress is surpassed, the fluid flows like a viscous liquid with finite viscosity. Thus, it is common to use the term “yield stress fluids” to represent soft rheologically-complex materials that behave like a solid at low stress amplitude and flow when subjected to stress amplitude that exceed a critical value (Dimitriou, 2014).

There are two types of yield stress (Mujumdar, 2002):

1. Static Yield Stress
2. Dynamic Yield Stress

Static yield stress is the lowest shear stress required to break the waxy gel structure, and the dynamic yield stress describes the state of the gel structure after it is broken.

Cheng (2000) proposed another yield stress point in addition to the two listed above (static and dynamic yield stress), in order to describe the complete yielding process. This third

yield stress is called elastic-limit yield stress, which is the limit stress for oil sample to preserve a reversible waxy crystal structure.

On the other hand, it is important to distinguish between two types of yield stress fluids, those with thixotropic or “non-ideal” and non-thixotropic or “ideal” behavior (Møller, 2009). The difference between these two types of fluids is possible to be verified using rheological measurements, with a gradually increasing the shear rate applied over oil sample from zero.

Thus, in the case of non-thixotropic yield stress fluid, the results show that the curve corresponding to the increasing shear rate coincides with the decreasing one, in the shear stress versus shear rate curve. This response proves that this type of fluids does not depend on the shear history; therefore, there is no problem in determining the yield stress value. Nevertheless, in experiments with an increase and subsequent decrease in the applied shear rate for thixotropic yield stress fluids, the increase curve shows higher values of shear stress and viscosity than the decrease curve, meaning that the value of yield stress decreases according to its shear history and the measurement duration.

Flow of waxy crude oils in pipeline with surroundings temperatures below its crystallization temperature, promotes the formation of a structured gel. The features of this gel can be determined using rheological test and experimental loops. When the crude oil achieves temperatures below the PPT (point of no-flow) in the cooling process or if the temperature is maintained in the PPT. If under these conditions, takes place an expected or emergency shutdown, the gel grows stronger and it is possible to measure its strength determining the pump pressure require to break the gel structure and restart the gelled line. The magnitude of this needed pressure can be calculated from a force balance in the gelled section of the pipeline, using rheological and experimental test in a pilot flow line (K. Oh, 2009).

Yield stress concept has been widely discussed in the last decade. Barnes and others author suggested the idea of non-existence of a true yield stress (Barnes, 1985; Hartnett 1989; Moller, 2009). Despite the controversial concept of yield stress, it is acceptable to use this concept like a representation of the shear stress value under which the fluid shows an elastic solid behavior with infinite viscosity; engineers and researchers generally accept it, as a practical and useful tool to design and operate processes.

Waxy crude oil can be classified as a yield stress fluid because it exhibits a transition from solid to liquid, the point of this transition is the yield stress. This point is

determined like the minimum shear stress that needs to be applied in order to restart the flow. This initial work required to produce a shear flow depends on the gel composition, shear and thermal histories developed during the gelation process (Venkatesan, 2005).

There are many studies of yield stress measurements. Following it is summarized some findings of these studies:

- With the decreasing of the final temperature of the cooling process, the yield stress value increases (Davenport and Somper, 1971). Other properties increment their values as a result of the decrease in the temperature, i.e. the storage modulus (G'), the loss modulus (G'') and the viscosity (Wardhaugh and Boger 1987; El-Gamal, 1998; Remizov et al., 2000; Chang et al., 2000, Webber, 2001; Venkatesan et al., 2003; Kané et al., 2004; Visintin et al., 2005; Chen et al., 2006; Hou and Zhang, 2007, 2010; Lopes-da-Silva and Coutinho, 2007; Lee et al., 2008; Li et al., 2009; Oh et al., 2009; Hasan et al., 2010; Dimitriou et al., 2011; Ghannam et al., 2012; Rønningsen, 2012). The increment of the above properties is associated with wax solubility reduction in oil when the temperature is reduced (Venkatesan et al., 2003)
- The yield stress value increases with the increase of the cooling rate. Under constant cooling rate condition, the yield stress depends on the final temperature in the cooling process (Singh et al., 1999; Webber, 1999; Lin et al., 2011).
- Yield stress value reduces and increases under low and high shear rate applied during the cooling process, respectively (Singh et al., 1999; Webber, 1999; Lin et al., 2011). Venkatesan et al. (2005) obtained an opposite finding, they observed that the yield stress increased with the shear rate for low values of shear stress and decreased with the shear rate for high values of shear stress during the cooling process. This finding can be explained through two competing effects that occur during dynamic cooling: the enhancement of material mobility that promotes the wax aggregation and the wax crystal breaking by shearing. Thus, the maximum yield stress is reached when the stress is just enough to obtain larger crystals without breaking its structure.
- Rønningsen (1992), Venkatesan et al. (2005), Chen et al. (2006) and Lin et al. (2011) found that higher cooling rate results in lower yield stress. Weber (2001) detected the opposite behavior in experiments with mineral lubricant oils, showing an increase of yield stress with cooling rate.
- Lee et al. (2008) found that the yield stress increases with the cooling rate for low values of cooling rates and reduces for larger values.

- Wardhaugh and Boger (1991b) observed that the aging time of 65 hours after a dynamic cooling did not affect the yield stress value or the equilibrium viscosity. In agreement with the above results, Chang et al. (2000) also found that the aging time does not affect the yield stress, as well, it does not have influence on the size and shape of the wax crystals.
- Jemmett et al. (2013) found that the initial cooling temperature influences the pressure necessary to restart the flow in a gelled pipeline. They observed that for a difference of 5°C in the initial temperature, the restart pressure was doubled.
- Peng (2008) evaluated the yield stress under three different loading conditions: in stepwise sequence, in a ramp-up way and with a constant value; finding that the strains at yield stress value fell into a narrow range, and keeps some relationship with the stress loading.

The main difficulty to determine the yield stress value is the variation of the properties of gel along the pipe. Furthermore, the presence of spatial temperature gradients and diffusion of wax forming molecules in the radial direction from the center of the pipeline to the wall, influence the heterogeneity of the gel formed, its structure and its strength.

Recent works contribute with refined models of the behavior of thixotropy materials.

- De Souza Mendes (2011) proposed the use of the shear rate equation based on the linear viscoelastic Maxwell constitutive equation for structure parameter, incorporating the characteristic relaxation time and the shear stress as the driving force for the breakage of structure.
- Teng and Zhang (2013) represented the rheological response of waxy crude oils through an elastic and a viscous stress term. In the elastic stress term, the shear modulus varies proportionally to a structural parameter and a nonlinear damping function. The viscous stress term is proportional to a structure-dependent consistency and a completely unstructured parameter. The results predicted by this model were very successfully for the restart problem after cooling at rest, but only in the destructuring stage.
- Dimitriou and McKinley (2014) proposed a rheological constitutive equation modeling the material deformation in two components: a linear viscoelastic and a plastic deformation. Their analysis was focused on the physical behavior of the waxy crude oil in its slurry state.

- Mendes (2014) presented a model that predicts the thixotropic phenomena around the flow curve of the fluid as a reversible structure parameter.

2.5.2.1 YIELD STRESS MEASUREMENT TECHNIQUES

The yield stress measurements have some limitations related to the equipment used, i.e. viscometer and/or rheometer geometries; and the procedures performed to obtain the experimental data.

The methods used to measure the yield stress can be divided in two main categories, dynamic or controlled rate measurements and static methods or controlled stress measurements (Rønningsen, 1992):

Dynamic or indirect methods:

- Direct extrapolation of shear stress value from the log-log flow curve.
- Extrapolation to zero shear rate of curves adjusted to general constitutive models, such as Casson, Cross, Herschel-Bulkley, Bingham, etc.).

Static or direct methods:

- The yield stress can be determined through stress relaxation test, and it is identified as the residual stress acting on a static body immersed in the sample after a constant shear rate application. Nevertheless, this technique tends to underestimate the yield stress compared to others techniques.
- Controlled stress test with cone-plate or concentric cylinder geometry can be used to determine the yield stress. This technique is based on the gradual increase in shear stress from zero. The first evidence of flow is registered (shear rate higher than zero), and this value is identified as the yield stress. Furthermore, concerning to the geometry used, the cone-plate device is more suitable to evaluate the non-Newtonian and time dependent fluids because the shear rate and shear stress are uniform throughout the fluid for small cone angles.
- Oscillatory test using a small amplitude sinusoidal oscillation of the shear stress is widely applied to determine the yield stress. This technique has been used in the study of waxy crude oils assessing the storage and loss moduli with increasing amplitude at low frequencies.

- Model pipeline test is also used to determine the yield stress by measuring the flow in response to an imposed pressure.

Controlled stress measurements give more accurate yield stress values because the variable of interest is carefully monitored. Thus, in the controlled stress measurements it is possible to perform a gradual increase of the stress applied to the oil, and identify the stress point at which the movement begins. Besides, during controlled shear rate measurements, the point of yield stress can be achieved before the measurement occurs. Therefore, the yield stress value needs to be measured by back extrapolation from a finite level of motion to a zero-motion point.

When the yield stress is determined through experimental measurements, it is possible to determine if the breakage of the gel structure occurs under an adhesive or cohesive way, based on the response of shear stress versus time, in the controlled shear rate measurements (Paso, 2014).

Adhesive Breakage occurs when the strength of the cohesive bonds is higher than the strength of the adhesive bonds, which means that the cohesive forces which correspond to the intermolecular forces which link similar molecules, are greater than the adhesive forces that represent the intermolecular force that link a substance to a surface.

Cohesive Breakage takes place when the adhesive forces are greater than the cohesive forces, which means that the gel network is weak, therefore this conditions is desirable for pipeline restart application (Paso, 2014).

2.5.2.2 CONSTITUTIVE MODELS FOR YIELD STRESS FLUIDS

Constitutive models are mathematical equations that describe the material behavior, i.e. the relationship between stress and deformation rate. Some cases where gelation occurs, more than one equation may be necessary to describe all the rheological system. It is important to quantify the influence of state variables (temperature and the effect of structure/composition) on each parameter model.

There are three types of rheological models:

1. Empirical models, i.e. Power Law model deduced from rheological measurements.

2. Theoretical models, i.e. Krieger–Dougherty model (Krieger, 1985). This kind of models is derived from fundamental concepts of structural composition.
3. Structural models, i.e. Cross model, taking into account consideration related to structure and kinetics of changes happening in the structure.

Constitutive models for yield stress fluids are those that require a certain value, which represents the stress needed to start to flow. Several proposed models described the viscous behavior, which represent the behavior of yield stress fluid: Bingham, Herschel-Buckley, Carreau and Cross models.

Bingham plastic model describe the fluids that exhibit a yield stress (σ_0) through the following equation:

$$\sigma - \sigma_0 = \eta \dot{\gamma} \quad (1)$$

Where:

σ is the shear stress,

σ_0 is the yield stress,

η is the viscosity and

$\dot{\gamma}$ is the shear rate.

Bingham model describes the linear relation between shear stress and shear rate with a constant slope, which correspond to value of plastic viscosity, and the intercept correspond to yield stress value.

Herschel–Bulkley Model is represented by:

$$\sigma - \sigma_0 = K \dot{\gamma}^n \quad (2)$$

Where:

σ is the shear stress,

σ_0 is the yield stress,

K is the consistency index,

$\dot{\gamma}$ is the shear rate and

n is the flow behavior index.

Herschel-Bulkley model considers that the fluid has yield stress (σ_0) and the flow above this yield stress is described by a power - law relationship. The model is recommended when the yield stress is measurable, and the other parameters can be determined using a linear

regression of $\log \sigma - \sigma_0$ versus $\log \dot{\gamma}$, the intercept and slope of this line correspond to K and n respectively (Stokes, 2004).

Cross and Carreau Models

For these models, the apparent viscosity (η_a) is presented like a function of the shear rate ($\dot{\gamma}$), viscosity at low and high shear rates. Equation (3) corresponds to Cross model. Carreau model is represented by equation (4).

$$\eta_a = \eta_\infty + \frac{\eta_0 - \eta_\infty}{1 + (\dot{\gamma}/\dot{\gamma}_b)^n} \quad (3)$$

$$\eta_a = \eta_\infty + \frac{\eta_0 - \eta_\infty}{[1 + (\lambda_c \dot{\gamma})^2]^N} \quad (4)$$

Where:

$(1/\dot{\gamma}_b)$ and λ_c are time constants related to relaxation times,

n and N are dimensionless exponents,

η_∞ is the viscosity in an infinite state. Usually, η_∞ is very low-magnitude and it is difficult to be determined experimentally, so η_∞ is often neglected (Abdel-Khalik et al. 1974; Lopes da Silva et al. 1992).

Generally, Carreau model has been widely used in studies in North America and the Cross model in Europe (Rao, 2014).

2.5.3 TIME-DEPENDENT FLUIDS

Some fluids, whose viscosity depends on shear time, can be classified in two categories: thixotropic and rheopectic fluids. Thixotropic fluids show decrease of apparent viscosity when a constant shear stress or shear rate is applied, followed by a gradual recovery when the stress or shear rate is removed in a finite time, so the microstructure of fluid reaches a new equilibrium state. Rheopectic fluid (also called anti-thixotropic materials) increase its apparent viscosity when the applied stress or shear rate is increased (Tropea, 2007).

Changes in rheological properties indicate the structural rearrangement caused by application of external forces. Thus, thixotropy is a consequence of structure rupture and rheopexy of structure build-up. Usually, external forces promote the rupture rather than a build-up of structure, so thixotropic effects are more common than rheopectics. Rheopexy is characteristic of materials with unusual intermolecular interactions, such as strong ionic interaction or nitrogen bonding (A. Ya. Malkin, 1994)

2.5.2.1 Thixotropic fluids

Thixotropic fluids show a decreasing viscosity when a shear strain is imposed, resulting in changes in its structure. Once, the strain is ceased, the structure rebuilds. Thus, in thixotropic fluids, the viscosity is a time-dependent property due to reversible changes in its structure. Thixotropy is the property possessed by certain materials, whose behavior is continuous and reversible time-dependent change when the viscosity is measured under a specific shear rate.

The continuous decrease in viscosity under shear strain accelerates the flow (Coussot, 2002). In this decreasing viscosity change and subsequent increasing flow, occur a phenomenon called avalanche which causes the structural destroy of the fluid and a tremendous viscosity decline. This avalanche behavior can be seen as the link between yield stress and thixotropy concepts (Møller, 2006).

The change in the microstructural composition of the material caused by shear rate application is called shear rejuvenation. On the other hand, the aging is the opposite mechanism and it can be expressed as the ability of the material to rebuild its microstructure once the shear is ceased.

In order to describe the thixotropy phenomenon, which is very common in the viscoelastic materials, some constitutive models introduce a structural parameter. This parameter gives an idea of how much the material can build up or break in a period of time, because of shear application and determine the structuring level of the gel (G.M. de Oliveira, 2015)

So as to describe the two mechanism of the microstructure, shear rejuvenation (break-down term) and aging (build-up term) are described by the structural parameter varying in the time as a function of some rheological parameters like yield stress, viscosity and viscoelastic moduli need, which need to be evaluated. Nevertheless, Coussot (2002) proposed expressions to describe the gel microstructure behavior.

$$\frac{d\lambda}{dt} = \frac{1}{T} - \alpha|\dot{\gamma}|\lambda \quad (5)$$

$$\eta = \eta_0(1 + \beta\gamma)^n \quad (6)$$

Where:

T is the characteristic aging time for buildup of the microstructure,

α determines the rate at which the microstructure is broken down under shear,

$\dot{\gamma}$ is the shear rate,

λ is the structural parameter of the material,

η_0 is the limiting viscosity at high shear rates and

β and n are parameters designating how strongly the microstructure influences the viscosity.

Equation (5) includes the increasing structural parameter under zero shear or aging in the first term at right side of the equation. The second term describes the decrease of structural parameter.

Equation (6) is a general viscosity function, which depends on the structural parameter, and other parameters related to the microstructure characteristics.

2.5.2.2 Thixotropic measurement techniques

The quantitative measurements of thixotropic behavior of fluids has some limitations due to certain characteristics like wall slip, shear banding, shear heterogeneities, sedimentation, irreversible changes in the microstructure of the oil sample as a consequence of the shear and thermal history. Some rheological techniques allow studying the thixotropic behavior, as hysteresis loop, stepwise changes in shear rate or shear stress, start-up and creep experiments.

Hysteresis loop

Green and Weltmann introduced the hysteresis technique in 1943, allowing the study the variation of the shear stress response to an increased and subsequently decrease in the shear rate applied in a range of zero to a maximum value. There are different possible responses, which were summarized in Figure 2.

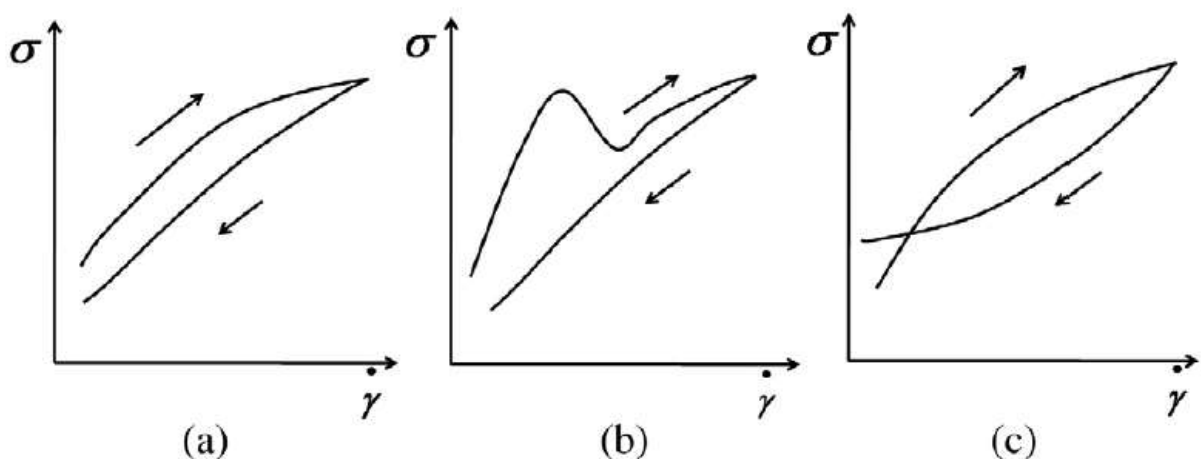


Figure 2. Possible hysteresis loop responses (Mewis et al. 2009).

Shape of the hysteresis loop and the area between their up and down curve, varies according to each fluid, as well as the conditions of the test, the range of the shear rate evaluated and the velocity of this variation.

Figure 2a corresponds to the classical shape of the hysteresis loop, but it can vary to those described by the chart in the middle and the right of the same figure (2b and 2c). In the case of the middle chart, an initial breakdown in the microstructure is shown resulting in a stress overshoot (peak), the subsequently reduction of the shear stress with the increase in the shear rate can cause shear banding and heterogeneities in the shear rate distributions at the sample. For the right chart in the Figure 2 suggested the formation of the structure at low values of shear rate.

An important limitation of the hysteresis loop technique is related to the dependence of the shear rate and time application, because it is not possible to separate the influence of each parameter. It is necessary to perform different test varying the shear rate range and the time of its application, to get the hysteresis loop that best describes the thixotropic character, i.e. for viscoelastic fluids, the application time of the increasing and decreasing shear rate needs to be faster because of the shorter time scales involve in viscoelastic relaxation (Bird et al., 1968).

Stepwise changes in shear rate or shear stress

Application of a constant shear rate or shear stress until the steady state is reached, and repeating this stepwise to achieve the initial conditions. Sudden applications of these steps (increasing or decreasing) in the shear rate or shear stress leads to viscosity and microstructure change under different flow conditions that can be simulated through the stepwise experiment. Figure 3 presents a typical response of a thixotropic material to this kind of experiments.

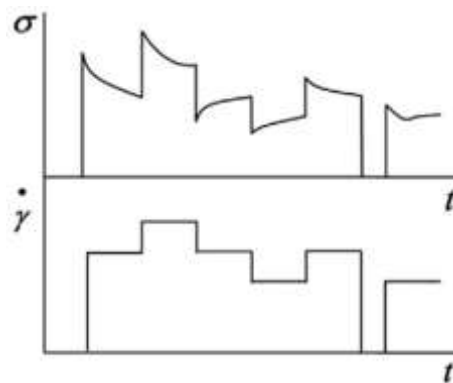


Figure 3. Response of the thixotropic material with a complex shear history to the stepwise experiments (Mewis et al. 2009).

Start-up and creep experiments

Sudden application of constant shear stress or shear rate are called start-up experiments. As result of this measurement, it is possible to record a stress overshoot followed by a decay stress value to a steady state. The overshoot recorded in this technique is usually associated with the yield stress (Butera et al., 1996). The peak that corresponds to overshoot usually increase with increasing shear rate for thixotropic systems.

Creep experiments consist in the application of a constant shear stress during a time interval and immediately this stress is removed to record the response of the sample, its recovery with the time of rest.

2.6 RESTART PROBLEM: PIPE FLOW EXPERIMENTS

The restart problem of gelled lines with waxy crude oil in the offshore petroleum industry, due to emergency and/or planned maintenance, it is related to the temperature decreases in the surroundings. Hence, the wax solubility decrease, causing the precipitation of wax molecules from crude oil under static conditions. Thus, under no flow conditions, precipitated waxes form a wax-oil network with gel features.

Table 1 presents an overview of the main restart studies done in laboratory pipeline reported in literature.

Table 1. Overview of laboratory pipeline shut-in and restart experiments (Paso, 2014).

Laboratory	Authors	Year	ID (mm)	Length (m)	L/D aspect ratio	Investigation
Atlantic Richfield Co.	Perkins and Turner	1971	7.9/8.5	15.24	1929/1793	Restart processes
BP	Smith and Ramsden	1978	6	15	2500	Fluid yield stress
ConocoPhillips Company	Lee et al.	2008	7.7	3.77	490	Adhesive and cohesive mechanisms

Laboratory	Authors	Year	ID (mm)	Length (m)	L/D aspect ratio	Investigation
IFP	Hénaut et al.	1999	50	0.79	15.5	X-ray scanning and gel properties
KAT	Phillips et al.	2011	6.35/12.7	15.24	2400/1200	Contraction flows and pressure
PetroChina Pipeline R&D Center	Cui et al.	2008	150/300	661	4407/2203	Pressures propagation processes
Shell Laboratory	Verschur et al.	1971	203/6	888/16	4371/2667	Pipeline restart processes
SPE&AGIP	Carniani and Merlini	1996	06/12	15	2500/1250	Influence of diameter and stress propagation
Utah Petroleum	El-Gendy et al.	2012	12.7	1.18	186	Advance imaging and pressure
	Ekweribe	2008	9.65	6.1	631,7	Valve positions
	Li et al.	1998	10	20	2000	Pressure transmission

These different research works were focused in the contraction flow, compressibility, pressure wave propagation and adhesive/cohesive fracture.

Contraction Flow

The impact of the thermal history plays an important role in the formation of waxy gel in field conditions. Various authors have found that under slower cooling processes the wax crystals formed are larger and produce a stronger gel (Venkatesan et al., 2005; Karan et al., 2000; Lee, 2008).

At field conditions it is observed a cooling rate range of 0.5 °C/h (0.0083 °C/min) to 10 °C/h (0.17 °C/min), using an insulated pipeline. Contraction flow is usually associated to

suction pressure along the pipeline because of the vacuum drop volume inside the line result of oil gelification.

Experiments performed by El-Gendy (2012), at laboratory scale showed that the pressure required to restart a gelled line decreased from 10 psig to 5 psig when the gel was formed and aged without any hydrostatic pressure head (around 12 psig). Lee et al (2008) also corroborated that the pressure required in restarting experiments was reduced by approximately 50% without hydrostatic pressure head.

Compressibility

Gel compressibility is related to segregated voids and entrained gaseous voids, which has an impact in the gel breakage process, axial stress localization and pressure wave propagation process.

Hénaut et al. (1999) measured the volume change with the pressure, using a controlled temperature lateral friction tester in a piston where the gelled oil was compressed. They found that at a temperature of 8 °C the gelled oil showed a volume contraction of 12% by application of 3000 kPa pressure. It was also observed that the compressibility values of gelled oil increased at lower temperature conditions. Shrinkage favors axial displacement of the gelled wax inside the pipeline. Thus, for increased compressibility conditions, a lower applied pressure is needed to restart the gelled line (Paso 2014).

Pressure wave propagation

Pressure wave propagation has a component in the axial segment of pipeline, which allows restart at smaller applied pressures than those predicted by force balance equations. Contraction and gel structure influence the pressure wave propagation. Cui et al. (2008) suggest that void compression process may reduce the pressure propagation velocity.

Adhesive or cohesive fracture

These two kinds of breakage were defined in the subsection 2.3. Lee (2008) found that gels formed at low cooling rates presented an adhesive breakage, and the gels formed at high cooling rate showed smaller crystal sizes and the rupture occurred through cohesive mechanism.

In the study of restart of gelled lines at temperatures of seabed in the offshore industry, the parameter of interest to be determined is the pressure required to break the gel formed and restart the flow inside the pipeline. The most simple and practical model considers the waxy oil as an incompressible fluid. Thus, it is possible to determine the minimum pressure

required through a forces balance between the applied pressure and the resistance to shear stress at the pipe wall (Borghi et al., 2003; Lee et al., 2008; Vinay et al., 2009; El-Gendy et al., 2012) as following equation:

$$\Delta P \frac{\pi D^2}{4} = \tau_w \pi D L \quad (7)$$

Where:

τ_w is the shear stress at the pipe wall,

L is the length of the pipe,

D is the diameter of the pipe and

ΔP is the pressure differential required to restart the gelled line.

Perkins et al. (1971) and Ajienka et al. (1995) proposed an equation to correlate the yield stress measured at rheometer (τ_w) with the minimum differential pressure, based on the geometrical parameter of the pipeline (Equation (8)).

$$\Delta P_{min} = \frac{4 \tau_w L}{D} \quad (8)$$

The above equation is a classical and conservative model, which is based on the hypothesis that the velocity of the pressure wave inside the pipeline tends to infinite value and the flow is considered incompressible.

This classical balance force is an over simplistic method to determine the minimum differential pressure to restart a gelled line, but is a powerful tool because it allows engineers to determine the pumping pressure for full size pipelines easily and fast (Borghi, 2003).

However, the correlation gives overestimated values for the restart pressures, in a factor of 4 to 5 times (Venkatesan et al., 2010).

3. MATERIALS AND METHOD

3.1 MATERIALS

The experiments were performed with a Brazilian waxy crude oil provided by Repsol Sinopec Brazil. This oil presents a dark color, characteristic smell and liquid behavior at ambient temperature.



Figure 4. Waxy crude oil sealed barrel of 50L provided by Repsol Sinopec Brazil.

Oil was received in four sealed barrels of 50 L (Figure 4). Oil samples were transferred to smaller containers, after being heated in accordance with the procedure in the section 3.1.1.

3.1.1 SAMPLING OF WAXY CRUDE OIL

Sampling of waxy crude oil was made through the following procedure:

- Samples in the original packaging (Figure 4), were pretreated at 60 °C using an oven.
- Samples were kept at 60°C for 8 hours. In that time interval, the oil was agitated every 30 minutes.
- After heating, the samples were transferred to 100 ml labeled bottles using a funnel (Figure 5).



Figure 5. 100 mL bottle of waxy crude oil.

3.1.2 PRETREATMENT OF WAXY CRUDE OIL BEFORE ANY TEST

In order to ensure a stable chemical composition before the rheological measurements, a pretreatment was applied to all oil samples. Each sample placed in 100 mL bottles (see Figure 5) was heated to 60 °C for at least 2 hours before any test of physicochemical or rheological characterization. This treatment avoided loss of the light, erased the thermal memory and promoted a good homogenization of the sample, ensuring the dissolution of all paraffin content in the crude oil.

3.2 EXPERIMENTAL SECTION

3.2.1 CHARACTERIZATION OF THE CRUDE OIL

3.2.1.1 Asphaltenes and Resins Determination

Percentages of asphaltenes and resins of waxy crude oil studied, were determined used an adapted procedure based on ASTM D6560 e ASTM D2007 standard test methods.

Asphaltenes Content Measurement

10 g of oil were weighed in a covered jar, subsequently heptane (Synth) was placed in the same jar in a 30:1 proportion of heptane and oil, respectively. This mixture placed in the covered jar was agitated for 24 hours at ambient temperature. Then the mixture was filtered under vacuum using Nylon 66 membrane (SUPELCO, 0.45 μm pore). The asphaltene (black solid) retained in the filter was washed with a small aliquots of heptane to remove oil residues. Asphaltene was dried at 78 °C for 3 hours and then weighed.

Resins Content Measurement

Quantification of resins was made from the maltene fraction (hydrocarbons plus resins) resulting from asphaltene extraction process. Initially, heptane was evaporated in a rotary evaporator in vacuum (95 °C; 200 mbar), resulting in deasphalted oil.

100 g of silica was dried at 100 °C and weighed after drying. This silica was packed in a glass column of 4.5 x 40 cm (length x diameter). Desphalted oil was eluted through this column using heptane as eluent. The elution process was repeated at least four times to ensure complete retention of the resins in the column. The elution was completed with heptane until only slight yellow coloration present in the column outlet.

After resin separation, silica was transferred to a round-bottomed flask and the solvent was evaporated in a rotary evaporator in vacuum (95 °C; 200 mbar) until the flask mass kept constant. The amount of resins was calculated by mass difference.

3.2.1.2 Karl Fisher Water

Oil emulsions formation has great influence in the rheological behavior of waxy crude oils. For this reason, if the amount of water present in the oil is high, an additional procedure needs to be performed in order to remove the water.



Figure 6. Karl Fisher equipment: T50 Titrator – Mettler Toledo.

Karl Fisher titration procedure is an analytical method used in the industry to determine the quantity of water in different fluids. The water content in the waxy crude oil was measured by equipment T50 Titrator, Mettler Toledo (Figure 6). This equipment is completely automated, requiring only add the sample to be analyzed. The solution used for measurements

was a Karl Fisher Hydranal Composite 5 solution and a toluene/methanol solvent (1:1). The test was performed according to established in the ASTM D6304-07 standard test method.

3.2.1.3 Total Acid Number (TAN) Determination

TAN is a measure of acidity that is determined by the amount of potassium hydroxide in milligrams that is needed to neutralize the acids in one gram of oil. The TAN is used to condemn nearly all-fluid types, thus a precise and accurate analysis is crucial, i.e. indication of potential corrosion problems.

The TAN in the waxy crude oil was measured by equipment T50 Titrator, Mettler Toledo (Figure 6). The test was performed according to the ASTM D664 standard test method. Oil sample was dissolved in toluene and propanol with a little water and titrated with alcoholic potassium hydroxide. A glass electrode and reference electrode were immersed in the sample and connected to a voltmeter/potentiometer. The inflection in the titration curve is the end point of the test, and the TAN is calculated from this volume of titrant.

3.2.1.4 Characterization of *n*-Paraffinic Fraction by Gas Chromatography

n-Paraffin fractions were determined using a gas chromatography (GC). The equipment used in this analysis was GC 2010, Shimadzu Plus (Figure 7).



Figure 7. GC 2010 Shimadzu Plus used in the characterization of paraffinic fractions.

1 μ L of oil sample was injected, with a temperature injector in 250 °C. The oven temperature was program at 50 °C, staying in that temperature for 2 minutes, and then with heating steps of 10 °C/min to 320 °C, this final temperature was maintained for 15 minutes, with a total run time equal to 44 minutes.

3.2.1.5 Characterization of *n*-Paraffinic Fraction by High-Temperature Simulated Distillation (HSTD)

n-Paraffin fractions were also determined by High-Temperature Simulated Distillation (HSTD) in a gas chromatographer (Agilent Technologies, 7890A) with a injector co on-column (COC) and flame ionization detector (FID) with temperature of 430 °C. Oil samples were diluted in carbon disulfide (CS₂) until a final concentration of 2% (in weight). Afterwards, it was injected 1 µL of solution, with an automatic injector (Agilent Technologies 7683 Series B) on a Wasson KC100 column. The column has a length of 6 m, an inner diameter of 530 µm, and a film thickness of 0.15 µm.

The gas flow rate in the column was equal to 22.5 mL/min. The initial column temperature was 40 °C heating to 430 °C with a heating rate of 10 °C/min. This final temperature of the column was kept for 5 min. Total time of the test was equal to 44 minutes.

Chromatographic data handling system (Agilent ChemStation software GC, B.03.02) was used for data acquisition. The curves obtained by chromatographic simulated distillation (SimDis) were made using the algorithm defined in ASTM D 7169 (2011) with SimDis software (AscentSimDis to netCDF A06.01 V1.012409) supplied by Instrumentation Wasson-ECE.

For the quantification, the detector signal is integrated every 0.1 minutes. The signal corresponding to the blank was removed from the data processing using the software SimDis (AscentSimDis is netCDF V1.012409 A06.01).

3.2.1.6 Pour Point Determination

ASTM D5853-11 standard test method was used to determine the pour point temperature of the oil sample.

Test jar with dimensions according to the established in the standard test method (height of 121.3 mm and inside diameter of 32 mm) was placed in and adequate apparatus to put into the thermostatic bath, which has a cavity to couple the test jar filled with the waxy crude oil.

The oil sample was heated at 60°C during two hours, and then it was placed in the test jar. Filling the test jar with the oil, it was closed with a polystyrene cork with a coupled thermometer in its center. The test jar was allowed to rest for 24 hours at ambient temperature.

Afterwards, using a thermostatic bath at 48 °C, the test jar filled with waxy crude oil sample was heated until the thermometer coupled to the test jar into the sample registered 45°C. At this time, test jar was transferred to the test jar carrying apparatus located in another

thermostatic bath at 21 °C (Figure 8). Every 3 °C decreased in the temperature of the oil sample, the test jar was removed from the carrying apparatus and inclined; when the fluid movement was observed, immediately test jar was replaced in the carrying apparatus, otherwise the tube was left for 5 seconds in a horizontal position. If any movement was observed after 5 seconds, the test jar was returned to the apparatus. When the oil sample registered 30 °C, the temperature of the thermostatic bath was changed to 0 °C. The criteria for defining the pour point, ASTM D5853-11, it is the absence of flow within 5 seconds when the test jar is put in a horizontal position. The measurements were performed in triplicate.



Figure 8. Test jar carrying apparatus in a thermostatic bath at 21 °C for pour point determination.

3.2.1.7 Density measurements

Density was measured at a density meter DMA 4500, Anton Paar (Figure 9) at temperatures of 60, 50, 40, 30, 20, 15.56, 10, 5, 4 °C. API gravity was calculated from the measure done at 15.56 °C, which corresponds to 60 °F.

Using a common syringe, the sample was inserted in the measurement cell until all its volume was completely filled by the sample. It made sure that there were no bubbles in the measuring cell, since the presence of air bubbles could give erroneous results. After the temperature stabilization in the measure equipment, the reading of density value was made. The measurements were performed in triplicate for each temperature.



Figure 9. Density meter DMA 4500 (Anton Paar).

3.2.1.8 Differential Scanning Calorimetry (DSC)

The Wax Appearance Temperature (WAT) was established as the onset of the exothermic peak during the cooling process that corresponds to the liquid-solid transition (crystallization phenomena).

Total energy released during cooling process can be quantified as proportional to the area between the base line and the exothermic peak. These enthalpies of crystallization were calculated from the integration of heat flow.

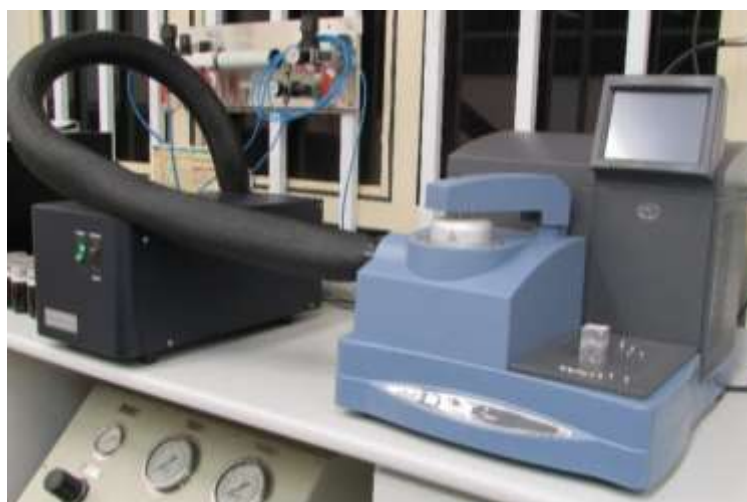


Figure 10. TA Instruments Q2000 equipment for DSC experiments.

The equipment used for DSC experiments was a TA Instruments Q2000 equipment (Figure 10), in the temperature range from 80 to -30 °C, with temperature scanning rates of 1.0 and 3.0 °C/min. The sample was heated to 80 °C for 10 minutes before being placed in the

calorimeter. During cooling process with two different cooling rates (1 and 3 °C/min), the paraffin crystallization produced a characteristic exothermic peak in the DSC curve. WAT was measured by the intersection point between the baseline and the tangent line of the inflection in the exothermic peak.

3.2.1.9 Wax Solubility Curve

The thermograms obtained from DSC analysis were also used to determine the concentration of precipitated paraffin (c_w) and the solubility curve of waxy crude oil. For this purpose, the total thermal effect of the wax precipitation in the sample at any measurement temperature (Q) was integrated at temperatures ranging from the WAT to the measurement temperature. Thus, the concentration of precipitated wax was obtained using Equation (9).

$$c_w \frac{\int_{T_w}^{WAT} dQ}{\bar{Q}} = \frac{Q}{\bar{Q}} \quad (9)$$

Where

c_w is the concentration of precipitated paraffin (% w/w),

T_w is the given temperature at which c_w is measured (°C)

dQ is the thermal effect of paraffin precipitation at the temperatures between T and $T + dT$ (J/g),

Q is the total thermal effect of paraffin precipitation at the temperatures ranging from WAT to T_w (J/g) and

\bar{Q} is 210 J/g, considered the thermal effect of wax precipitation for crude oils with an unknown molecular structure (Chen et al., 2004; Yi and Zhang, 2011; Coto et al., 2011).

3.2.1.10 Rheo-optical measurements

The microstructure of waxy crude oils was obtained using a microscopic accessory (Figure 11) at the controlled-stress rheometer - Thermo Scientific, Haake Mars III (Figure 13). All the experiments were performed using cone-plate geometry (polished cone with 60 mm diameter and angle of 1 degree). The images were taken using a lens with 20 times magnification and crossed polarizers. In order to determine the Wax Appearance Temperature (WAT), the oil was cooled from 60 to 5 °C using different cooling rates (0.5, 1.0 and 3.0 °C/min) without shearing. The WAT was recorded when the first wax crystal was visually identified.



Figure 11. Rheoscope module of controlled-stress rheometer - Thermo Scientific, Haake Mars III.

Another important variable studied using rheo-optical tests, was the influence of aging time in the formation of crystals at the different temperatures. The concept of aging of the wax deposition is related to the porous-like behavior of the gel network in which wax molecules is keeping diffuse due to the radial variation of temperature and wax concentration (Singh, 2001). Experiments were carried out for three different aging times of 0, 1 and 5 h, controlling the cooling rate and temperature.

3.2.2 RHEOLOGICAL MEASUREMENTS

The rheological tests were performed in a controlled-stress rheometer - Thermo Scientific, Haake Mars III (Figure 13). The cone-plate geometry was selected with cone size of 60 mm in diameter and angle of 1 degree (Figure 12). The gap between the cone and plate was 0.052 mm and the sample amount required for each measurement was approximately 1 mL. Peltier element inside of rheometer was used to control the temperature of the oil samples.

Prior to any test in the rheometer, oil samples were heated in a thermostatic bath at constant temperature of 60 °C. The heating of the samples was performed for at least 2 hours to eliminate their thermal history. The samples were placed in the gap between the cone and plate at the initial temperature of each test (60 °C) and sheared for 10 minutes at a constant rate of 10 s^{-1} in order to erase their thermal and shear history, respectively. The rheological analysis was performed in order to get some oil parameters such as yield stress and viscosity.



Figure 12. Cone-plate geometry with cone size of 60 mm.

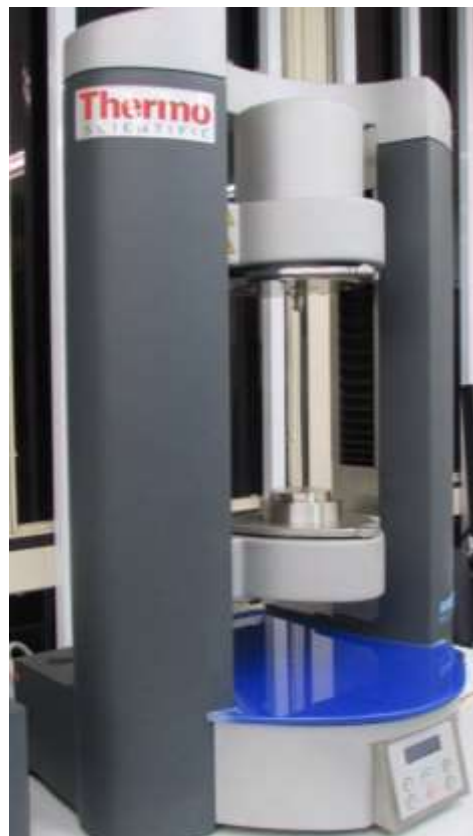


Figure 13. Controlled-stress rheometer - Thermo Scientific, Haake Mars II

3.2.2.1 Viscosity and Flow Curves

Viscosity tests were performed under a constant shear rate of 1 s^{-1} and three cooling rates of 0.5, 1.0 and $3.0 \text{ }^{\circ}\text{C}/\text{min}$ in triplicate. The initial temperature of the tests was $60 \text{ }^{\circ}\text{C}$ and the final one was $5 \text{ }^{\circ}\text{C}$.

Another rheological protocol was used to evaluate the influence of the shear rate variation between 10 and 250 s^{-1} , under constant temperatures of 60, 50, 40, 30, 20, 15, 10, 5 and $4 \text{ }^{\circ}\text{C}$. After each measurement, the analyzed oil sample was substituted by a new sample, to avoid shear history stored in. From these measurements were obtained flow curves whose experimental values can be fitted to constitutive models that describe the rheological properties of waxy crude oil. The flow curves were adjusted by the data analysis software of Haake Mars III Rheometer, evaluating two rheological models: Cross and Herschel –Bulkley models.

3.2.2.2 Oscillatory Test

Oscillatory tests were performed applying an oscillatory stress amplitude sweep, starting at 1 Pa until 3500 Pa with a frequencies values of 0.5 Hz and 1 Hz; immediately after the cooling sample process, from 60 to $5 \text{ }^{\circ}\text{C}$ with a cooling rate of $1 \text{ }^{\circ}\text{C}/\text{min}$.

This shear stress sweeping is an important step in the sequence of rheological studies, because it allows verifying regions of elastic response, creep, fracture and shear thinning in the yielding process or gel breakage.

3.2.2.3 Gelation Temperature

The rheological measurement used to determine the gelation temperature was oscillatory test during a cooling process with an initial temperature of 60 °C to 5°C, using a cooling rate of 1 °C/min.

Once it was identified the region where the gel formed presents elastic response as a function of the shear stress, from the oscillatory stress amplitude sweep. A shear stress amplitude was chosen from the linear region (elastic response from oscillatory test of above section), in order to ensure that the gel preserves its elastics features without suffering any change in its structure. In this particular case, the stress amplitude used was 1 Pa and a low frequency was fixed in 0.5 Hz. The measurements were done in triplicate.

3.2.2.4 Gel behavior by Oscillatory Test

Oscillatory tests were performed in order to evaluate the response of the storage and loss moduli during frequency sweep (0 to 100 Hz) under a small stress amplitude (1 Pa) to ensure that the gel kept in the region of the elastic response (linear region defined from preliminary oscillatory test).

After of pretreatment protocol for rheological measurements, the oil sample were cooled to 5 °C with a rate of 1 °C/min. Once the oil sample reach the test temperature, it was kept in this temperature during four different aging times: 0, 1, 5 and 24 hours, to evaluate the influence of aging time in the gel structuring over a wide pulsation range.

3.2.2.5 Yield Stress

Yield stress value was determined using two rheological methods, the first one is called oscillatory stress amplitude sweep under a low frequency and the second one the strain-controlled measurements. The results of the yield stress measurements were compared with the experiments in the horizontal loop.

Oscillatory Stress for Yield Stress Determination -Controlled Shear Stress

Static tests were performed by applying an oscillatory stress amplitude sweep, starting at 1 Pa to 3500 Pa with a frequency of 0.5 Hz; after cooling sample process from 60 to

5 °C with a cooling rate of 1 °C/min, assessing four aging time (0, 1, 5 and 24 hours) with the oil sample kept at 5 °C.

Start-Up Measurements for Yield Stress Determination – Controlled Shear Rate

After a cooling process of the sample from 60 to 5 °C at a cooling rate of 1 °C/min, with the oil sample kept at 5 °C, aging time of 0, 1, 5 and 24 hours were evaluated. The dynamic tests were performed applying constant shear rates of 0.0001; 0.001; 0.01; 0.1 and 1 s⁻¹, during 30 minutes.

3.2.2.6 Thixotropy

The thixotropic behavior of the waxy crude oil was evaluated using two different techniques. The hysteresis loop technique and start-up experiments.

Hysteresis loop test

The hysteresis loop tests were carried out to evaluate the changes in the viscosity and the shear stress resulting from the shear rate sweep from 0 to 100 s⁻¹, and 100 to 0 s⁻¹ range that was applied immediately after the increased stage. Each stage, increased and subsequently decreased was measured during 1 minute.

A second range of shear rate in the hysteresis technique was evaluated, varying the shear rate from 0 to 1000 s⁻¹ in the first stage of the assessment, and just immediately the decrease stage from 1000 to 0 s⁻¹. Each stage was performed with a duration time of 1, 3 and 5 minutes, in order to evaluate the influence of time of shearing over the hysteresis loop characteristic of the waxy crude oil.

Start-up Experiments

A constant shear rate of 0.0001; 0.001; 0.01; 0.1 and 1 s⁻¹ was imposed on the oil sample during 30 minutes, after a cooling process from 60 to 5 °C at a cooling rate of 1 °C/min with the oil sample kept at 5 °C, aging times of 0, 1, 5 and 24 hours were evaluated

3.2.3 RESTART EXPERIMENT IN THE HORIZONTAL LOOP

The problem of restart of gelled lines related to the yield stress of the waxy crude oil after cooling under quiescent conditions was studied in order to confirm the findings achieved through the tests performed on the rheometer.

Figure 14 shows a schematic diagram of the restart experiments components: two heated tanks, a cold bath, a pipeline and the pressurization system.

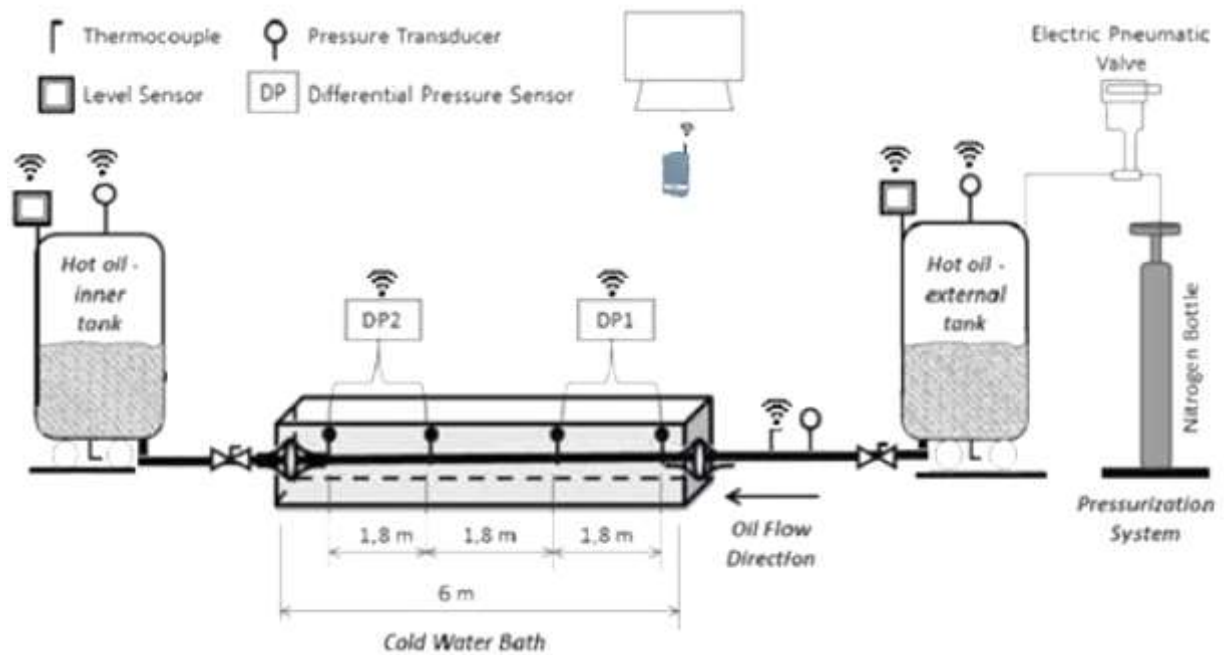


Figure 14. Schematic diagram of apparatus for the restart experiments (Geest, 2015).

Therefore, the experimental study of restart of a production line blocked with gelled waxy crude oil was carried out in a copper tubing of 1 inch diameter and 6 meters long of test section which is immersed in a water bath.

The water bath has two differential pressure gauge, the first one (DP1) is placed in the entrance and the second (DP2) is situated at the end of the test section. These sensors operate with wireless transmission.

The inner and external tanks (Figure 15 and Figure 17) have the same features: volume of 50 liters where the waxy crude oil is storage. They remained mechanically agitated and heated to 60 °C during the experiments in order to ensure a good homogenization of the waxy crude oil and the effective dissolution of all paraffin content in the crude oil.

The pressurization system consists of two nitrogen tanks, the first one whose function is to apply pressure to the waxy crude placed in the external tank, and the second nitrogen tank is a stock, in order to ensure the supply of nitrogen to the pressurization system (Figure 18). There is an electric pneumatic valve BR240S, that connects the nitrogen tank and the external tank.

3.2.3.1 Test Protocol for Restart Experiments

Before any testing oil samples was stored in the inner tank (Figure 15) for 2 hours at 60 °C under stirring. In this stage, the paraffin was dissolved in the oil. At the same time, the temperature of the water bath (Figure 16) was maintained at 55 °C, heating the test section.



Figure 15. Inner tank of horizontal flow loop.



Figure 16. Test section in the water bath.

To start the procedure, all valves that connect the inner tank, the test section and the external tank were opened, and the horizontal pipeline was filled with the waxy crude oil until achieve the same level in the both tanks. The tanks were open to atmosphere during the filling procedure; the temperature of the water bath was decreased to 5 °C. When the oil temperature in the test section reached approximately 5 °C, gelled waxy crude oil was aged for 1, 5 or 24 hours to check if the pressure required to restart the flow in the pipeline increase with the aging time. After aging the gel, the pressurization system was switched-on, initiating the restart test.

Time of pressure application was taken into account in the restart tests. The pressure was kept constant for 30 minutes after each increment. Initially, the tanks are at atmospheric pressure, then the pressure was increased using a nitrogen cylinder coupled to the external tank (Figure 18), to about 0.1 bar, maintained it during 30 minutes. The restart flow was verified after each pressure increased through the sensors responses in the LABVIEW panel (Figure 19) for monitor the experiments.



Figure 17. External tank of horizontal flow loop.



Figure 18. Pressurization system for restart experiments.

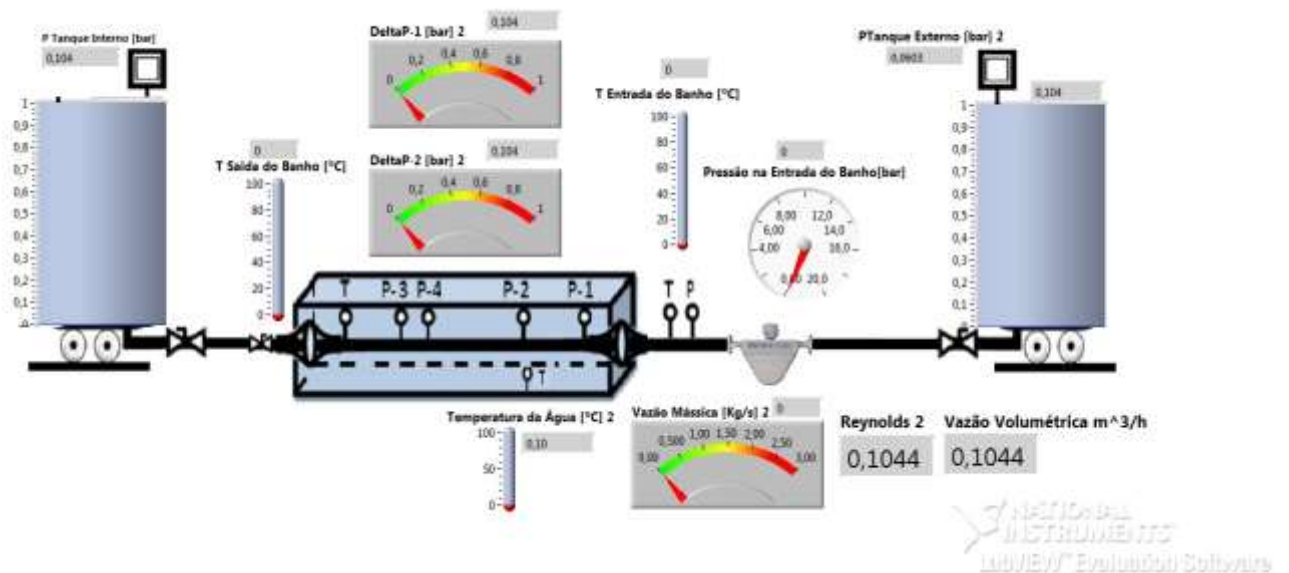


Figure 19. Labview panel for monitoring the restart experiments.

4. RESULTS AND DISCUSSION

In this section, it will be presented, analyzed and discussed the results of the physicochemical and rheological characterization performed for a Brazilian waxy crude oil, plus experiments of the restart of gelled pipeline. The analysis of the results aims to find a relationship between full characterization of a waxy crude oil and the pilot scale experiments results, to determine the pressure needed to restart a gelled pipeline with this particular waxy crude oil.

4.1 CHARACTERIZATION OF THE CRUDE OIL

4.1.1 ASPHALTEN AND RESIN CONTENTS

Asphaltenes and resins content were determined for the waxy crude oil studied in accordance with the ASTM D6560 e ASTM D2007 standard test methods, respectively. The results are presented in the Table 2.

Table 2. Asphaltenes and resins content for the waxy crude oil.

% Asphaltenes	2.5
% Resins	5.1

It is important to determine the content of resins and asphaltenes in the crude oil to discard deposition problems due to these constituents. Asphaltenes and resins are oil constituents that also can precipitate and form solid deposits in production lines. The main difference between resins and asphaltenes is the solubility of these constituent in heptane. Resins are miscible with heptane, and asphaltenes are insoluble in an excess of heptane. However, resins and asphaltenes are very similar in their structure, though the resins have a lower molecular weight compared with asphaltenes, <1000 g/mole (Chamkalani, 2012). Resins tends to associate with the asphaltenes, influencing their solubility in the oil. Thus, Leontaritis and Mansoori (1987) suggested employing the ratio of resins to asphaltenes as an index of asphaltenes stability, based on the hypothesis that resins provide asphaltenes stability by coating or peptizing them.

Thus, the greatest amount of resins found in the crude oil ensures the asphaltenes stabilization, whereby gelation of the crude studied is consequence of gelation of solid deposits of paraffin.

4.1.2 WATER CONTENT – KARL FISHER

The determination of water content in the waxy crude oil studied is presented in the Table 3. Due to the low water content is possible to affirm that it is not enough to form emulsions that modify the rheological behavior of the oil. Therefore, the low water content does not represent any risk in the development and reproducibility of rheological and scale-laboratory experiments.

Table 3. Water content of the waxy crude oil.

Samples	Water Content [%]
Sample 1	0.13
Sample 2	0.13
Sample 3	0.13
Mean	0.13

4.1.3 TOTAL ACID NUMBER (TAN) CONTENT

Table 4 shows the results for the TAN analysis. Total acid number (TAN) for the waxy crude oils was determined by potentiometric titration according to the ASTM D-664 procedure.

Table 4. Total Acid Number (TAN) content of the waxy crude oil.

Samples	mg/g KOH
Sample 1	0.170
Sample 2	0.156
Sample 3	0.165
Mean	0.164 ± 0.005

The acid content is directly related to the presence of naphthenic acids in crude oil. The low total acid number (TAN) in the oil studied indicates that no problems occur due to scale or corrosion, which may cause solid deposition.

4.1.4 CHARACTERIZATION OF n-PARAFFINS FRACTION BY GAS CHROMATOGRAPHY (GC)

Figure 20 shows the n-paraffinic fraction analyzed by gas chromatography (GC). Although the standard test methods used were ASTM D5917-15 and ASTM 7360-11. The visualization was possible approximately to C40, due the column used in the chromatograph had sensitivity to hydrocarbons C8-C40. The mass percentage of each carbon atom of the paraffins of the crude oils can be seen in the Table 5.

Table 5. Mass percentage for some carbon atoms of the n-paraffin of the waxy crude oil.

Carbon Number	%wt	Carbon Number	%wt
C8	8.28	C25	1.04
C9	8.60	C26	1.10
C10	6.60	C27	0.98
C11	7.29	C28	0.97
C12	6.23	C29	0.68
C13	6.82	C30	0.52
C14	4.82	C31	0.38
C15	4.81	C32	0.28
C16	3.63	C33	0.19
C17	3.83	C34	0.15
C18	2.85	C35	0.11
C19	2.72	C36	0.04
C20	2.48	C37	0.05
C21	0.70	C38	0.02
C22	0.88	C39	0.03
C23	0.94	C40	0.02
C24	1.00		

The n-Paraffin fractions of a waxy crude oil correspond to hydrocarbons with carbon chains between C18 and C50. This analysis was carried out with an internal standard, which is

used to determine the concentration of the n-alkanes in the waxy crude oil between C8 and C40. Thus, the mass fraction results between C18 and C 40 were added to find the percentage of n-alkanes, which corresponds to waxes.

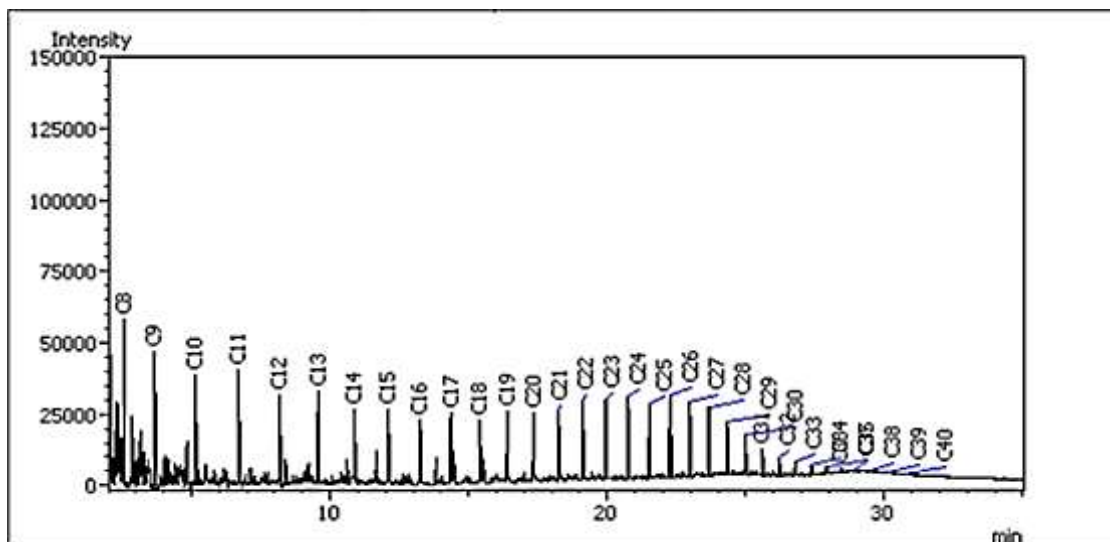


Figure 20. Chromatogram analysis for waxy crude oil.

4.1.5 CHARACTERIZATION OF n-PARAFFINS FRACTION BY HIGH TEMPERATURE SIMULATED DISTILLATION (HSTD)

High-Temperature Simulated Distillation (HSTD) determines the boiling point (BP) distribution crude oils. The gas chromatographic simulation of this BP determination can be observed in the Figure 21.

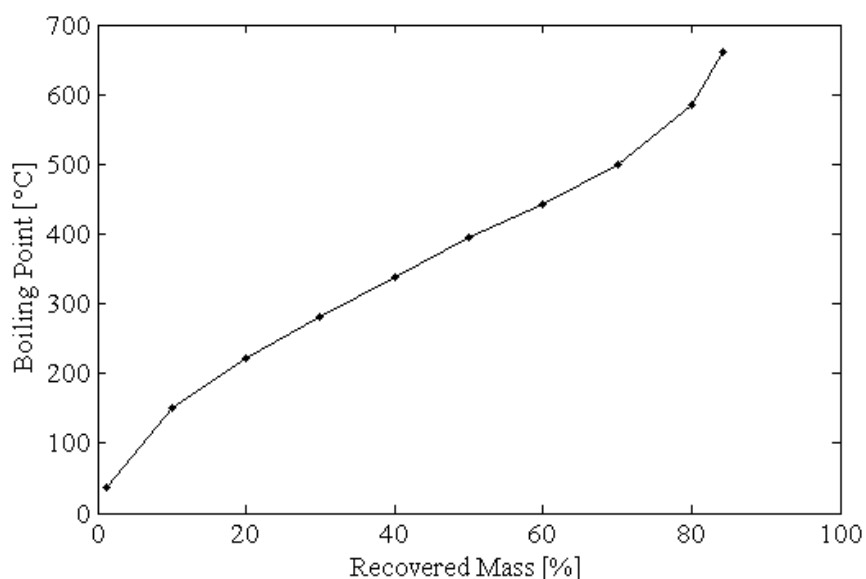


Figure 21. Boiling point versus recovered mass of waxy crude oil.

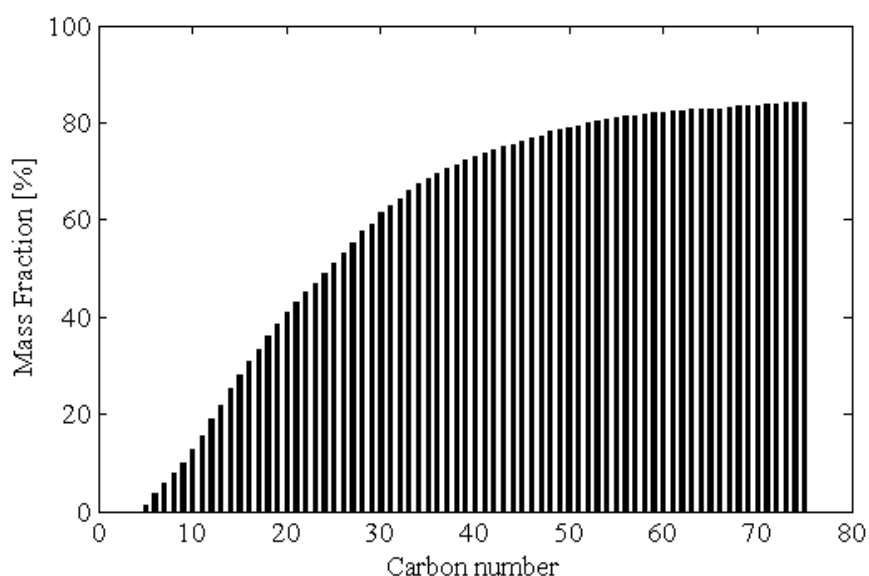


Figure 22. HSTD analysis for waxy crude oil.

The high-temperature simulated distillation (HSTD) analysis (Figure 22) shows a high mass percentage for the hydrocarbons between C18 and C50, confirming the presence of n-alkanes, iso-alkanes and cyclic alkanes in these oils. The presence of light hydrocarbons, which are solvent for the paraffins, was also verified for this oil.

4.1.6 POUR POINT TEMPERATURE

Assays for determining the pour point temperature were performed in triplicate for the waxy crude oil, based on the ASTM D5853 standard test method in quiescent condition. The results are shown in Table 6.

Table 6. Pour point temperature of waxy crude oil.

Oil Samples	Pour Point Temperature (°C)
Sample 1	15
Sample 2	15
Sample 3	18
Mean	16 ± 2

The value of 16 °C is a qualitative measure, which indicates the no-flow condition for the waxy crude oil studied. At temperatures below of this value, a significant amount of wax is precipitated resulting in the increase of gel strength. The cooled of waxy crude oil at temperatures equal or less than the pour point under static conditions, promote the strength of

this crystal networks in conditions where planned or unplanned shutdown occurs at ambient temperature below the pour point. Therefore, it is important to define prevention strategies in order to avoid that the waxy crude oil into the pipeline reaches the pour point temperature.

4.1.7 DENSITY

Density measurements were performed for the waxy crude oil as it was received. The data are shown in Table 7. Density values were determinate for 60, 50, 40, 30, 20, 15.56 (60 °F), 10, 5 and 4 °C. The results are also presented in the Figure 23.

The measurement obtained at 15.56 °C was used to calculate de API gravity in order to classify the waxy crude oil studied as a medium oil.

Table 7. Density of waxy crude oil.

Temperature (°C)	Density Sample 1 (g/cm ³)	Density Sample 2 (g/cm ³)	Density Sample 3 (g/cm ³)	Mean Density (g/cm ³)
60	0.83543	0.83464	0.83690	0.83566 ± 0.00083
50	0.84378	0.84382	0.84377	0.84379 ± 0.00002
40	0.85056	0.85055	0.85053	0.85055 ± 0.00001
30	0.85761	0.85765	0.85767	0.85764 ± 0.00002
20	0.86481	0.86484	0.86484	0.86483 ± 0.00001
15.56	0.86926	0.86948	0.86932	0.86935 ± 0.00008
10	0.87548	0.87520	0.87498	0.87522 ± 0.00017
5	0.87915	0.87917	0.87928	0.87902 ± 0.00005
4	0.88021	0.88019	0.88033	0.88024 ± 0.00006
API gravity			30.94	

API gravity and density measurements are one of the preliminary diagnostic test done at petroleum industry in order to identify problems related to wax precipitation and deposition. This property is not only important to determine the quality of crude oil, also has direct insight into capability of crude oil to inhibit the precipitated waxes. The wax particles suspensions are caused by the difference between gravities of the wax crystals and the crude oil.

Figure 23 shows a linear trend between density and temperature. The same trend was found for waxy crude oils by several authors (Ekaputra 2014 and Kelechukwu 2011).

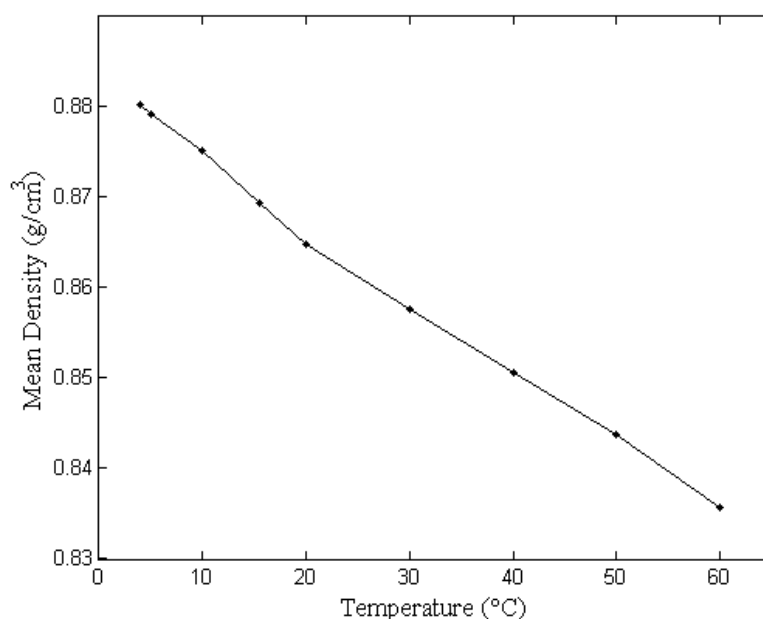


Figure 23. Density versus temperature of waxy crude oil.

4.1.8 DIFFERENTIAL SCANNING CALORIMETRY (DSC)

Figure 24 shows the DSC thermograms for the waxy crude oils studied for two cooling rates (1 and 3 °C/min). It is possible to identify two exothermic peaks corresponding to two crystallization events. From the first peak, at higher temperature, it was obtained the Wax Appearance Temperature (WAT), while the second one corresponds to the second crystallization event. The results are summarized in Table 8.

Table 8. Values from DSC characterization of waxy crude oil.

	1 °C/min		3 °C/min	
	Temperature (°C)	Thermal Effect (J/g)	Temperature (°C)	Thermal Effect (J/g)
1° Exothermic Peak (WAT)	50.02	0.3137	47.58	0.3738
2° Exothermic Peak	26.83	9.212	26.10	9.707

DSC thermograms show the presence of two exothermic peaks in the cooling process of the oil sample. The first peak at high temperatures is smaller than the second; the

values of the thermal effect as well as the temperatures of each peak are presented in the Table 8 for the two cooling rates evaluated.

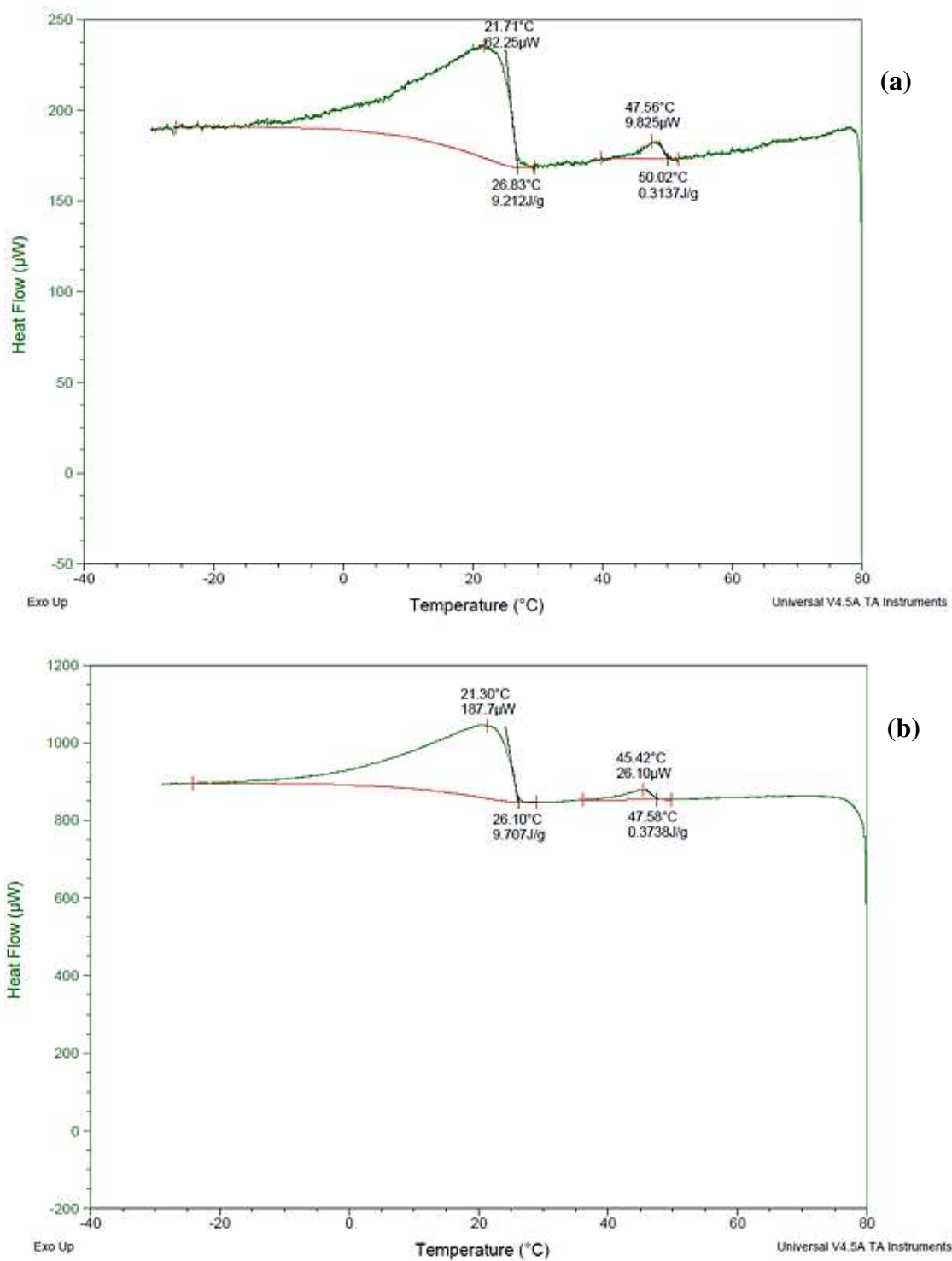


Figure 24. DSC thermograms of waxy crude oil for a cooling rate of 1 °C/min (a) and 3 °C/min (b).

The first peak of the thermogram indicates the WAT, but this peak has a thermal effect smaller, around 30 times, than the second one, which means that there is a higher content of paraffin with low molecular weight whose transition effect between liquid and solid takes place at temperatures below the WAT (around 26 °C). Thus, it was confirmed that there are serious problems in the flow assurance at temperatures lower than 26 °C for the oil under study.

On the other hand, temperature of the exothermic peaks decrease with the increasing cooling rate as other authors found it (Y. Zhao et al., 2014; Oliveira, 2012). It was verified that for a larger cooling rate, lower temperatures were recorded for the two exothermic peaks. This small difference can be associated to the different nucleation and crystallization rate of the paraffins in the oil (Paso *et al.*, 2009)

4.1.9 WAX SOLUBILITY CURVE

Figure 25 shows the wax solubility curve obtained for the waxy oil. The value of concentration of wax precipitated at different temperatures was calculated through the equation (9), using the thermogram data obtained in the previous section.

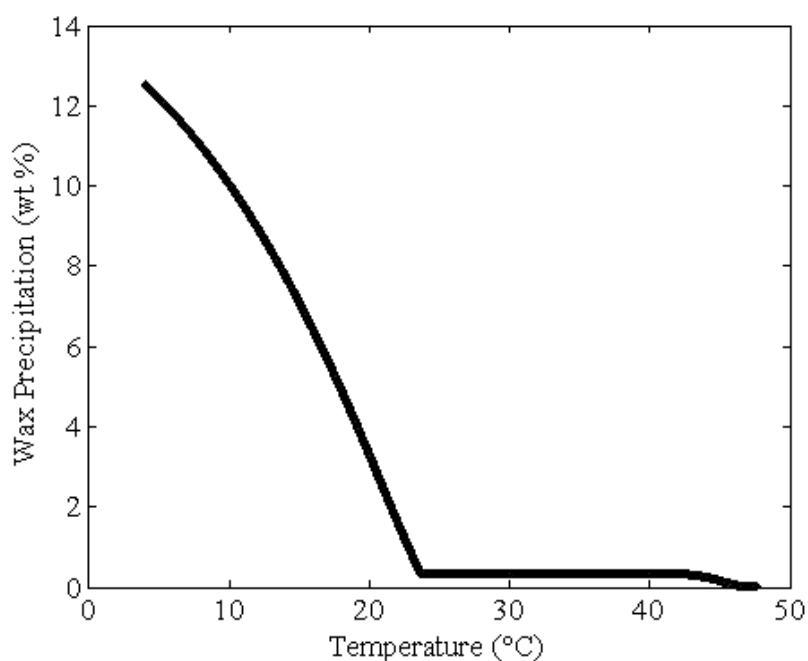


Figure 25. Wax precipitation curve determined by DSC thermogram at cooling rate of 3 °C/min.

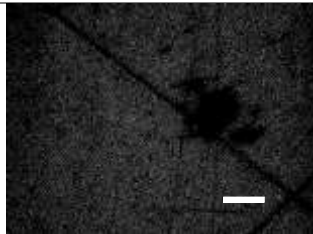
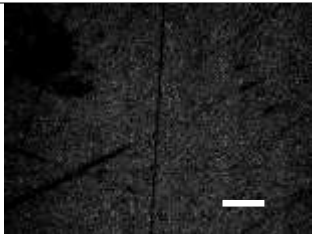
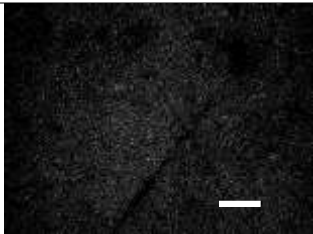
At temperatures above the WAT, it does not exist any wax crystal precipitated, so the value of c_w is zero. At temperatures below the WAT, the concentration of precipitated paraffin increase with the decrease of the temperature.

The solubility curve was calculated using the results obtained in the DSC thermogram at a cooling rate of 3 °C/min. It is possible to identify that at WAT value (50 °C) begins to precipitate a small percentage of paraffins reaching a maximum value of 0.35% at a temperature of 41 °C. This percentage remained constant until reach the temperature corresponding to the second exothermic peak or second crystallization event, which occur at 26 °C where oil sample began to precipitate greater amount of paraffin with the temperature decrease. Thus, the average temperature of the seabed (about 4 °C) is expected to precipitate 12.5% of the total paraffin content in the oil.

4.1.10 RHE-OPTICAL MEASUREMENTS

The wax appearance temperature was also established by using polarized light microscopy. Table 9 shows the WAT and the microstructures of the waxy oil at these temperatures. In the micrographs, the paraffin crystals appear as white particles dispersed in a black isotropic background due to their optical characteristics (Rønningsen and Bjørndal, 1991; Lira-Galeana and Hammami, 2000). The results showed that the WAT was 56.5, 55.3 and 55.1 °C for the three cooling rates evaluated, 0.5, 1.0, 3.0 °C/min, respectively. Similar to observed in DSC method, it was observed a tendency of the WAT decreases with the increase of cooling rate.

Table 9. Effect of cooling rate on the WAT and microstructure of the first wax crystals obtained by rheo-optical experiments. Scale bar = 10 μ m.

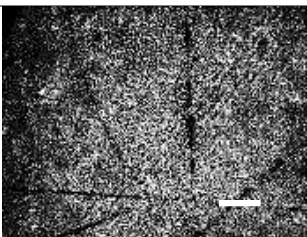
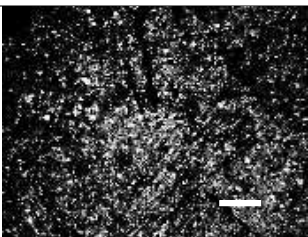
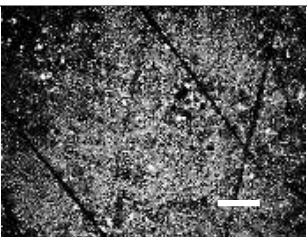
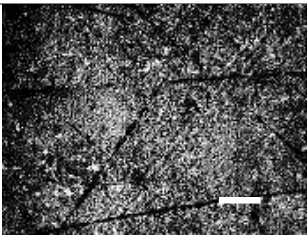
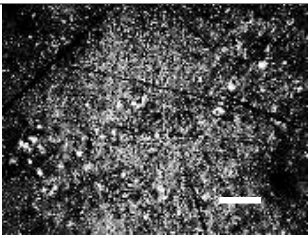
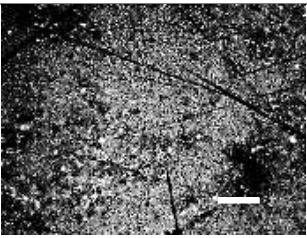
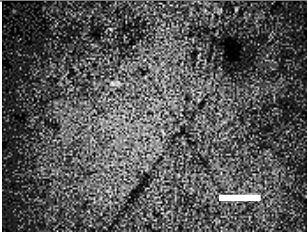
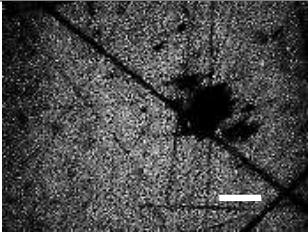
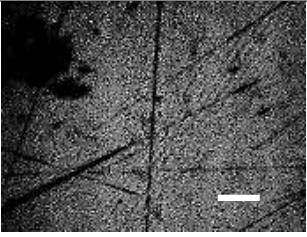
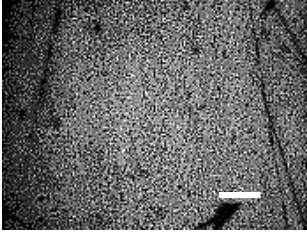
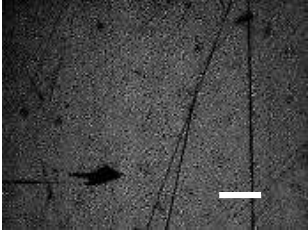
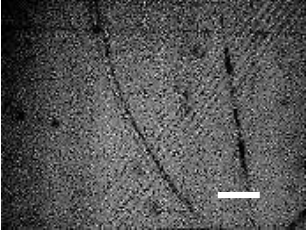
	3.0 °C/min	1.0 °C/min	0.5 °C/min
WAT (°C)	55.1	55.3	56.5
Micrographs			

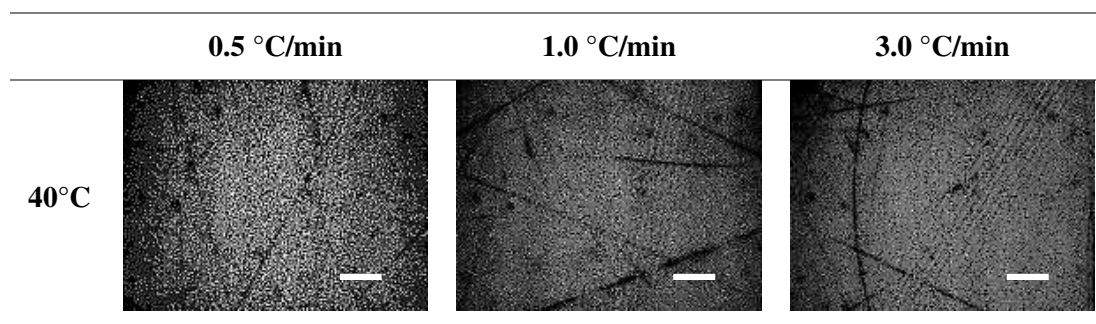
The microscopy provided higher WAT values in comparison with that from DSC, which can be explained by the sensibility of the microscopy analysis to detect the presence of

very small wax crystals in their nucleation stage. Thus, this technique can be considered the most accurate for WAT measurements (Lira-Galeana and Hammami, 2000).

The cross-polarized micrographs of the waxy crude oils during cooling (Table 10) showed that the amount of wax crystals increased with the decrease of temperature. In general, the crystals showed a globular shape, similar to crystals observed by other authors (Rønningsen and Bjørndal, 1991; Venkatesan *et al.*, 2003; Yi and Zhang, 2011), which can be attributed to the presence of asphaltenes in their composition that are responsible for the globular shape. The comparison between the different cooling rates showed that the crystals were bigger as the cooling rate was higher (Table 10), similar to the trend found by Hénaut (1999).

Table 10. Micrographs of waxy crude oils at different temperatures and cooling rates of 0.5, 1.0 and 3.0 °C/min. Scale bar = 10 μ m.

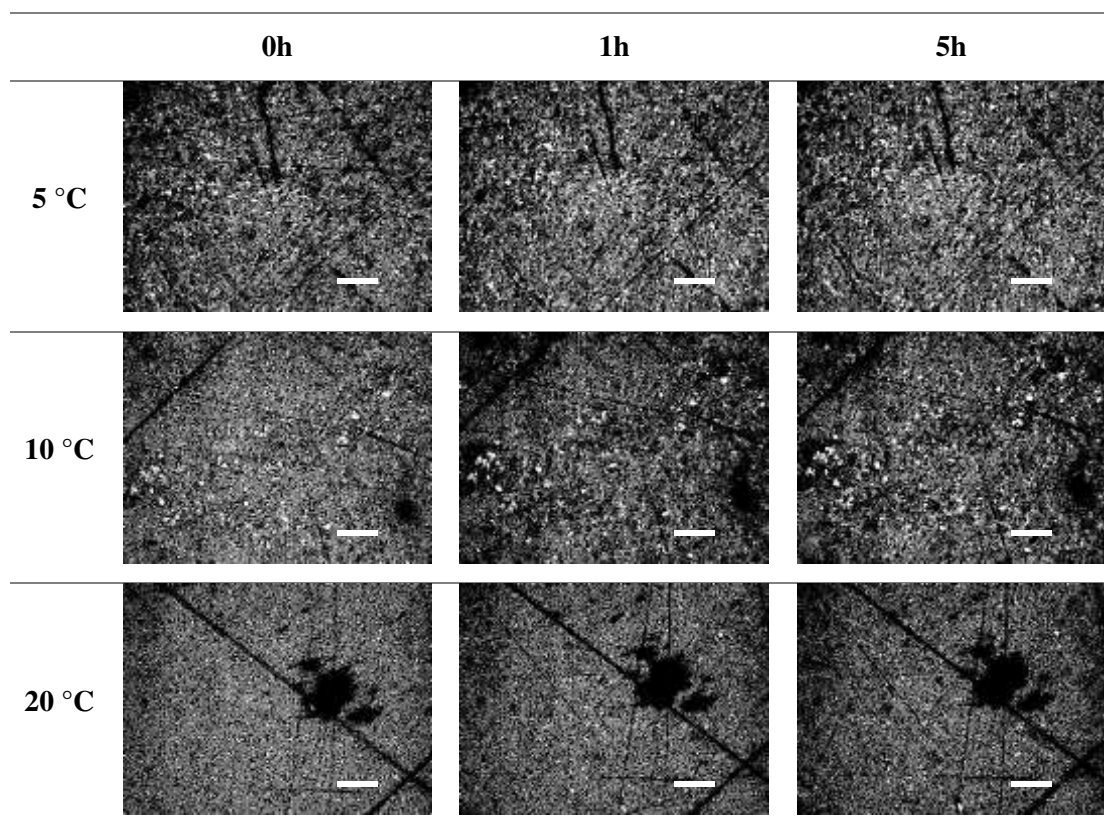
	0.5 °C/min	1.0 °C/min	3.0 °C/min
5 °C			
10 °C			
20 °C			
30 °C			

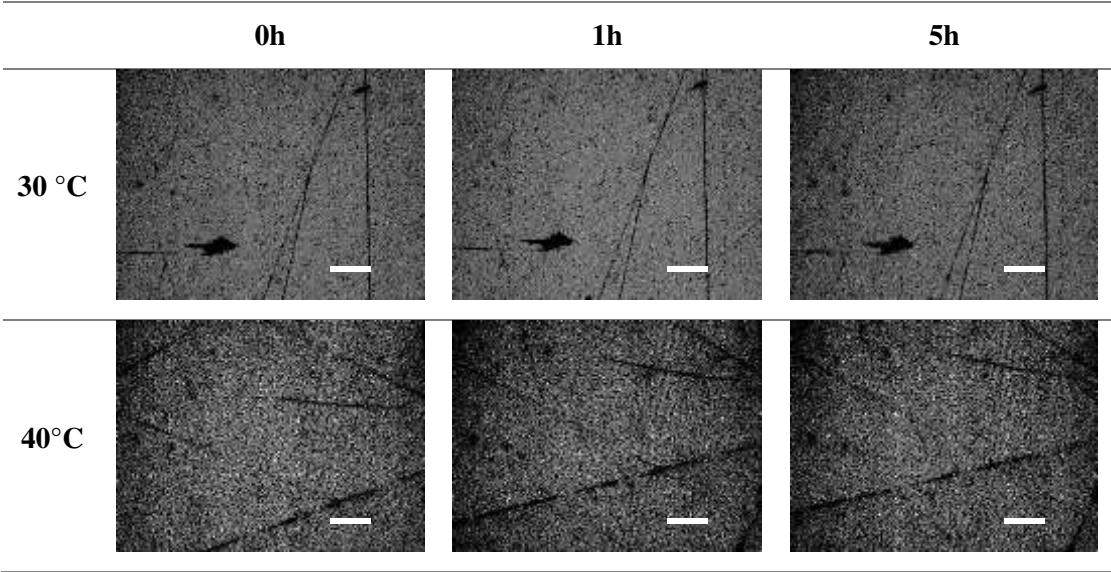


The influence of the aging time over the structure of the gel was studied. The samples of the waxy oil were cooling at specific rate (0.5, 1.0 and 3.0 °C/min), up to different final temperatures (5, 10, 20, 30 and 40 °C).

The micrographs of the oil samples are shown in the Table 11. In these images are possible to observe the increase of the amount of paraffin crystals with the aging time, at constant temperatures below the WAT. On the other hand, the amount of crystals increased with the decrease in the final temperature in the cooling process, at the same cooling rate.

Table 11. Micrographs of Waxy Crude Oil at different temperatures with a cooling rate of 1°C/min and aging time of 0h, 1h and 5h. Scale bar = 10 μ m.





4.2 RHEOLOGICAL CHARACTERIZATION MEASUREMENTS

4.2.1 VISCOSITY AND FLOW CURVES

The effect of temperatures on the viscosity of the waxy crude oil was verified by rheological measurements at a fixed shear rate of 1 s^{-1} , this low value of the shear rate does not delay the appearance of crystals. Figure 26 shows the measured viscosity as a function of the inverse temperature.

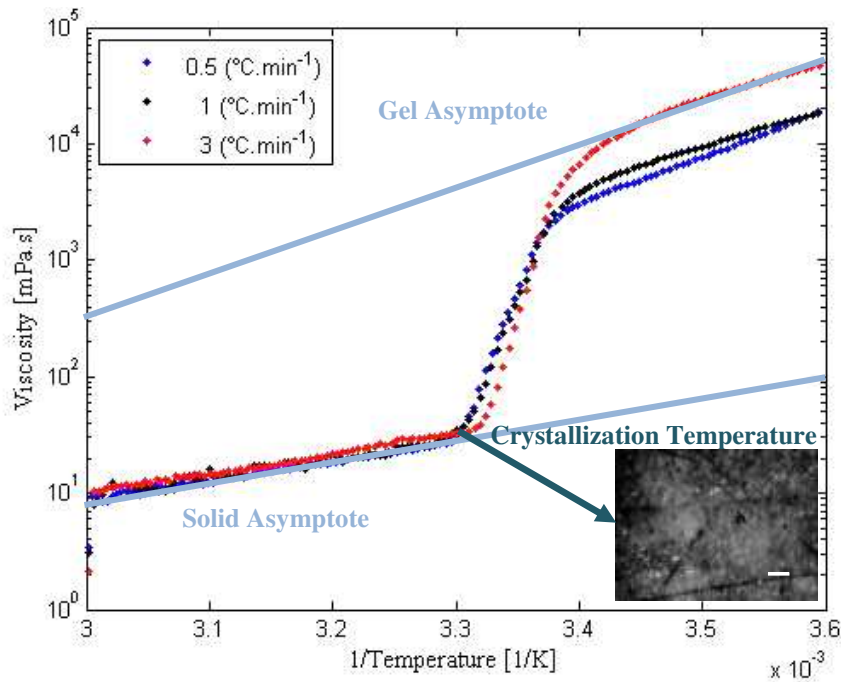


Figure 26. Rheological measurements for waxy crude oil at shear rate of 1 s^{-1} and cooling rates of 0.5, 1.0 and 3.0 °C/min. Scale bar = 10 μm .

The evaluation of the viscosity versus temperature curve showed three distinct regions and each one can be appropriately fitted by the Arrhenius equation:

$$\eta = Ae^{(Ea/RT)} \quad (10)$$

The first region corresponds to temperatures above the WAT, where the oil has a Newtonian behavior, it has drawn the solid asymptote which slope corresponds to the value of (Ea/RT) , thus was calculated the activation energy of waxy crude oil evaluated at cooling rate of 3 °C/min, $E_{sol} = 63974$ J/mol (at first region). When the temperature decreased, it was observed a point that the slope curve exhibited a sharp increase and the second region was started. This point have been considered as crystallization temperature (Table 12), where a significant amount of wax crystals increasingly precipitates and start to interact (Marchesini *et al.*, 2012). In the second region of the curve (Figure 26), a sharp rise in the viscosity due to the formation of higher amount of crystals and the increase of crystals length, contributing to the development of a gel-like structure. Finally, in the third region there was a more accentuated increase of the viscosity compared with the first region. In this case, as the oil was cooled under shear, there was a tendency of the gel structure to break while it was formed simultaneously (Visintin, 2005). For the third region was also calculated the slope of the gel asymptote. In the same way that was calculated the activation energy for the gel asymptote, was obtained the $E_{gel} = 32409$ J/mol. The E_{sol} is around two times higher than the E_{gel} . These values are in agreement with those reported in the literature for crude oils (Rønningsen 1991; Visintin, 2005; Alcazar-Vara, 2011). Table 12 shows the mean results calculated from the values obtained from the oscillatory measurements made in triplicate.

Table 12. Crystallization temperature of waxy crude oil at different cooling rates.

Cooling Rate (°C/min)	Crystallization Temperature (°C)
0.5	30.17 ± 0.00
1.0	29.77 ± 0.27
3.0	28.23 ± 0.46

The values of crystallization temperature obtained by rheological measurements were much smaller than WAT (first peak) obtained by DSC (Table 8) and microscopy (Table 9) and were higher than the pour point measurements (Table 6). Thus, this crystallization

temperature obtained by viscosity measurements adjusted by the Arrhenius equation can be associated with the gelation temperature, where a certain volume of precipitated wax material is necessary to develop an interlocking network, modifying the rheological properties of the waxy crude oil.

Other rheological tests were performed with controlled shear rate in the rotational method. The flow curves are shown in the Figure 27, and they represent the variation of the shear stress as a function of the shear rate under constant temperature. Waxy oil shows a strong change in its Newtonian behavior at temperatures below 30 °C, showing large variations of shear stress between 0 and 160 Pa, during the same shear rate variation (10 s^{-1} to 250 s^{-1}).

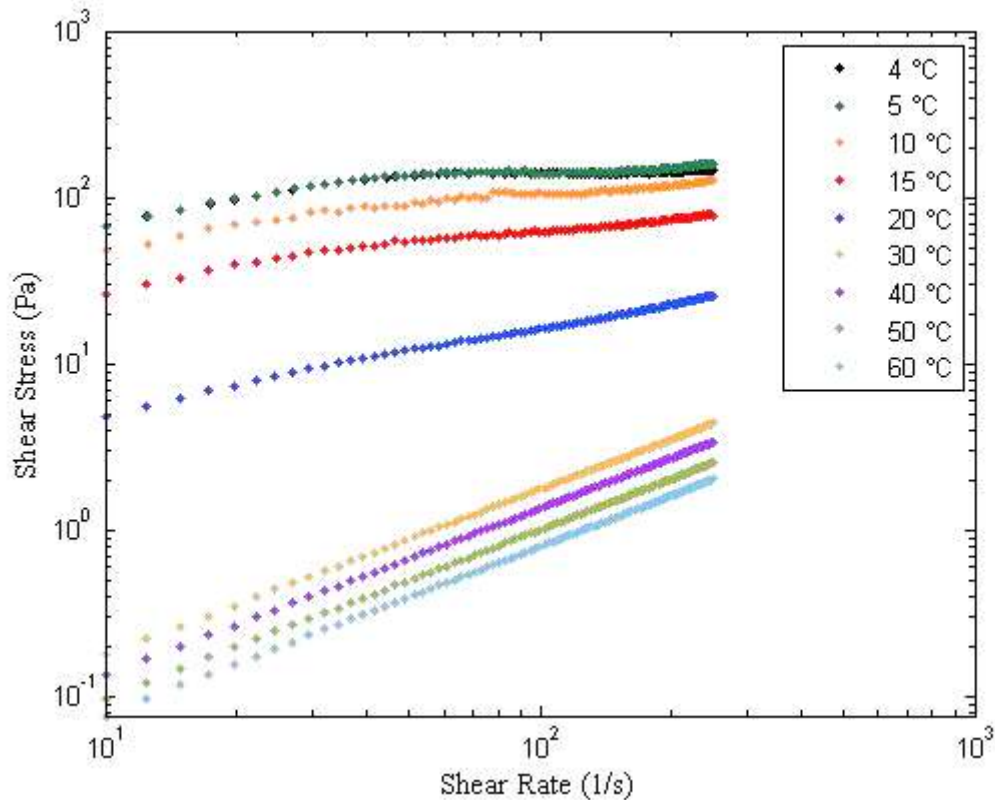


Figure 27. Flow curve of waxy crude oil at different temperatures.

It was possible to adjust the behavior of each curve at different temperatures to a rheological model as shown in the Figure 28 and Table 14. Figure 28a shows the flow curves that presents a Newtonian behavior which corresponds to 60, 50, 40, and 30 °C; Figure 28b presents the flow curves that corresponds to Non-Newtonian behavior (20, 15, 10, 5 and 4 °C).

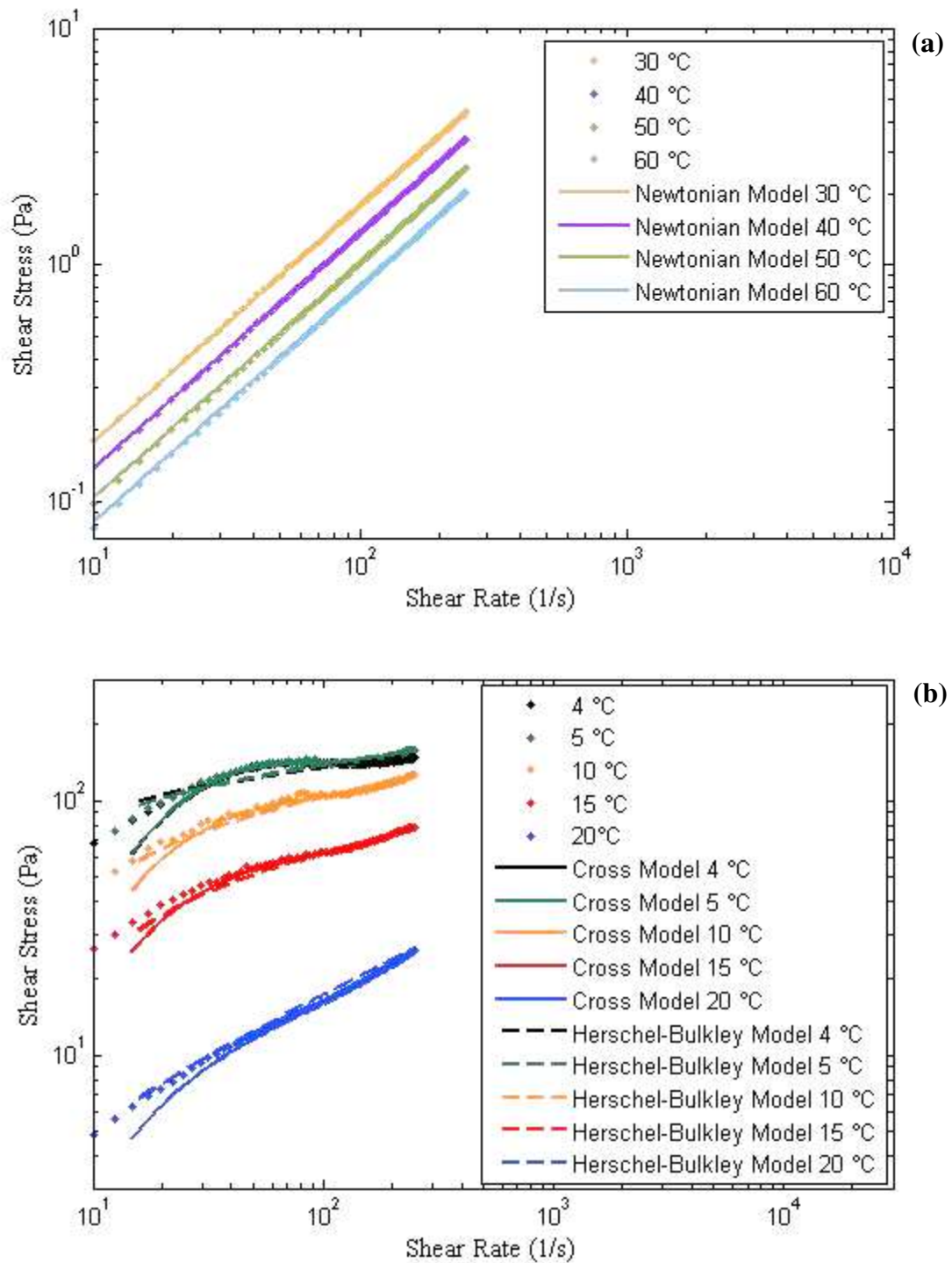


Figure 28. Flow curves adjusted to the rheological models: Newtonian behavior (a) and non-Newtonian behavior (b).

For the flow curves, which present a Newtonian behavior, the data results were fitted and the parameters are presented in the Table 13. Shear stress varies proportionally with the shear rate multiplied by a constant, which corresponds to the value of viscosity. This viscosity increased with the decreasing temperature.

Table 13. Fitted parameters for the flow curves with Newtonian behavior.

Temperature (°C)	η (Pa s)	Correlation Coefficient r
60	0.008075	0.9999
50	0.01017	1
40	0.01357	0.9999
30	0.01763	1

In order to describe the rheological behavior of Non-Newtonian flow curves, two rheological models were considered, Cross and Herschel-Bulkley models.

Table 14. Parameters of the Cross model for the waxy crude oil.

Temperature (°C)	η_0 (Pa s)	η_∞ (Pa s)	$\dot{\gamma}_b$ (s ⁻¹)	n	Correlation Coefficient r
20	0.6051	0.06396	26.63	1.137	0.9999
15	3.254	0.1592	25.91	1.287	0.9999
10	5.713	0.2195	25.84	1.283	0.9942
5	7.054	0.3398	33.92	1.538	0.9952
4	7.326	0.2257	32.27	1.43	0.9968

Cross model adjusted the whole data range including the zero-shear rate viscosity (η_0), the shear thinning region and the constant infinite shear viscosity (η_∞).

Flow curves fitted using the Cross model presented a good adjust, with correlation coefficient values approximately equal to 1. The zero shear and high shear rate increased with the decreasing of the temperature (Table 14).

The dynamic yield stress can be determined from Cross model using the next expression: $\tau_0 \sim (\eta_0 \times \dot{\gamma}_b)$.

Table 15. Dynamic yield stress values by Cross model fitted.

Temperature (°C)	τ_0 (Pa)
20	16.11
15	84.31

Temperature (°C)	τ_0 (Pa)
10	147.62
5	239.27
4	236.41

This dynamic yield stress is an engineering design parameter that indicates the minimum stress required to maintain the flow, after the gel structure was broken and the flow was initiated.

Other common rheological model used to describe the waxy crude oil at temperatures below its gelation temperature is the Herschel–Bulkley model.

Table 16. Parameters of the Herschel–Bulkley model for the waxy crude oil.

Temperature (°C)	τ_0 (Pa)	K	n	Correlation Coefficient r
20	7.772	0.1846	0.8296	0.9999
15	50.77	0.1037	1.018	0.9969
10	98.03	0.003461	1.634	0.9819
5	139.9	5.418e-7	3.129	0.9721
4	139.6	6.475e-10	4.194	0.9334

Figure 29 shows the adjusted of two models evaluated. The Herschel-Bulkley model did not present a good adjust to the experimental values obtained by measurements at rheometer at 4 and 5 °C (Figure 29a), but the Cross model presented good adjustment to these lower temperatures and for the 20, 15 and 10 °C too, which also presents Non-Newtonian behavior. The adjusted curve with Herschel-Bulkley model presented a good agreement just for temperatures of 20, 15 and 10° C. Thus, it is recommended the use of Cross model to describe the rheological behavior for waxy crude oils below its gelation temperature.

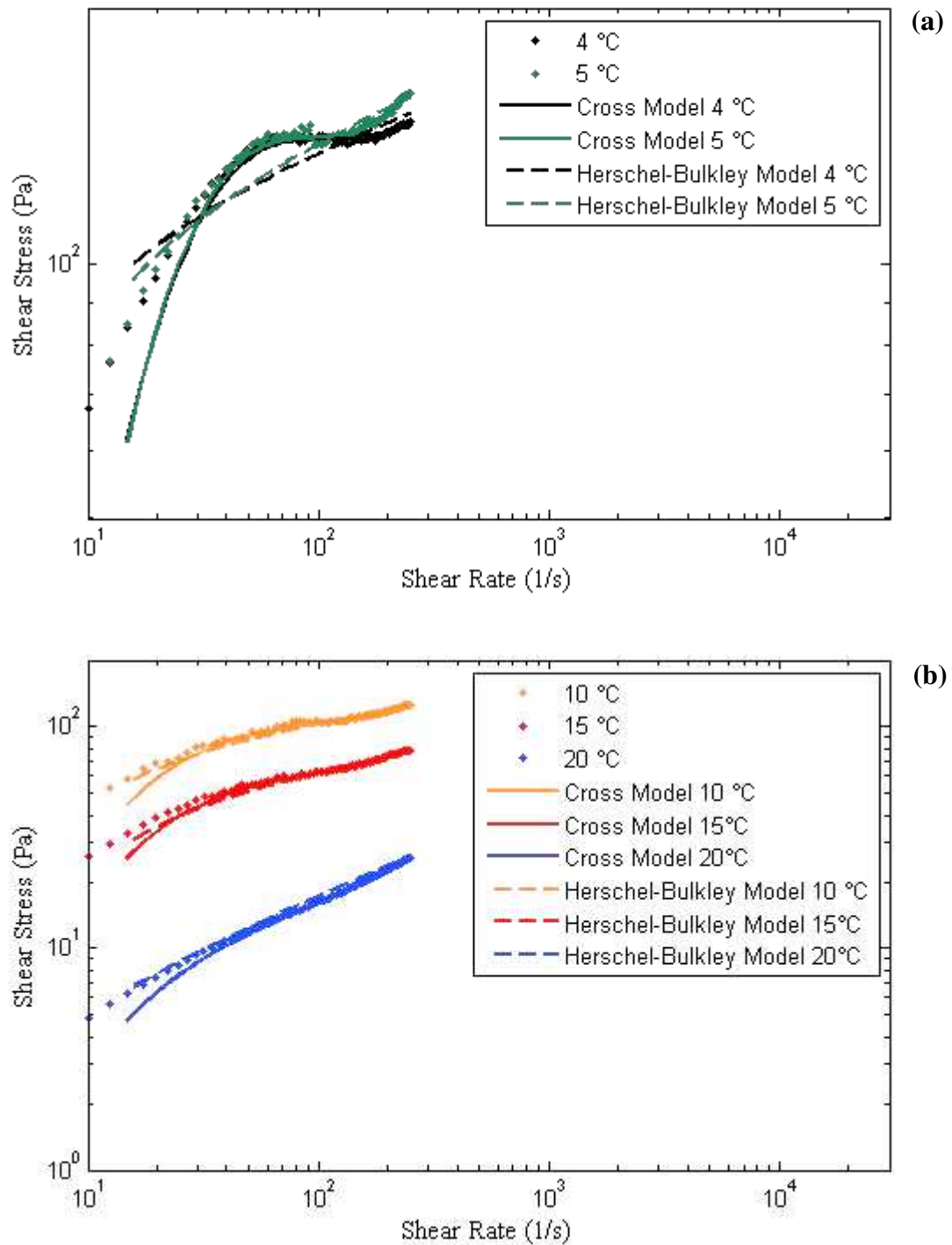


Figure 29. Flow curves adjusted to the rheological models for non-Newtonian behavior: 4 and 5 °C (a), 10, 15 and 20 °C (b).

Figure 30 shows curves of viscosity as a function of shear rates at different temperatures. It was observed that at higher temperatures (30 to 70 °C), the viscosity behavior is independent of the shear rate applied. For the lower temperatures (4 to 20 °C), the viscosity

decrease with the increasing shear rate. The viscosity also increases with decreasing temperature at any shear rate value.

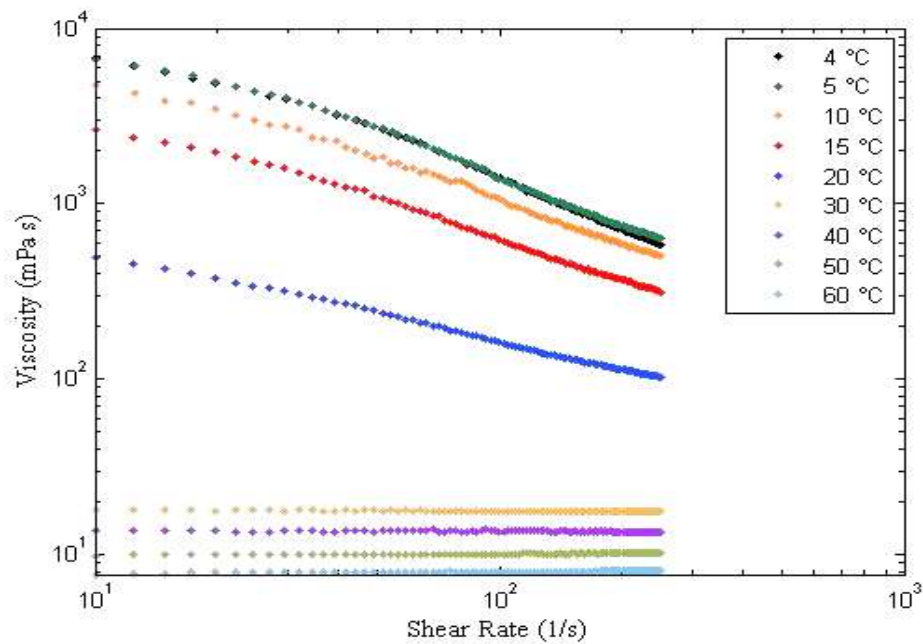


Figure 30. Viscosity versus shear rate at constant temperatures.

Viscosity of the waxy crude oil under different shear rates (10, 20, 50, 80, 120 and 250 s^{-1}) is presented in the Figure 31. It is possible to notice that the viscosity decreases with the increasing temperature until reach a temperature where the behavior of viscosity is independent of the shear rate applied, in this case at 30°C . Viscosity keeps constant with the variation of the shear rate for temperatures above 30°C .

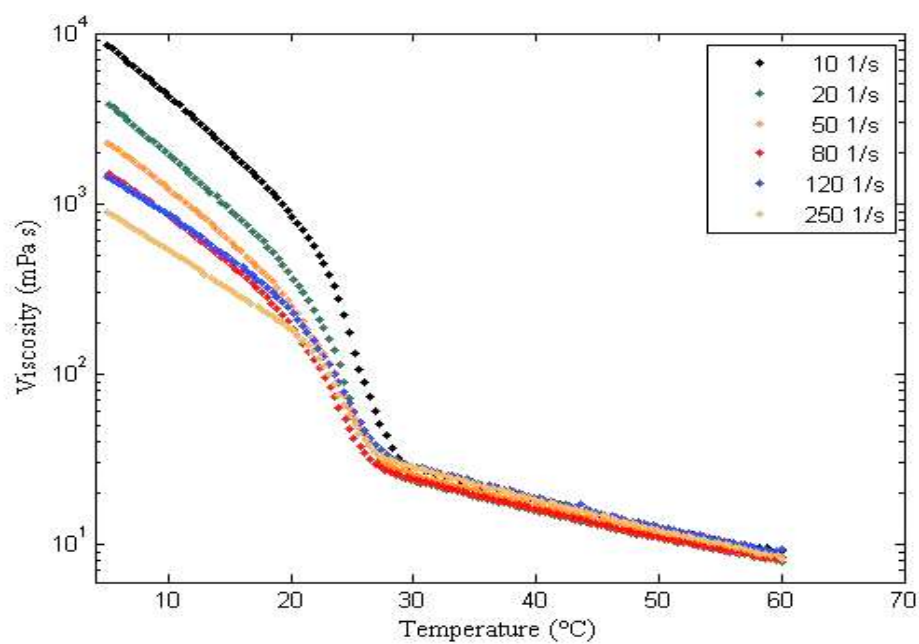


Figure 31. Viscosity of waxy crude oil under different shear rates.

4.2.2 OSCILLATORY TESTS

Oscillatory tests were performed as a preliminary rheological test, that allow identify the different region in the wax crystal structuration. In this rheological measurement, the oscillation amplitude was increased linearly from 0.001 to 3500 Pa to capture all the yielding process of the gel when it keeps at 5°C under a fixed low frequency (0.5 Hz and 1 Hz).

Figure 32 shows the variation of the storage (G') and the loss moduli (G'') as a function of the shear stress sweep. It is possible to recognize a first linear region, which corresponds to the elastic response of the gel at low values of shear stress (between 1 and 190 Pa). In this region, G' and G'' keep on a constant value until the point A, this responses indicate that the interlocking waxy network formed was not destroyed when the shear stress was inferior to 190 Pa. When the stress amplitude exceeds 190 Pa, G' and G'' decrease gradually with the increasing stress, that corresponds to the creep response that represent a partial damage of the crystal wax structure. The point B, where G' and G'' have the same value, it is called fracture point. After point B is identified G' becomes lower than the G'' , that means the change of solid-like behavior of the oil sample to liquid-like. For shear stress values above the point C, the structure of the gel network is completely destroyed (Chang and Boger, 1998 and 2000).

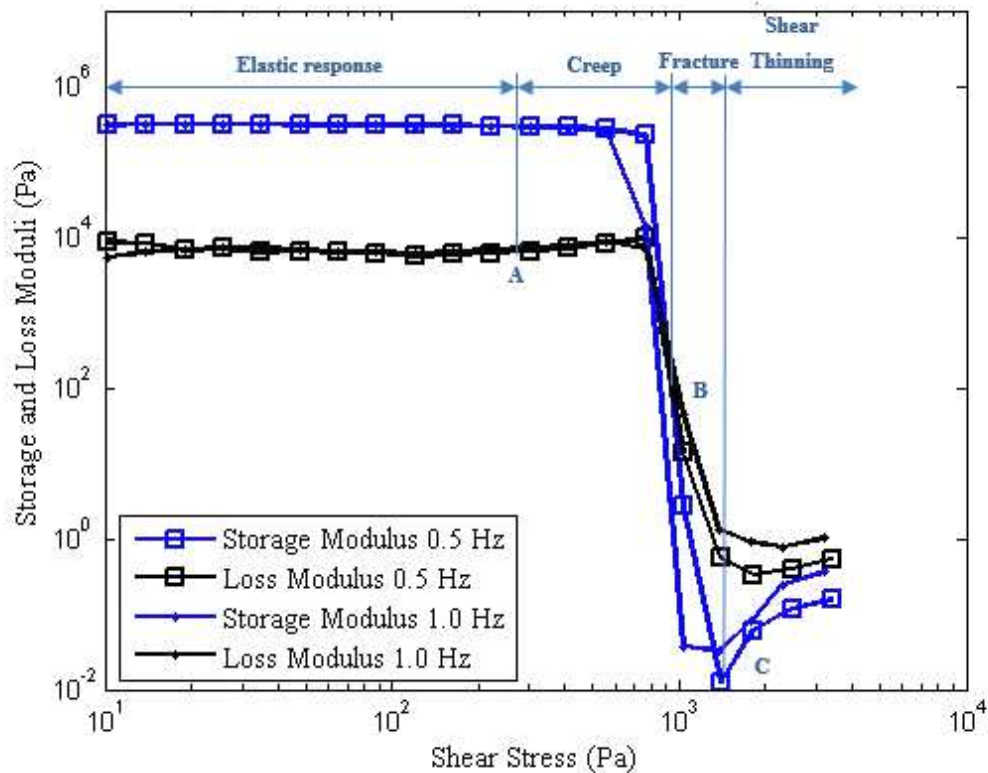


Figure 32. Oscillatory test for waxy oil at 5°C under 0.5 and 1.0 Hz without aging.

Two different frequencies were evaluated, 0.5 Hz and 1.0 Hz to assess its effect on the yielding process. It is shown in Figure 32 that the measurements at the two different values of frequencies result in the similar values for the G' and G'' responses. Thus, for the two frequencies evaluated the region boundaries point are independent of the time scale used in the oscillatory test, because the transition points between elastic response and creep, creep and fracture, occur at the same shear stress values.

4.2.3 GELATION TEMPERATURE

Oscillatory rheological measurements during the cooling of the waxy crude oils were used to determine the gelation temperature. Figure 33 shows the storage (G') and loss (G'') moduli of the waxy crude oil as a function of temperature. The results were obtained within the linear viscoelastic region of samples (with no structural damage), fixing the stress amplitude at 1 Pa under 0.5 Hz. At high temperatures, the loss modulus (G'') was higher than the storage modulus (G'). However, the decrease of temperature led to the increase of both viscoelastic moduli. Below certain temperature, the elastic behavior predominates on the viscous character due to the crystallization of paraffins, confirming the structural transition to the gel state (Visintin *et al.*, 2005). The temperature where G' is equal to G'' (G' - G'' crossover) is considered the gelation temperature (Figure 33, Figure 34 and Figure 35).

Table 17 shows the mean values of gelation temperature for the waxy crude oil evaluated at different cooling rates, these measurements were done in triplicate. The gelation temperature was almost identical, just 1 °C of difference between cooling rates evaluated. The higher value of gelation temperature was verified for the slower cooling rate (0.5 °C/min), which can be explained by the favoring of the formation and aggregation of paraffin crystals at longer times of cooling (Chang *et al.*, 2000; Visintin *et al.*, 2005). Thus, the slower the cooling rate, the higher is the storage modulus (G'), resulting in a displacement of the crossover to a higher temperature.

Table 17. Gelation temperature of the waxy crude oils at different cooling by oscillatory test.

Gelation Temperature (°C)	
0.5 °C/min	25.52 ± 0.93
1.0 °C/min	23.13 ± 0.17
3.0 °C/min	22.79 ± 0.03

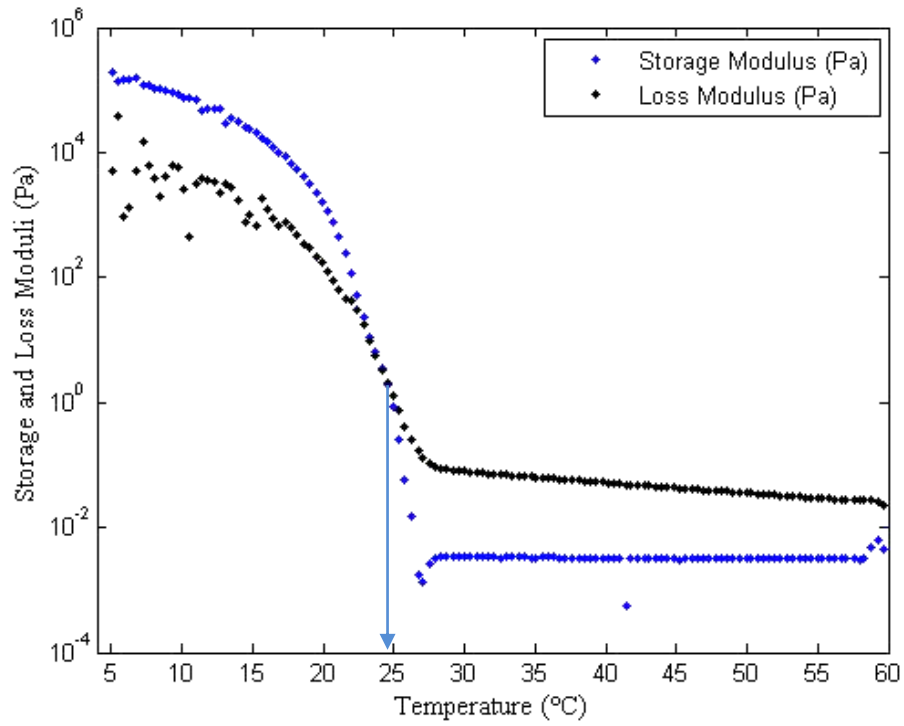


Figure 33. Typical behavior of G' and G'' versus temperature for determination of gelation temperature obtained at cooling rate of 0.5 $^{\circ}\text{C}/\text{min}$.

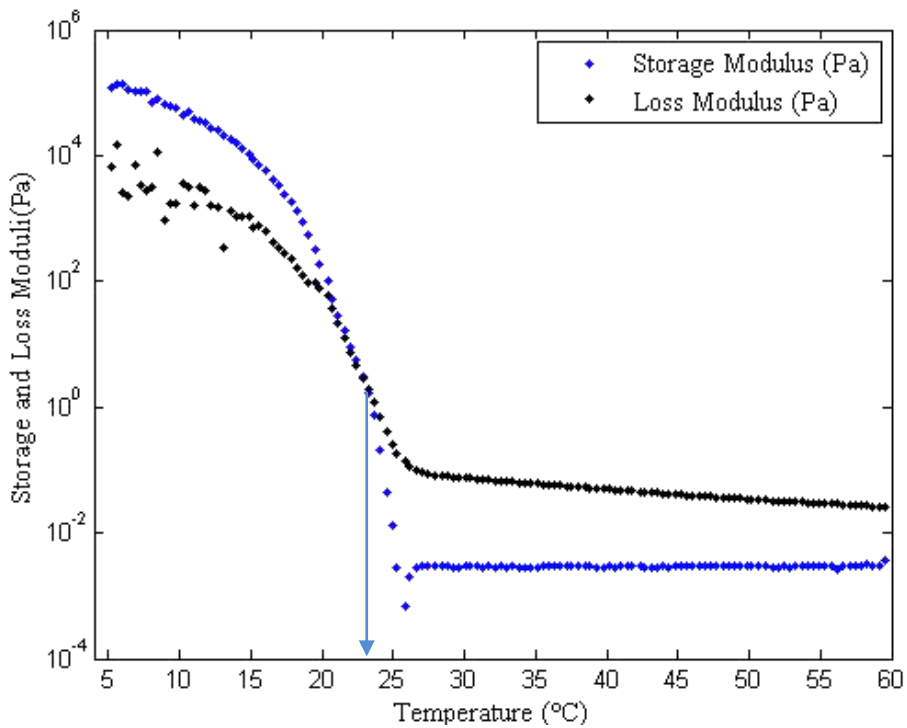


Figure 34. Typical behavior of G' and G'' versus temperature for determination of gelation temperature obtained at cooling rate of 1.0 $^{\circ}\text{C}/\text{min}$.

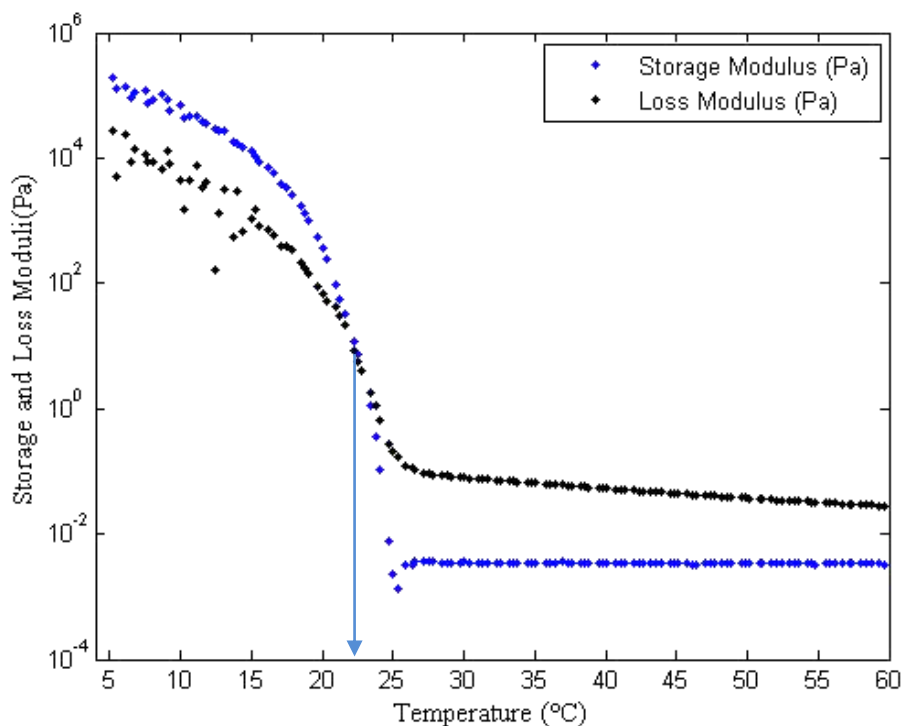


Figure 35. Typical behavior of G' and G'' versus temperature for determination of gelation temperature obtained at cooling rate of $3^{\circ}\text{C}/\text{min}$.

4.2.4 GEL BEHAVIOR BY OSCILLATORY TESTS

Oscillatory tests were performed, varying the frequency between 0 and 100 Hz under small stress amplitude of 1 Pa to ensure no disturbance of the gel structure and allows to characterize it. Tests were performed after the rheological protocol was applied, the oil sample were cooled to 5°C with a rate of $1^{\circ}\text{C}/\text{min}$, aging the gel during 0, 1, 5 and 24 hours.

The experiments allowed the gel characterization and corroborated that crystallized waxy crude oil pertain to the category of themoreversible strong gel (Hénaut, 1999). Figure 36 shows the variation of the storage and loss moduli with the frequency sweep applied. For all the aging times studied, the storage modulus were higher than the loss modulus, this behavior can be associated to the presence of a microstructure in the gel formed (Barnes, 1997). The magnitude of the storage modulus showed an increase with the aging time. In the case of the loss modulus, it stayed in a constant value independent of aging time, and its magnitude was lower than the storage modulus. The both moduli presented a slight variation with the frequency as was found by Lapasin and Pricl (1995), thus the moduli behavior was relatively independent of the frequency over a pulsation range evaluated.

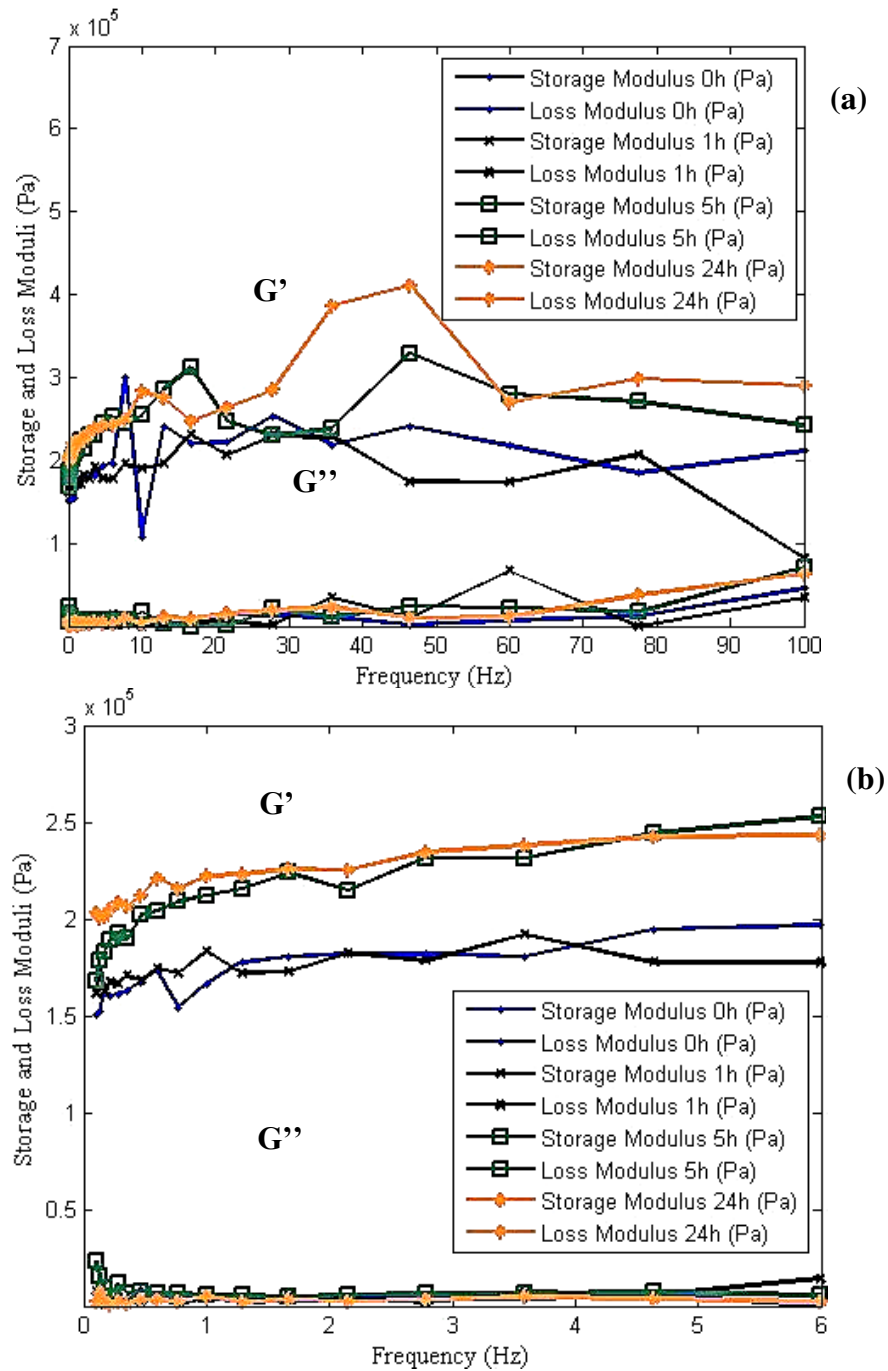


Figure 36. Gel behavior at 5 °C under stress amplitude of 1 Pa for the different aging time: 0-100 Hz (a) and zoom of 0 to 6 Hz (b).

4.2.5 YIELD STRESS

4.2.5.1 Oscillatory Stress Amplitude Sweep for Yield Stress Determination

Oscillatory test is one of the most common methods employed to determine the yield stress value in the literature and the oil industry, because this procedure have a connection between the steady-state analysis and the oscillatory flows (Tarcha, 2015). Thus, the

experiments were performed using an oscillation shear stress increasing from 1 to 3500 Pa. The protocol for the rheological measurements was applied to oil sample and then they were cooled to 5 °C, this temperature were kept during 4 different times (0, 1, 5 and 24 hours) to assess the effect of aging time over the yield stress value. The tests were executed under a fixed low frequency of 0.5 Hz.

As it was presented in the preceding section (4.2.2), oscillatory tests show the response of the storage and loss moduli to an oscillatory stress amplitude sweep, defining three different regions associated with yielding process (elastic response, creep and fracture). Thus at the point B or point of fracture (Figure 32) where the value of the storage and loss moduli are equal in magnitude, this stress value is taken as the Yield Stress (Wardhaugh and Boger, 1991; Chang *et al.*, 1998).

Figure 37 to Figure 40 presents the storage and loss moduli variation with the shear stress sweep applied over the structured gel of waxy crude oil at 5°C. At the beginning of the test, when was applied lower stress amplitude, the storage and loss moduli stay in a constant value. Despite of the loss modulus presents an oscillation in the first stage of measure, this oscillation occurs around a constant value until its stabilization. In this region, which corresponds to the linear viscoelastic region, the storage modulus is higher than the loss modulus because the material is gelled (Andrade, 2014). With the continue increase of the stress amplitude, both moduli decreased gradually because of the beginning of fracture process of the gelled structured material. In this stage, the storage modulus decrease faster than the loss modulus until the both moduli had the same value (fracture point) and the loss modulus becomes higher than the storage modulus, indicating that the structure was destroyed. The shear amplitude interval where the crossover between the storage and loss moduli took place were summarized in the Table 18.

Table 18. Yield stress for different aging time measured by oscillatory test.

Aging Time (Hours)	Static Yields Stress (Pa)
0	[905-976]
1	[976-1053]
5	[1426-1533]
24	[2134-2197]

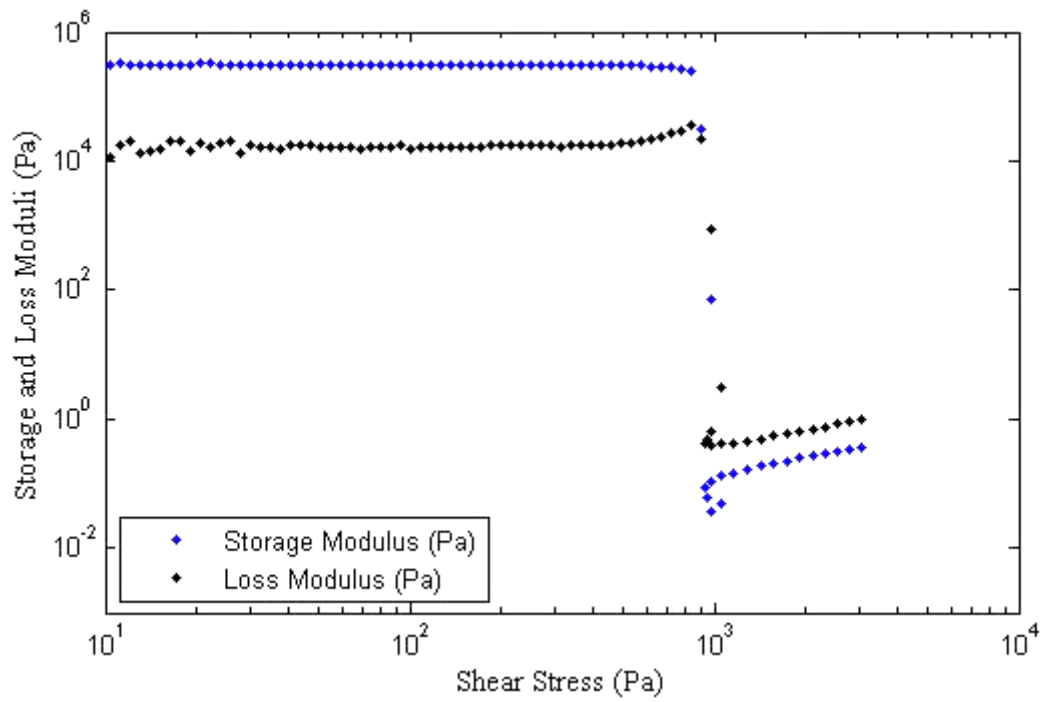


Figure 37. Oscillatory measurements for yield stress determination without aging times.

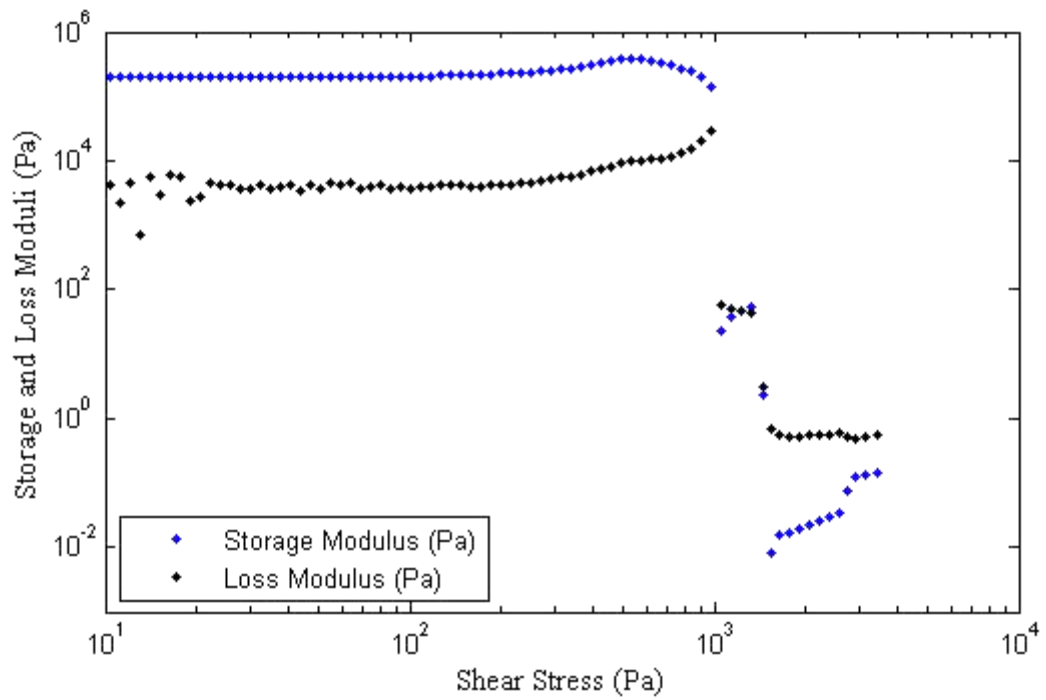


Figure 38. Oscillatory measurements for yield stress determination with aging time of 1 hour.

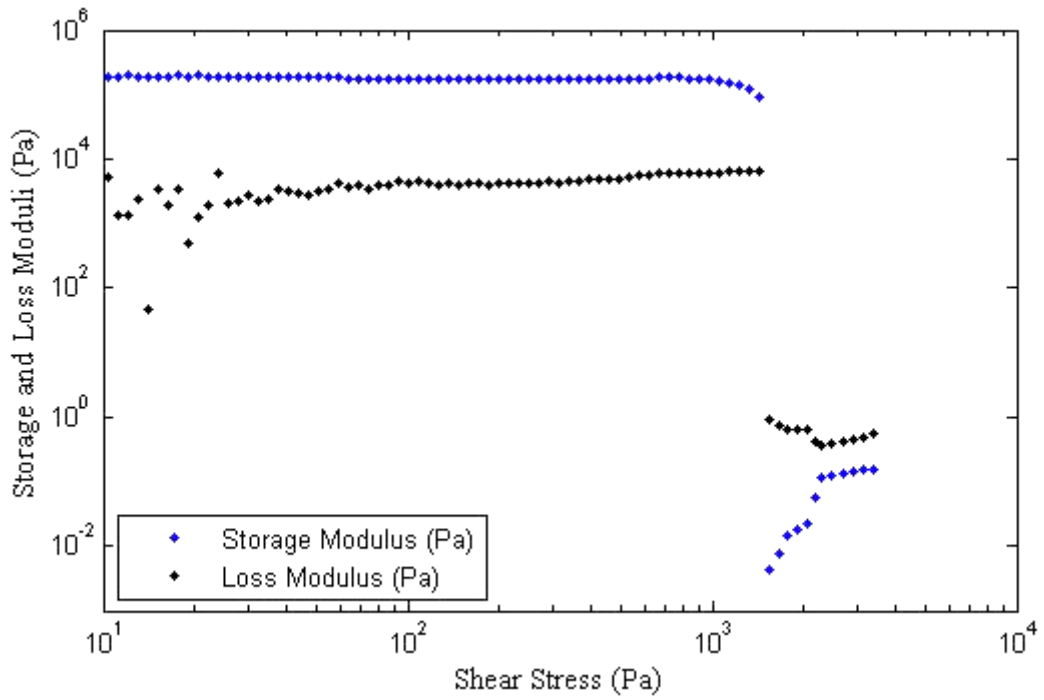


Figure 39. Oscillatory measurements for yield stress determination with aging time of 5 hours.

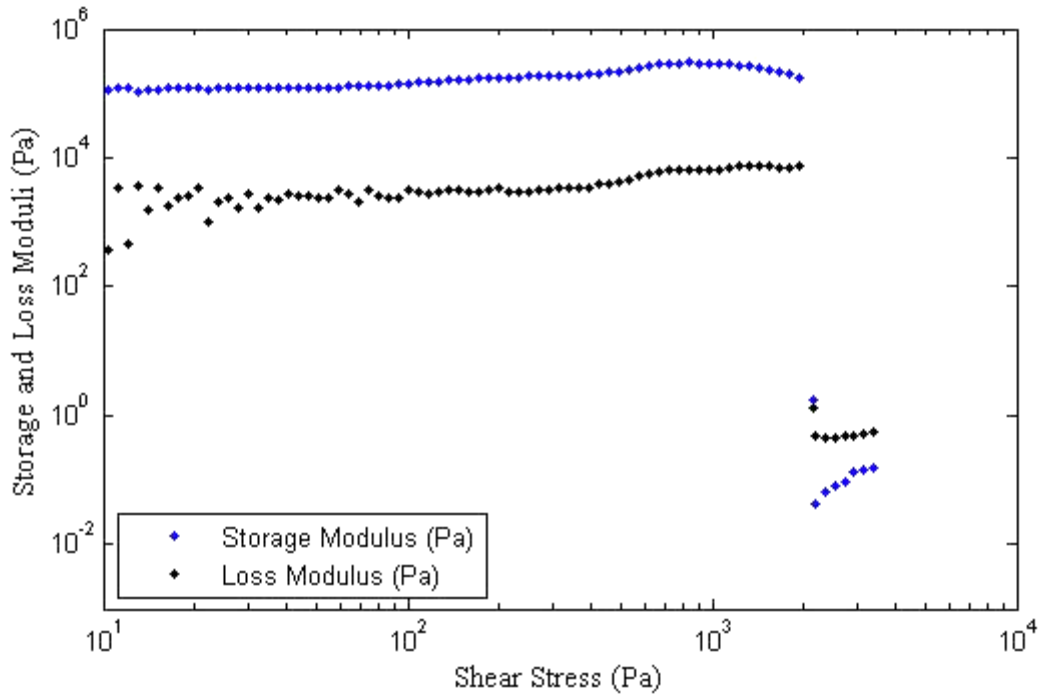


Figure 40. Oscillatory measurements for yield stress determination with aging time of 24 hours.

The first value in the intervals (Table 18) corresponds to a stress amplitude where the storage modulus was larger than the loss modulus, just before of its crossover. While the

second value in the interval corresponds to a stress amplitude where the loss modulus is greater than the storage modulus, which ensures that the gel structure was broke. So that, this second value in the interval was taken as a yield stress value for further calculations.

Yield stress increases with the aging time because of the structural evolution that takes place with the time as reported by Wardhaugh and Boger (1991). The storage and loss moduli kept constant at low shear stress values (elastic response region) for the different aging time evaluated.

4.2.5.2 Strain-Controlled Measurements for Yield Stress Determination

In the strain-controlled measurements, the oil samples were cooled to 5 °C with a rate of 1 °C/min followed by the pretreatment protocol, four different aging times (0, 1, 5 and 24 hours) were evaluated. Subsequently the samples were suddenly subjected to a constant shear rate during 30 minutes, in this study were applied the following shear rates values: 0.0001, 0.001, 0.01, 0.1 and 1.0 s⁻¹.

Figure 41 to Figure 44 show the response of the shear stress under shear rates and aging times evaluated as a function of time.

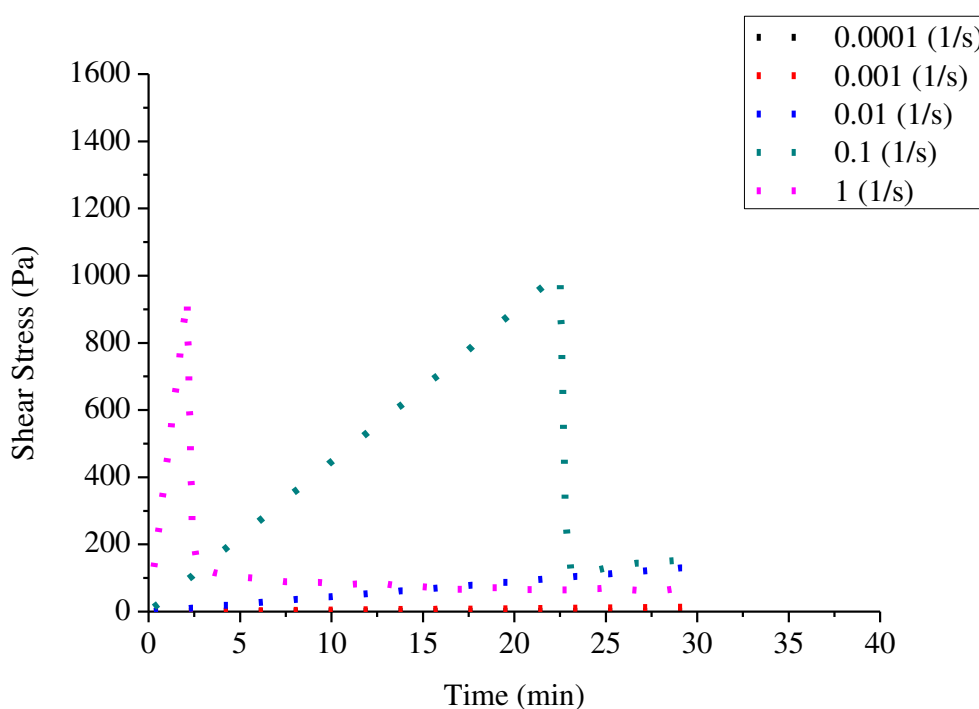


Figure 41. Yield stress determination by strain rate-controlled measurement without aging time.

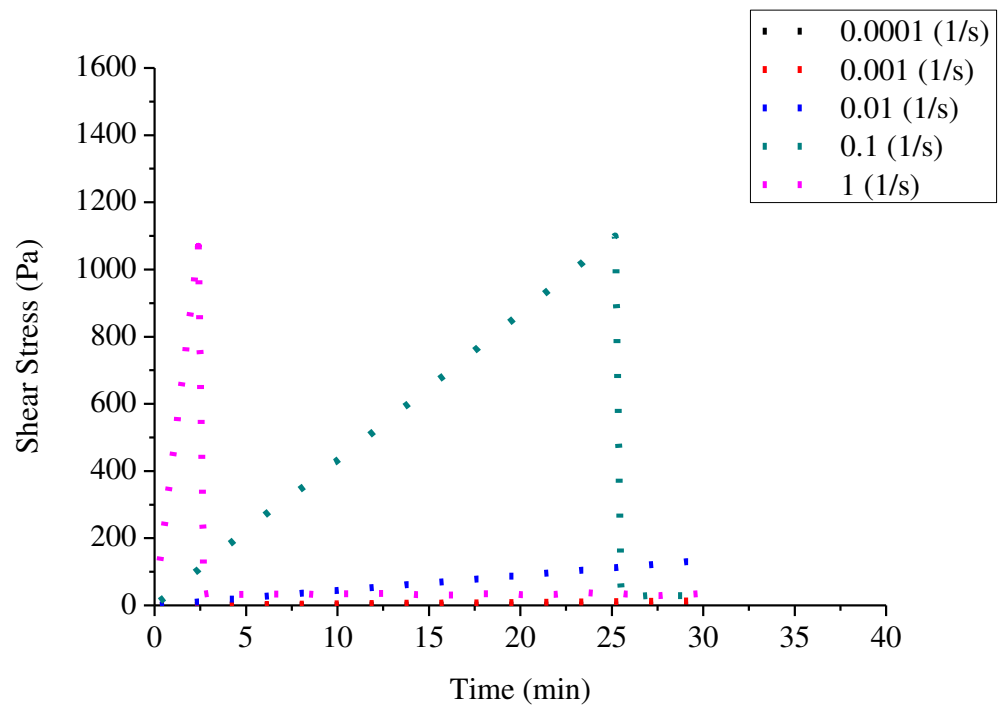


Figure 42. Yield stress determination by strain rate-controlled measurement for aging time of 1 hour.

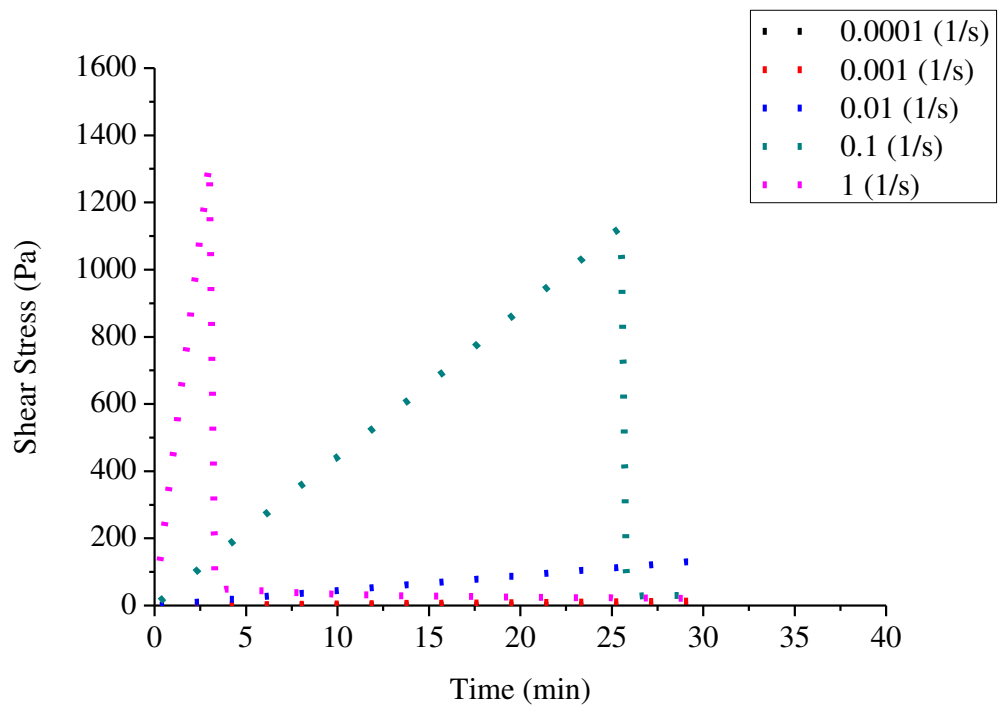


Figure 43. Yield stress determination by strain rate-controlled measurement for aging time of 5 hours.

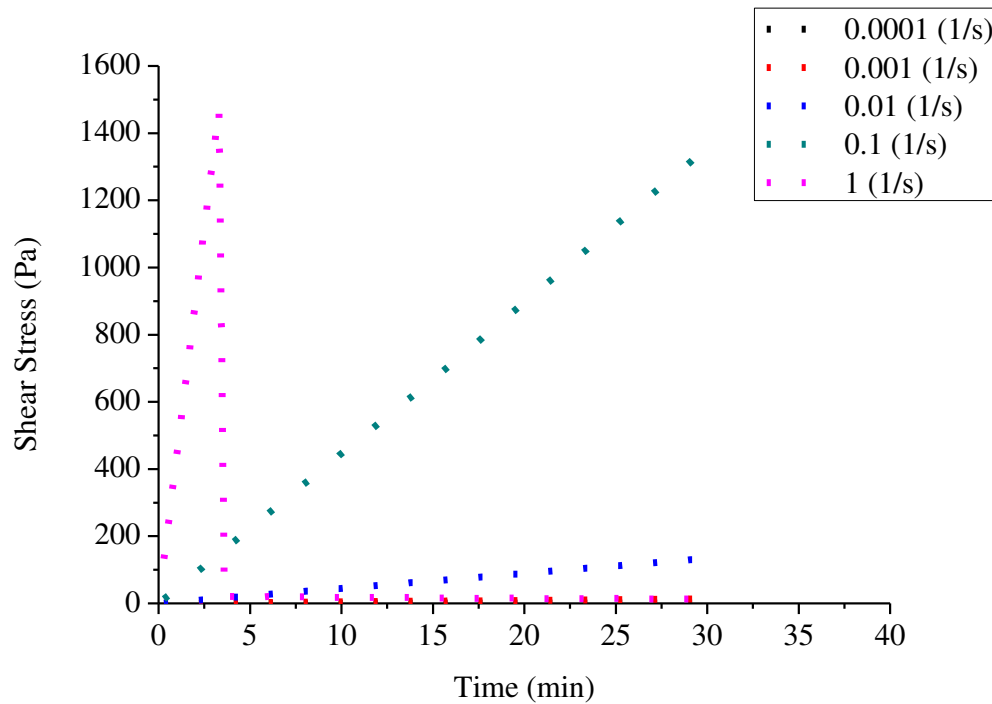


Figure 44. Yield stress determination by strain rate-controlled measurement for aging time of 24 hours.

The lower shear rate values (0.0001 , 0.001 and 0.01 s^{-1}) presents a slightly linear increased of the shear stress with the time; just in the case of the higher shear rate assessed (0.1 and 1 s^{-1}), the curves showed an overshoot stress value that increases with the aging time (Figure 45 and Figure 46). This overshoot stress is associated with the yield stress (Liddell and Boger, 1996).

After overshoot took place in the higher shear rate evaluated, it was presented a sudden decay to a steady state value as was explained by Mewis (2009) and it is often associated with the final degraded gel residual yield stress. These response represents a typical ideal cohesive breakage with a weak wax gel network, which means that the strength of the adhesive bonds is higher than the strength of the cohesive bonds, hence the fracture occurs cohesively, which is desirable for pipeline restart applications (Paso, 2014).

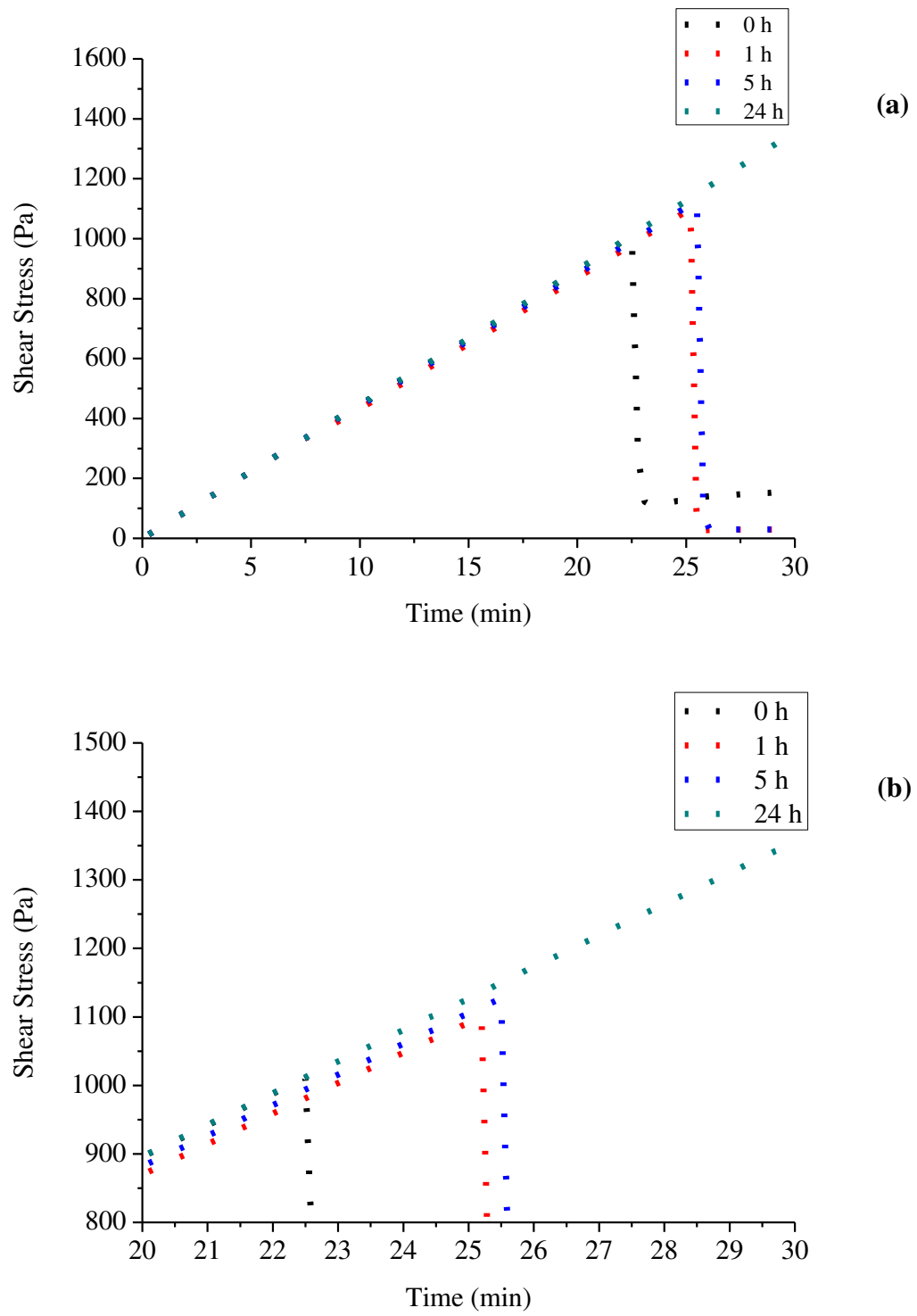


Figure 45. Yield stress determination by strain rate-controlled measurement under 0.1 s^{-1} (a) and 0.1 s^{-1} zoom (b)

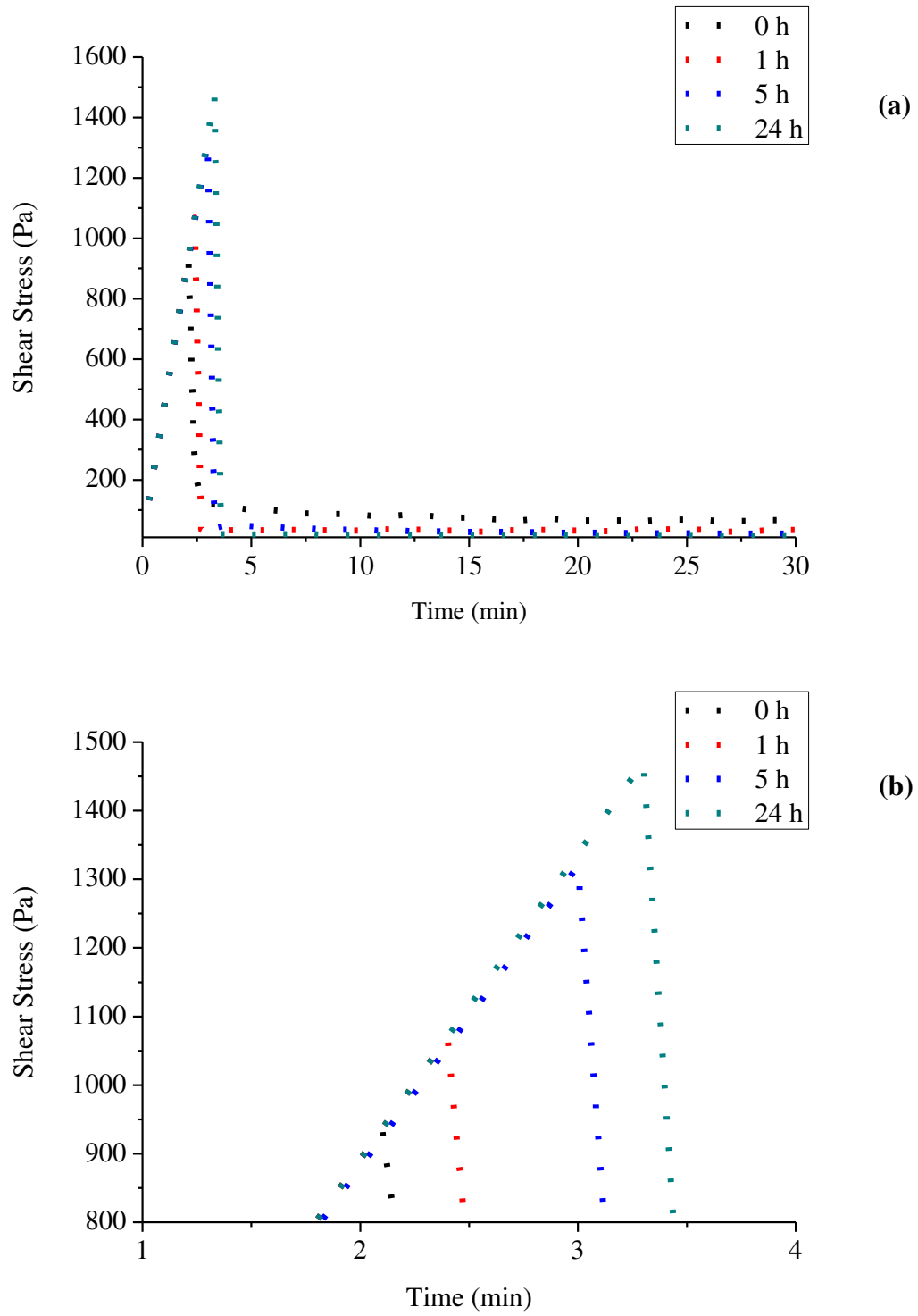


Figure 46. Yield stress determination by strain rate-controlled measurement under 1 s^{-1} (a) and 1 s^{-1} zoom (b)

Results of strain-controlled experiments are summarized in the Table 19. In these experiments were also verified that the yield stress value increase with the aging time for the shear rate which presented an overshoot stress response (higher shear rate values). In the case

of the lower shear rate values, where did not present an overshoot, is necessary to maintain the time of application for more than 30 minutes to get at overshoot point.

Table 19. Yield stress (overshoot stress) for different aging time by strain-controlled measurements.

Aging Time (Hour)	Yield Stress (Pa)	
	0.1 s ⁻¹	1.0 s ⁻¹
0	1011	936
1	1101	1070
5	1127	1320
24	-	1471

4.2.6 THIXOTROPY

4.2.6.1 Hysteresis loop test

Hysteresis of waxy crude oil was studied using the hysteresis loop technique, where the shear rate was increase linearly from zero to a maximum value, followed by decreasing it to zero at the same rate, under isothermal conditions. The measurements were performed after the pretreatment protocol, and the subsequently cooled of the oil sample to 5 °C with 1°C/min as a cooling rate. The sheared programs tested were divided in two categories: Hysteresis tests varying the shear rate range and the second kind of hysteresis test assessing the shearing time application.

Hysteresis test varying shear rate application:

- Shear rate was increase linearly from 0 to 100 s⁻¹ in 1 minute and immediately the sample was sheared from 100 to 0 in 1 minute.
- Shear rate was increase linearly from 0 to 1000 s⁻¹ in 1 minute and immediately the sample was sheared from 1000 to 0 in 1 minute.

The above procedures were made in order to evaluate the difference in the range of shear rate tested.

Hysteresis test at different shearing time application:

The following three procedures were applied with the claim of determine the influence of test duration on hysteresis loop results:

- Shear rate was increase linearly from 0 to 1000 s^{-1} in 1 minutes and immediately the sample was sheared from 1000 to 0 in 1 minute.
- Shear rate was increase linearly from 0 to 1000 s^{-1} in 3 minutes and immediately the sample was sheared from 1000 to 0 in 3 minute.
- Shear rate was increase linearly from 0 to 1000 s^{-1} in 5 minutes and immediately the sample was sheared from 1000 to 0 in 5 minute.

Hysteresis loop consists in two curves, the first one corresponds to the increase of the shear rate applied, and the second one consists in the decrease of the same shear rate range. The area delimited by these two curves has been used as a characteristic for thixotropy (Ahmadpour, 2014).

Difference between the shear rates ranges applied to the oil sample during the same time of 1 minute was noted. Thus, when the experiment were performed slower, 0 to 100 s^{-1} and 100 to 0 s^{-1} one minute each, a smaller difference between the both hysteresis curve (up and down curves) was recorded, which can be explained by the microstructure of gel has more time to come closed to the steady state. The faster experiments with a sheared procedure of increase shear rate from 0 to 1000 s^{-1} and subsequently decrease the shear rate from the 1000 to 0 s^{-1} showed a higher difference in the shear stress values on ascending and descending curves (Figure 47a) compared with the smaller range evaluated. These test confirmed the time dependent feature of the waxy crude oil.

Figure 47b shows that the viscosity values in the up curse are higher than those recorded in the down curve, confirming the thixotropic character of the waxy crude oil.

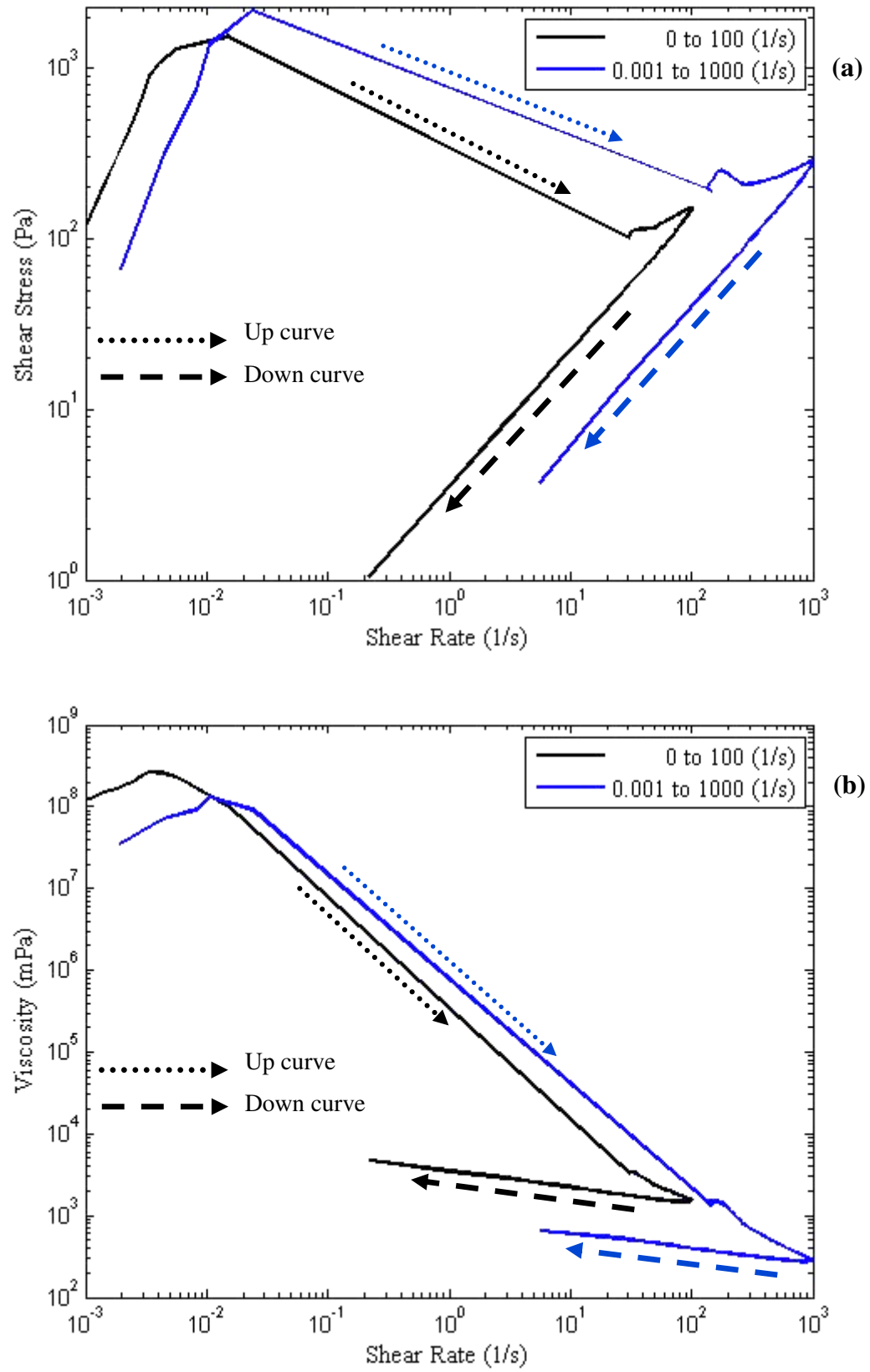


Figure 47. Hysteresis loop for 0 to 100 s^{-1} and 0 to 1000 s^{-1} : Shear stress versus shear rate (a) and viscosity versus shear rate (b).

Figure 48 shows the first sheared procedure done (linear increasing of shear rate from 0 to 100 s^{-1} in 1 minute and from 100 to 0 in 1 minute), which was repeated three times, in order to obtain the next two loops. It was identified that the second and third loop are exactly overlap, indicating that there is no active resistance to the flow, once the gelled pipeline was restarted in a test temperature of 5°C (Sun, 2015).

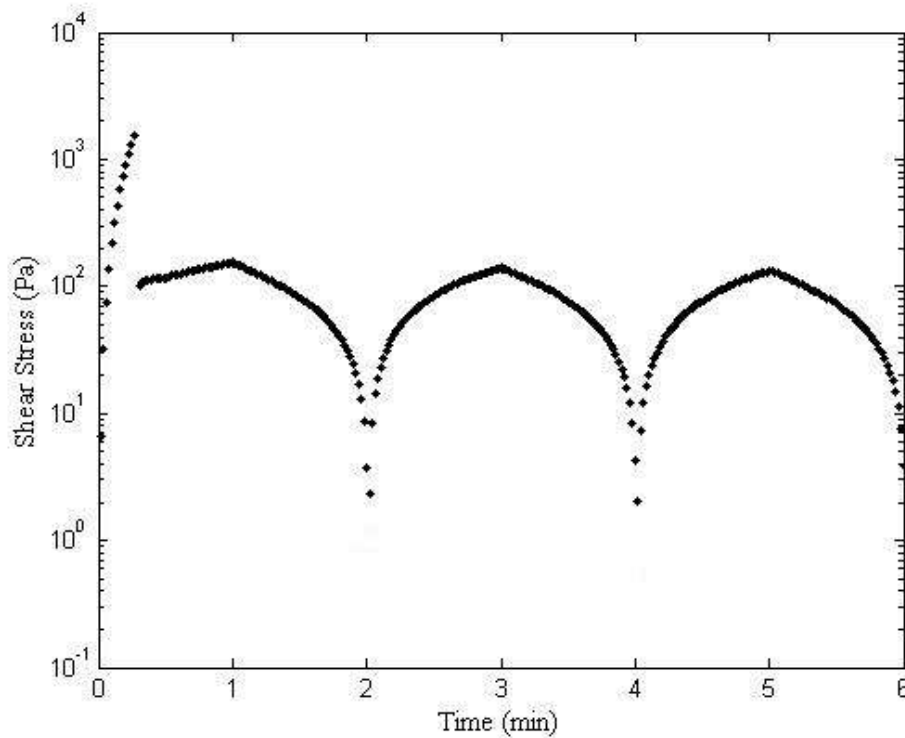


Figure 48. Shear stress versus time for three consecutive loops from 0 to 100 s^{-1} .

Taking into account that the hysteresis loop has limitations related to the shear rate and time effects, tests were performed varying the time of application of shear rate for the up and down curves.

Figure 49a shows the response of the shear stress under shear rate variation in the hysteresis test for different times as well as the Figure 49b shows the behavior of the viscosity under the shear rate application. The duration times evaluated were 1, 3 and 5 minutes, where the increasing of stress overshoot with the test time was observed.

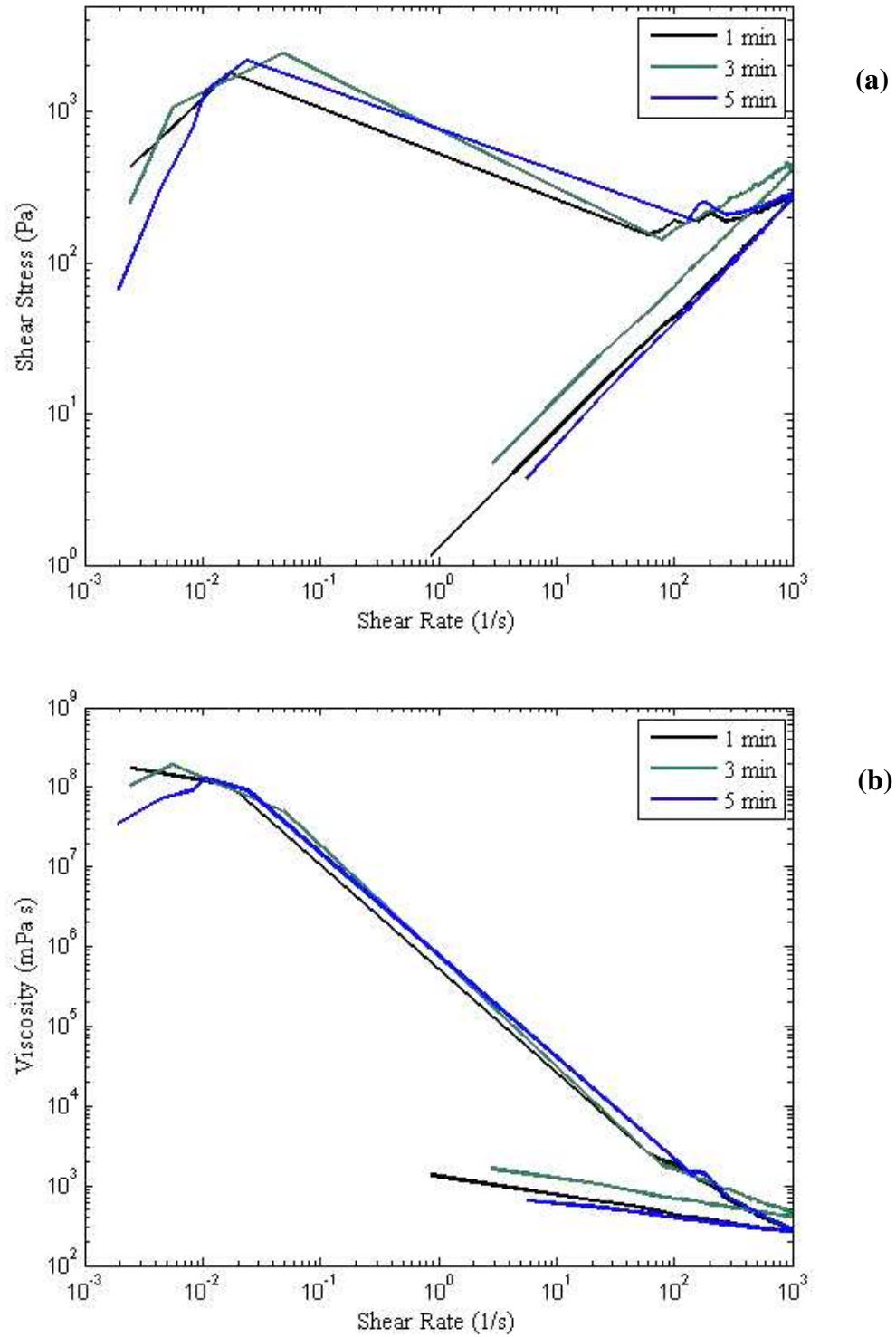


Figure 49. Hysteresis loop between 0 and 1000 s^{-1} applied at different duration times. Shear stress versus shear rate (a) and viscosity versus shear rate (b).

Table 20. Stress overshoot from the hysteresis loop at different test time.

Test Time (min)	Stress Overshoot (Pa)
1	1802
3	2183
5	2424

Hysteresis loop area is usually used as a measure of the thixotropic behavior of a fluid. Thus, the area enclosed between up and down curves obtained in the linear increasing and subsequently decreasing shear rate at different times. Shear stress and viscosity response were measured and the results are shown in the Table 21.

The test time that corresponds to 3 minutes shows the larger area between up and down curves, compared with 1 and 5 minutes tests. However, the loop area of the hysteresis test increase with the time increase for the different evaluated times.

Table 21. Hysteresis loop areas as a measure of thixotropy of waxy crude oil

Test Time (min)	Area 1 (Pa/s)	Area 2 (Pa/s)	Difference (Pa/s)
1	2.675×10^5	1.514×10^5	1.161×10^5
3	4.024×10^5	2.340×10^5	1.684×10^5
5	3.858×10^5	1.485×10^5	2.374×10^5

4.2.6.2 Star-up Experiments

This technique was described in the section 4.2.5.2 and it was employed to determine the yield stress value.

For this evaluation technique, a constant shear rate was imposed after cooled the sample to 5 °C with a cooling rate of 1°C/min. The constant shear rate studied were 0.0001, 0.001, 0.01, 0.1 and 1 s⁻¹, applied during 30 minutes to the oil sample.

The stress overshoot results recorded in the experiments using 0.1 and 1 s⁻¹ are present in the Table 19.

Figure 41 to Figure 44 show all the start-up experiment performed in this section and the Figure 45 and Figure 46 present only the shear stress response varying with the time for the test performed under 0.1 and 1 s⁻¹, respectively. For the different aging times evaluated, it was encountered that the stress overshoot in the start-up increases with increasing aging time

as other authors have been observed (Cheng, 1986; Lapasin and Pricl, 1995). This confirms once again the time dependent nature of the waxy crude oil and it is possible to affirm that applying a constant shear stress value, lower than the static yield stress on a gelled line during enough time, the gel structure will break and the flow will be restarted.

This fact can be observed in the higher shear rate assessed, in the case of the 1 s^{-1} , the overshoots for the different aging time appeared in the first 5 minutes of total 30 minutes test, keeping the trend of increasing the shear overshoot with the aging time. On the other hand, the results recorded under 0.1 s^{-1} , the stress overshoots for the different aging time (0, 1 and 5h) were registered from 22 minutes, and 30 minutes were not enough to reach the overshoot stress when the test was conducted for the aging time of 24 hours.

4.3 RESTART EXPERIMENTS IN THE HORIZONTAL FLOW LOOP

Experiments for restart flow in the horizontal loop were carried out in order to determine the pressure at which the restart of the gelled line happened. The pipeline contain a waxy crude oil cooled to 5°C , which was kept in that temperature during 1, 5, and 24 hours in order to evaluate the effect of the aging time in the pressure value for restart a gelled line under quiescent conditions. After the waxy oil remained inside the line during set aging times, it was applied pressure in the flow line, using a nitrogen cylinder coupled to the external tank. The pressure was kept constant for 30 minutes at time of each increase pressure, until observed restart of the flow in the gelled line in the monitoring panel of LABVIEW (Figure 19). This restart experiment through gradual increases pressure was performed because it corresponds to the majority of situations that occur in oil fields (Lee *et al.*, 2008).

4.3.1 AGING TIME OF ONE HOUR (1h)

Figure 50 shows the most relevant variables measured during the restart experiments for the first test made for the aging time of 1 hour:

- Inlet pressure in the pipeline: Value that needs to be recorded once the flow was reestablished (bar)
- Differential pressures placed in the test section(bar)
- Pressure in the external tank (bar)
- Pressure in the internal tank (bar)
- Level of waxy oil in the external tank
- Level of waxy oil in the internal tank

Figure 50 summarizes the procedure that was carried out with the oil. Four increments in pressure were made for this experiment, each of them with a duration of 30 minutes. In the first three increments of pressure, where the gelled oil (5 °C) did not flow, the level values of the tanks kept constant. The values of the differential pressures presented oscillations once the pressure was incremented, but these values stabilized. The inlet pressure in the inner tank is recorded as zero during the experiment because it was open to the atmosphere all the experiment time. Thus, in this first three increment pressure steps, no change in the monitored variables were registered.

In the fourth increase, the inlet pressure in the pipeline decreased gradually and the pressure in the external tank decreased in the proportional way, confirming that the gel structure were broken and the flow inside the pipeline was started. While this happened, the external tank level decreased and the internal tank level increased. Thus, this pressure was registered as the needed to restart the gelled line.

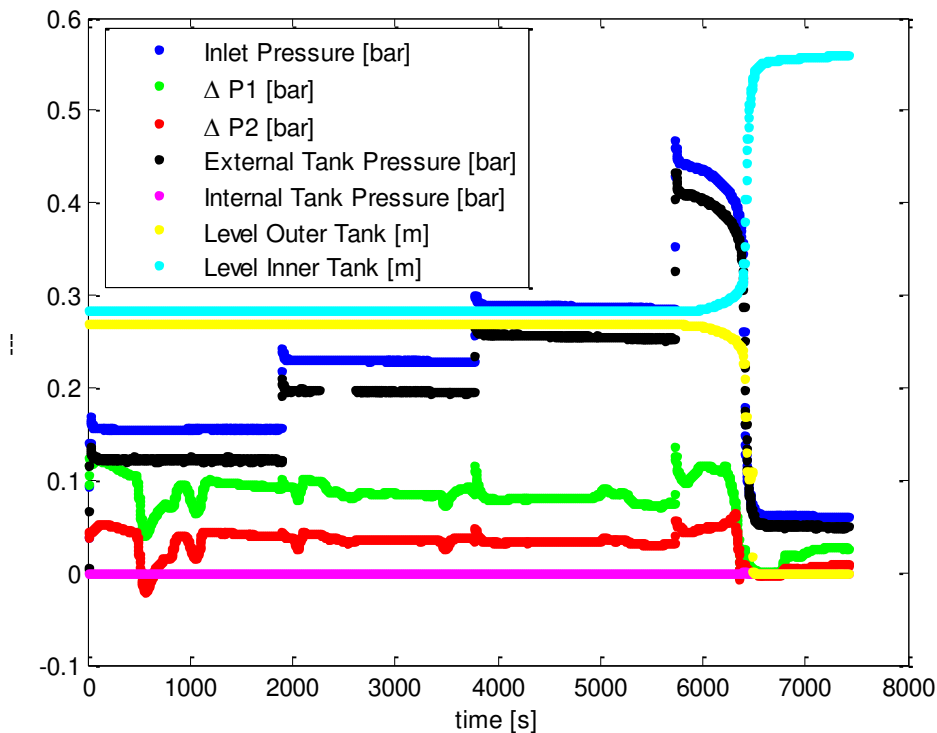


Figure 50. All variables measured in the restart experiments for the first test with aging time of 1 hour.

Figure 51 shows in detail the inlet line pressure, level inner tank, and the differential pressures. The first increase in pressure was approximately 0.17 bar. Waxy crude oil stayed under this pressure around 2000 seconds and no change was observed, so a new increased pressure were applied until 0.25 bar during the next 2000 seconds. The next increased raised

approximately 0.30 bar but once again no variation were recorded. The last increase pressure reached 0.47 bar and the flow was restarted in the pipeline. It was determined that the minimum pressure to restart the gelled line is between 0.30 and 0.47 bar.

Other variable recorded in the restart process was the inner tank level. Figure 51 shows that the precise moment when the pressure drops. The inner tank level increased until a constant value, confirming the fact no movement or flow took place inside the line before 0.47 bar was applied in the line.

Differential pressures were also kept constant before the pressure reached the 0.47 bar value, with small oscillations with each increased pressure. Total differential pressure on the flow line is shown in the Figure 51 as ΔP . This result was calculated based on the values of the inner tank level and the value of inlet line pressure. This ΔP value of 0.44 bar is necessary to restart the flow under this experiment conditions.

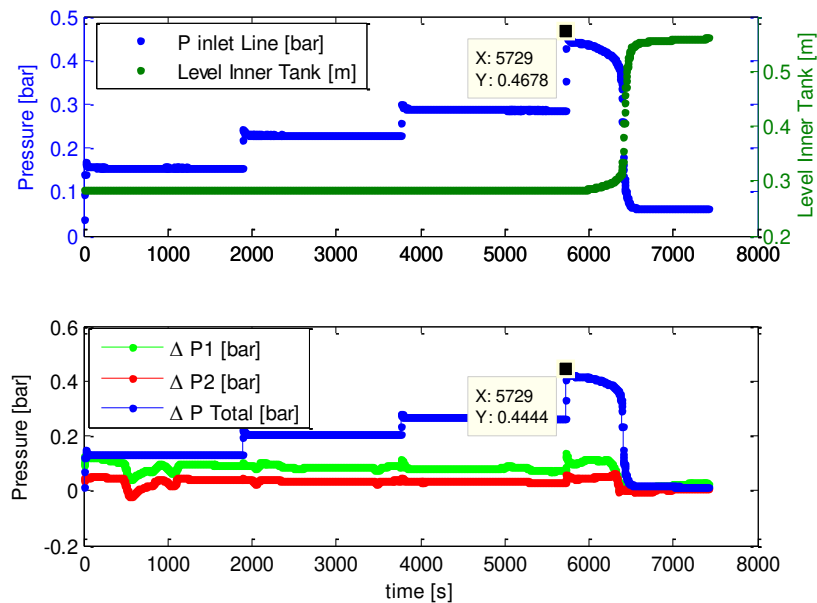


Figure 51. Detail of the pressure and level of inner tank for the first test with aging time of 1 hour.

Temperature sensors also recorded the waxy oil temperature at the inlet of the line, at the outlet of the line and at the water bath where the test section is submerged. Initially the temperature of the water bath and the outlet of the line stayed constant at 5°C during the first three increments of temperature. When the oil began to flow, a peak was observed in the data recorded by the both oil temperature sensors (Figure 52). This confirmed that the gelled waxy oil was displaced in the section test.

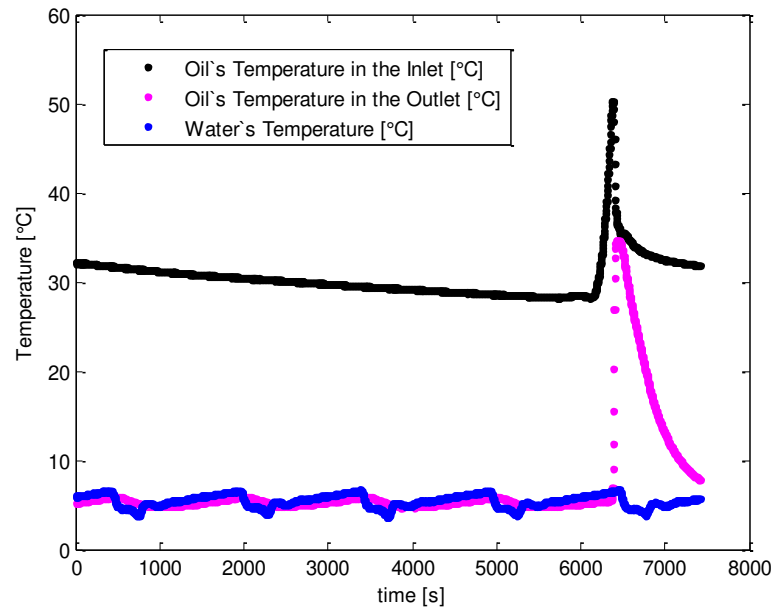


Figure 52. Temperature recorded for the restart experiment with aging time of 1 hour.

Figure 53 and Figure 54 show the results for the second and third experiments carried out for an aging time of 1 hour. The response of measured variables were very similar to the first experiment performed, obtaining values of the final increase of the pressure of 0.50 bar and 0.55 bar for the second and third test, respectively; and a total pressure drop needed for gelled line restart of 0.48 bar and 0.53 bar for the second and third experiment, respectively.

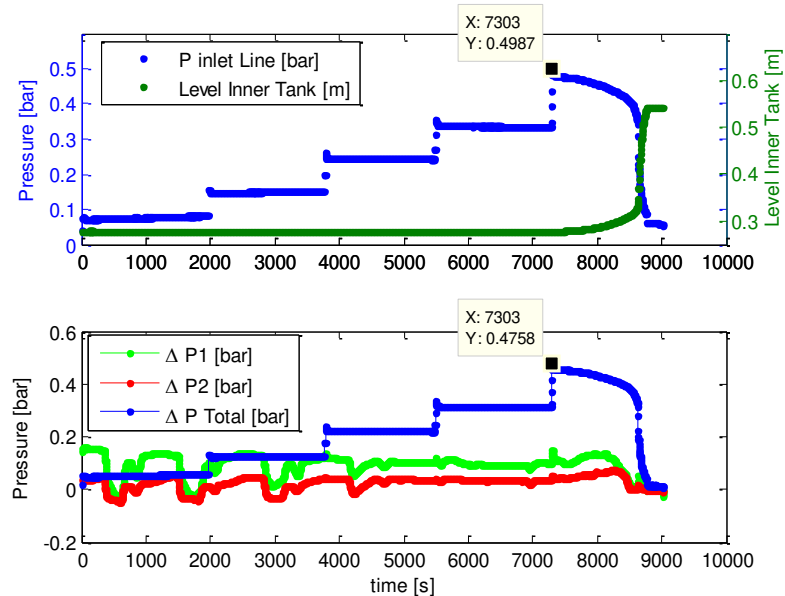


Figure 53. Detail of the pressure and level of inner tank for the second test with aging time of 1 hour.

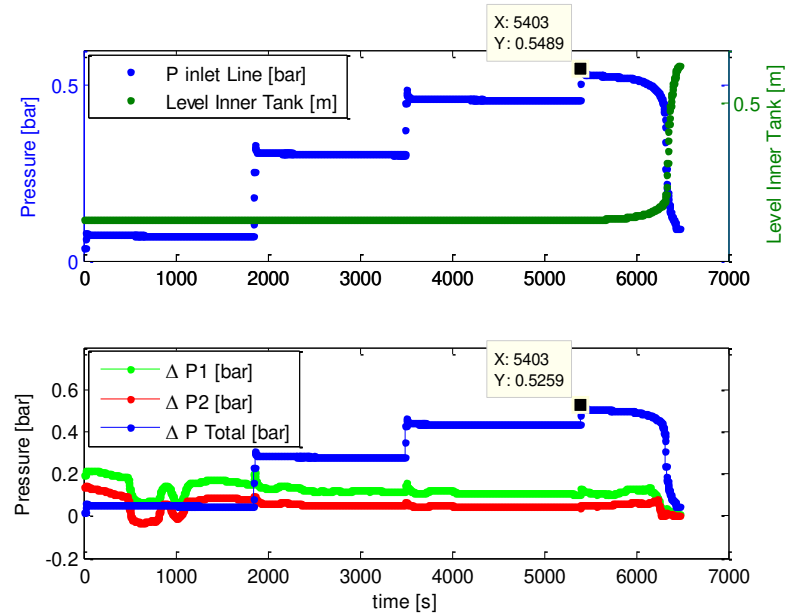


Figure 54. Detail of the pressure and level of inner tank for the third test with aging time of 1 hour.

Figure 55 and Table 22 present the summary of the results from the restart experiments for an aging time of 1 hour. The pressure value at the flow was restart for the three experiments were closed. Applied pressures and their steps were not equal because the valve used to control is a flow control valve, which makes difficult the pressure control. Thus, the pressure required to restart the flow of the gelled line aging during 1 hour is 0.51 bar.

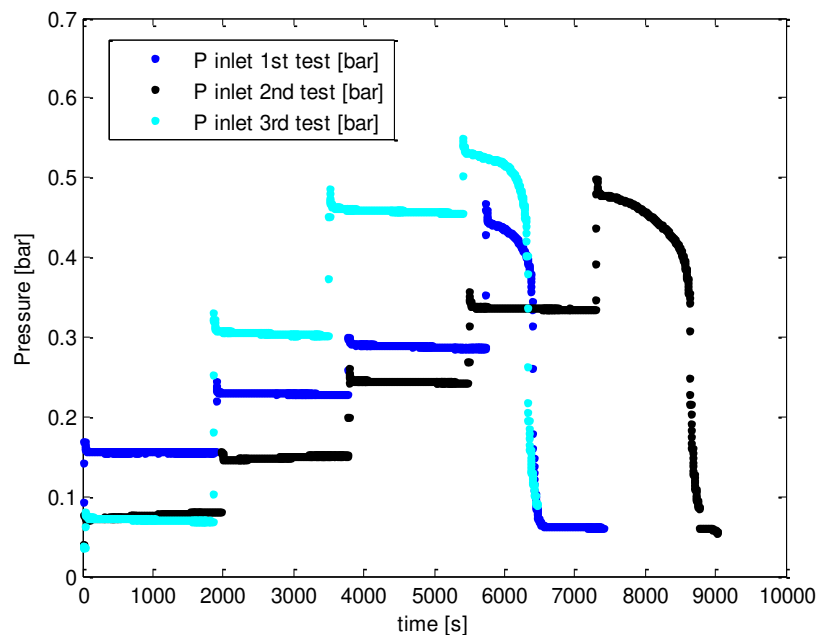


Figure 55. Comparison between results for experiment with aging time of 1 hour.

Table 22. Inlet line pressure and ΔP total for the restart experiments with an aging time of 1 hour.

	Inlet line pressure (bar)	ΔP total (bar)
1st Test	0.47	0.44
2nd Test	0.50	0.48
3rd Test	0.55	0.53
Mean	0.51 ± 0.03	0.48 ± 0.03

4.3.2 AGING TIME OF FIVE HOURS (5h)

The procedure performed for tests with aging time of 5 hours was the same as described in the previous section for the 1 hour experiments, varying only aging time to 5 hours. Figure 56 shows the same tendency of the experiments with an aging time of 1 hour (Figure 50), when the pressure increased steps raised 0.4 bar the gelled line restarted to flow.

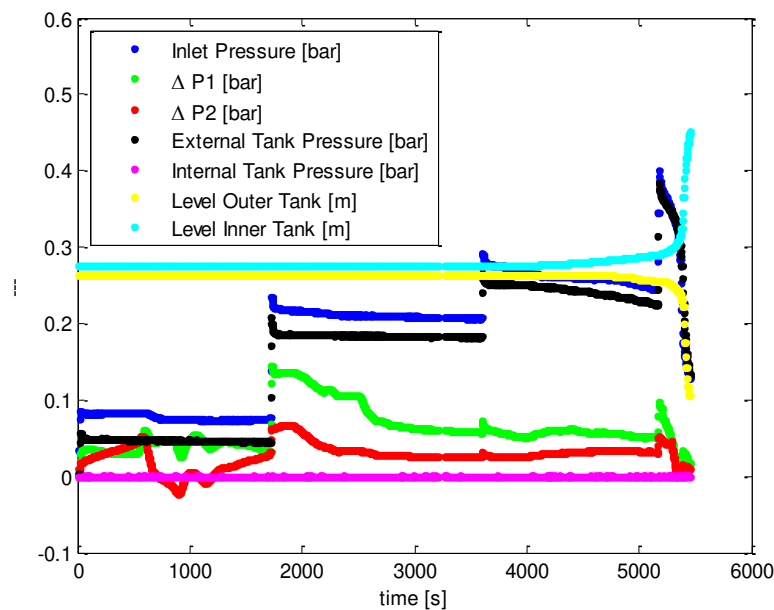


Figure 56. All variables measured in the restart experiments for the first test with aging time of 5 hours.

Figure 57 and Figure 58 show approximately the same value for the restart the movement inside the gelled line (around 0.4 bar) compared with the experiments with aging time of 1 hour.

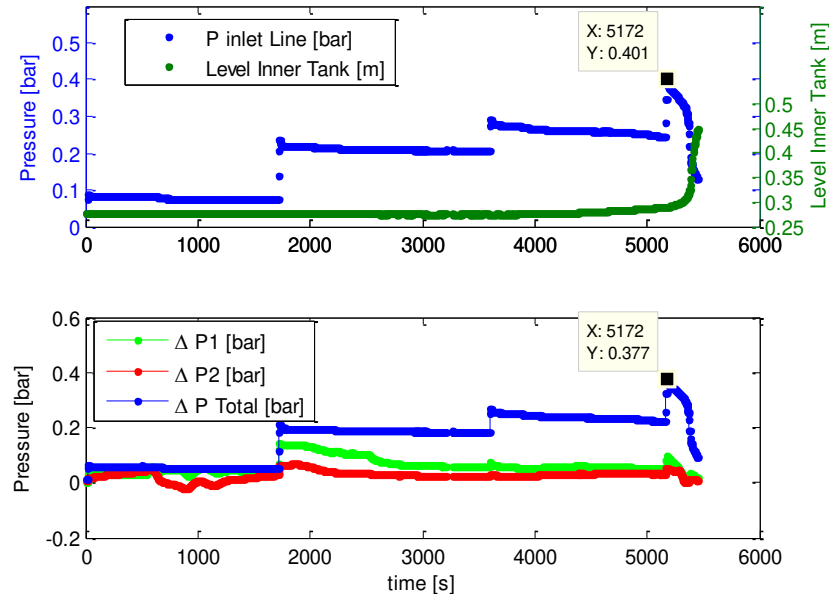


Figure 57. Detail of the pressure and level of inner tank for the first test with aging time of 5 hours.

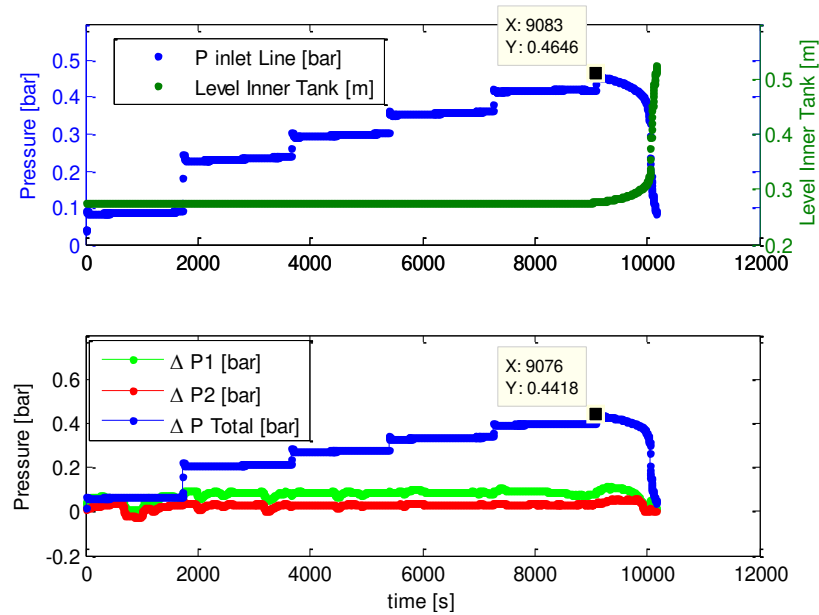


Figure 58. Detail of the pressure and level of inner tank for the second test with aging time of 5 hours.

Figure 59 and Table 23 present the summary of the results obtained for the restart experiments for aging time of 5 hours. There is no significant variation compared to experiments an hour of aging.

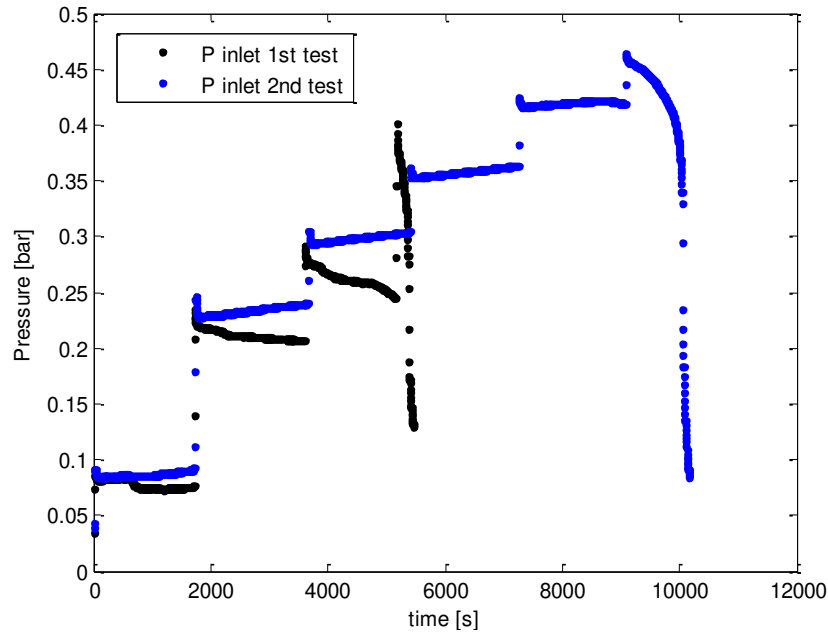


Figure 59. Comparison between results for experiment with aging time of 5 hour.

Table 23. Inlet line pressure and ΔP total for the restart experiments with an aging time of 5 hours.

	Inlet line pressure (bar)	ΔP total (bar)
1st Test	0.40	0.38
2nd Test	0.46	0.44
Mean	0.43 ± 0.03	0.41 ± 0.03

4.3.3 AGING TIME OF TWENTY-FOUR HOURS (24h)

Two experiments were made to evaluate the restart pressure of gelled line aging during 24 hours. Figure 60 shows the variables measured in the first test. The results are very similar to those obtained for the smaller aging times.

Figure 61 and Figure 62 present in detail the results obtained for the first and second test with aging time of 24 hours. In the second experiment, when the pressure reach 0.56 bar in the increased pressure steps, it was necessary approximately 1000 seconds to restart the flow of the gelled line.

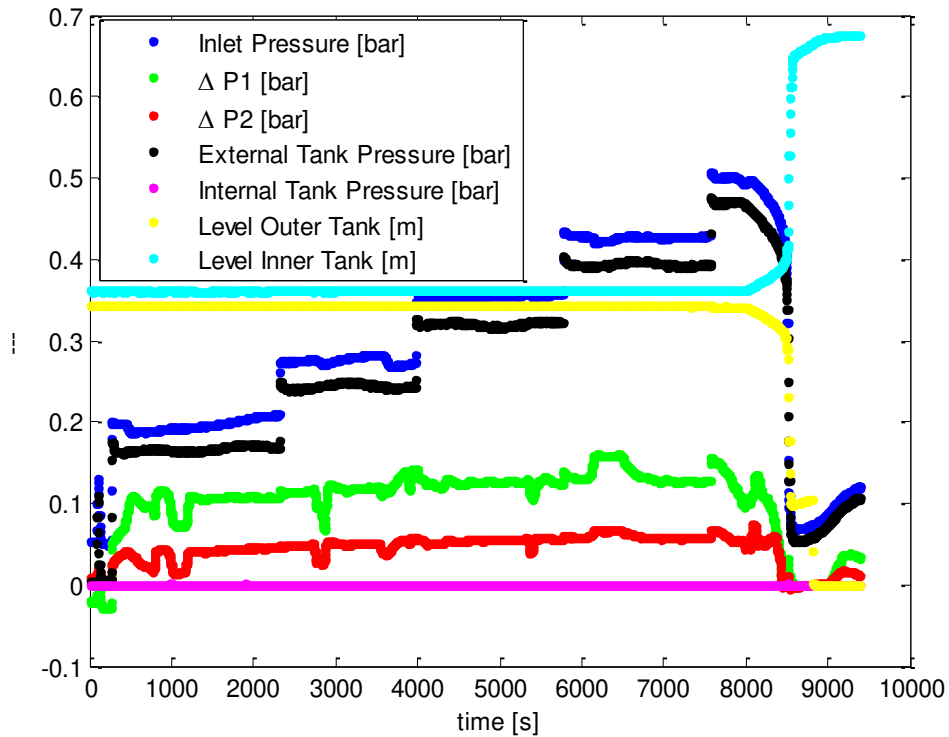


Figure 60. All variables measured in the restart experiments for the first test with aging time of 24 hour.

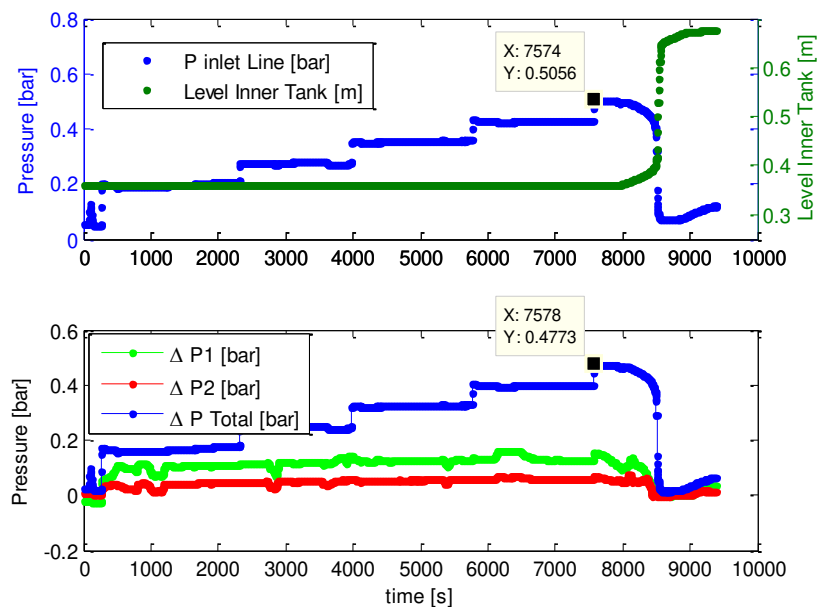


Figure 61. Detail of the pressure and level of inner tank for the first test with aging time of 24 hours.

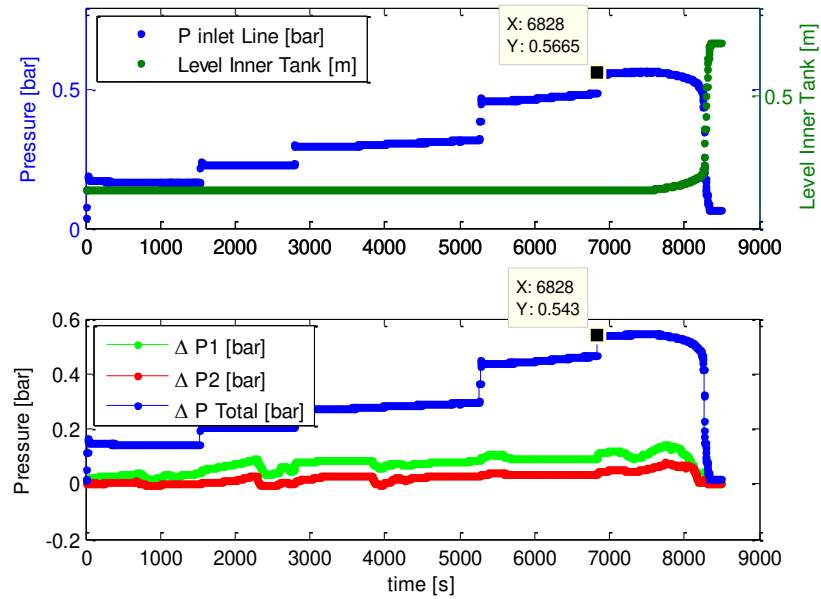


Figure 62. Detail of the pressure and level of inner tank for the second test with aging time of 24 hours.

Figure 63 and Table 24 summarized the results recorded for the restart experiment with aging time of 24 hours. The values obtained from these experiments are slightly higher compared to those obtained with shorter aging times.

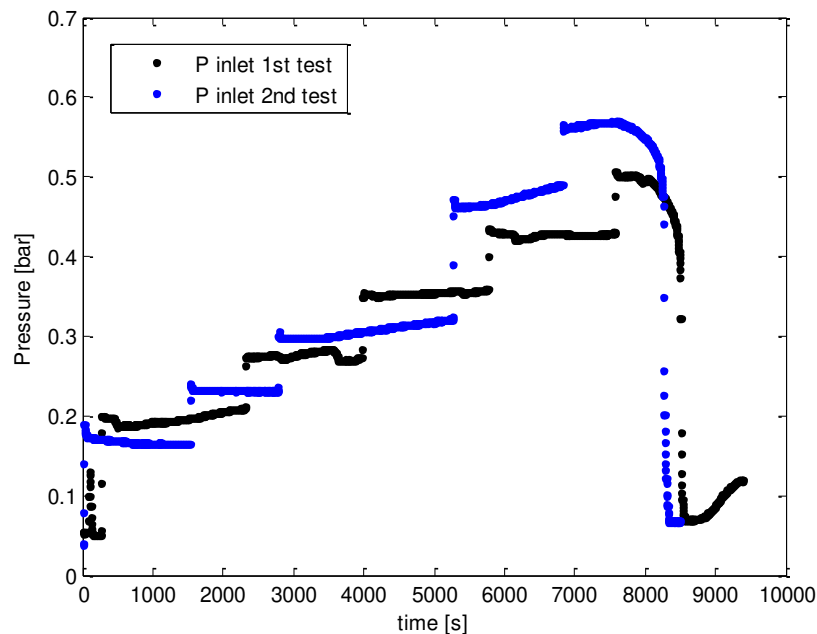


Figure 63. Comparison between results for experiment with aging time of 24 hours.

Table 24. Inlet line pressure and ΔP total for the restart experiments with an aging time of 24 hours.

	Inlet line pressure (bar)	ΔP total (bar)
1st Test	0.51	0.48
2nd Test	0.57	0.54
Mean	0.54 ± 0.03	0.51 ± 0.03

4.3.4 COMPARISON BETWEEN DIFFERENT AGING TIMES

Contrary to the results obtained by rheological measurements and to those suggested by the literature review, no relationship between the aging times and the pressure required to restart the flow in a gelled line was found. For each experiment, the pressure varies between 0.40 and 0.57 bar through the different aging times. Figure 64 summarizes the restart pressure found for the aging times evaluated.

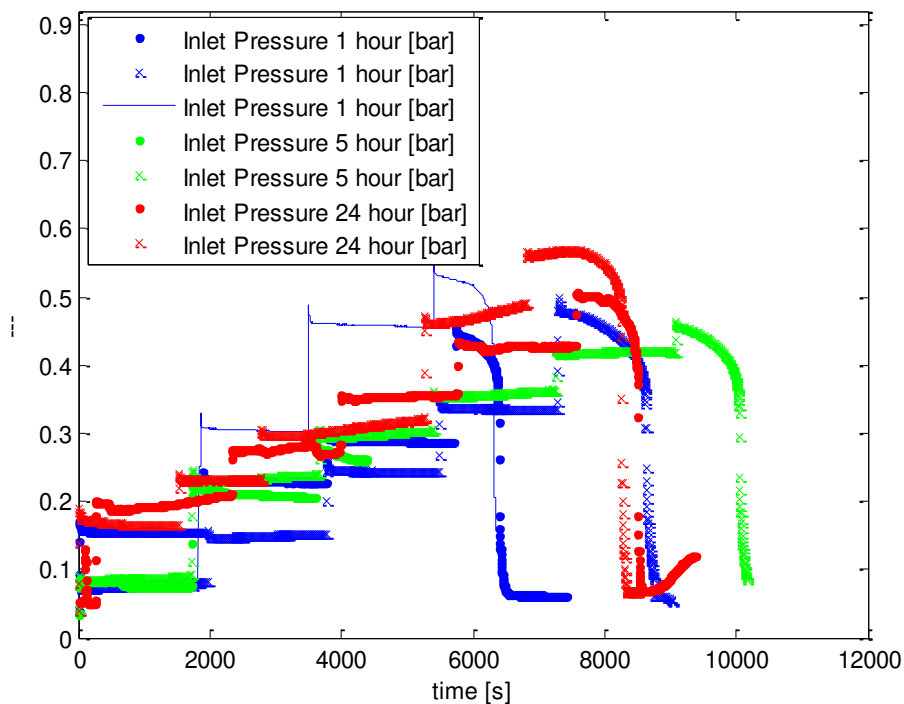


Figure 64. Restart pressure for the different aging times evaluated.

The increase pressure in the gelled line, using nitrogen as pressurization system (see Figure 18), makes that the shearing over the gel, causing a decrease in its strength. This fact

confirms again that the gel strength is a dependent variable of time and stress shearing, so these variables have an important role in the restart of gelled lines.

4.4 COMPARISON BETWEEN MODEL PIPELIN AND CONTROLLED STRESS RHEOMETER

The restart pressure obtained from the scale-laboratory experiments were compared with the yield stress values obtained from the oscillatory measurements for the different aging times evaluated, using the following equation:

$$Break\ pressure = \frac{Break\ force}{\pi R^2} = \frac{Failures\ strength \times 2\pi RL}{\pi R^2}$$

Resulting in the equation (7) presented in the chapter 2:

$$\Delta P_{min} = \frac{4 \tau_w L}{D}$$

ΔP_{min} from the balance force is calculated based on the results presented in the Table 18 for the yield stress obtained by oscillatory measurements at Controlled Stress Rheometer.

Table 25 presents the comparison between the pressures differential obtained by oscillatory test at the rheometer and those recorded by flow line experiments. As expected, the restart pressure obtained through the force balance overestimated this value, compared with the minimum pressure obtained by pilot scale experiments in a flow line with diameter of 1 in and length of 6 m.

Laboratory measures overestimated the restart pressure, so it is necessary to use empirical factors to scale the laboratory results to field conditions. However, it has not found a constant empirical factor that can be reproduced. Borghi and Corra (2003) found that the yield stress determined using the classical balance force equation; it was 3 times higher than the yield stress results from the model pipeline. Davenport and Somper (1970) noticed the same trend, restart pressure calculated from rheological data are larger than pressures evaluated with model pipelines or pilot rigs. Fleming *et al.*, (2013) present that that the restart pressure calculated from rheological test is around 20 to 30 times higher than the measured necessary pressure in a model line.

These overestimated results indicate that is necessary to include parameters such as the oil compressibility, viscoelasticity, and others, in order to make a better estimation of the minimum required pressure to restart the flow in a gelled line.

Table 25. Comparison between restart pressures obtained by rheological measurements and by flow line measurements.

Aging Time (Hours)	Yield Stress (Pa) by Oscillatory test at rheometer	ΔP_{min} from equation (7) (bar)	ΔP measured in the flow line (bar)	$\frac{\Delta P_{min}}{\Delta P_{measured}}$
0	976	9.22	-	-
1	1053	9.95	0.48	21
5	1533	14.49	0.41	35
24	2197	20.76	0.51	41

5 CONCLUSIONS

An experimental study of the restart flow in a gelled line was performed using physicochemical and rheological characterization and experiments at pilot-scale laboratory in a horizontal flow line of a Brazilian waxy crude oil.

A pretreatment protocol was applied before any test in order to ensure a good reproducibility of the results. Physicochemical characterization showed lower contents of asphaltenes, resins, water, acids, compared with the fraction of paraffin, which confirmed the waxy nature of the crude oil.

The critical temperatures in the precipitation, sedimentation and deposition process were determined for the waxy crude oil studied.

The definition of the critical temperatures allowed stablishing regions of risk associated with the wax crystallization and gelation. The zero risk region is defined by the temperature above the WAT, where the oil behaves as a Newtonian fluid. The WAT is defined as the temperature at which the first wax crystals begin to appear. WAT and the pour point (no flow) temperatures delimit an intermediate risk region. In this intermediate region is located the gelation temperature, point where the solid behavior of the oil predominates over its liquid behavior during the cooling process. In a continuous cooling process of a waxy oil, wax starts to precipitate when the cloud point is reached and, from this point, the liquid behavior is continuously reduced while the solid behavior is increased, but the liquid still predominates over the solid behavior. When the oil reaches the gelation point an inversion happens and the oil shows a predominant solid behavior which increases up to the pour point, where is reached a no-flow condition.

Wax appearance temperature (WAT) were determined under different cooling rates, using a DSC analytical technique and rheoscope modulus coupled to a rheometer with polarized light. The optical techniques gave higher values of WAT compared to the DSC technique. This is due to WAT allows to visually monitor the crystal formation in real time while the oil sample was cooled.

The gelation temperature was identified as a temperature where the Newtonian behavior of the waxy crude oil changes to a complex Non-Newtonian behavior. This temperature was determined under different cooling rates by oscillatory test at the rheometer.

For the WAT and gelation temperature determination shows that this temperature decreased with the increasing cooling rate.

The pour point temperature of the waxy crude oil was determined under static conditions, which represents the temperature where no movement or flow is observed during the cooling process of the oil.

The viscosity measurements showed that the waxy crude oil behaves like Newtonian fluid at temperatures above 30 °C. Below this value, the behavior of fluids was adjusted by Cross model. Cross model was successful in describing the flow curves for Non-Newtonian conditions because its parameter represents the low and high stress behavior of this kind of complex fluid.

The flow curves were also fitted to Herschel-Bulkley model. However, this model did not fit the flow curve results at lower temperatures (4 and 5°C). Herschel-Bulkley model is recommended, just when the magnitude of yield stress is known and it is possible to adjust the shear stress response above the yield stress to a power law model.

Preliminary oscillatory tests showed that during the elastic response at lower shear stress amplitude, the storage modulus kept constant and greater than the loss constant modulus value. At shear rates closed to the fracture ($G' - G''$ crossover) shear stress, both moduli began to decreased until the breakage of wax crystal structure. Two different frequencies were evaluated in order to assess the effect in the stress point boundary for elastic response, creep, fracture and shear thinning regions. The response of G' and G'' were very similar, confirming that the oscillatory response was independent for the two different time scales (or frequencies) evaluated.

Frequency sweep was also evaluated by oscillatory tests with the objective of corroborate the crystallization process of waxy crude oil at different aging times. The recording of the G' and G'' response under a frequency sweep, showed higher values of G' than those for the G'' . On the other hand, G'' was kept constant for every aging time evaluated while the G' shows a slightly increase with the rise of the aging time. This response is associated to the presence of gel microstructure.

Static yield stress values was evaluated through different procedures at temperature of interest (5°C): Oscillatory Stress Amplitude Sweep, Strain-Controlled Measurement and Start-Up experiments at a 1-inch size horizontal flow line. Results showed that the start-up at horizontal flow line results differ in the yield stress values determined with the other two rheological techniques.

The yield stress evaluated in the horizontal flow line shows very small values when compared with those recorded by other rheological measurements. These values were calculated using the simple force balance, which presents a correlation between pressure

differential with the static yield or yield stress. Thus, the error in this measurement can be associated to other important characteristics like viscoelastic behavior, oil compressibility and other; that need to be taken into account for the accuracy of yield stress determination.

Yield stress measured with the two above mentioned rheological techniques showed good agreement between them. Yield stress values between 936 Pa (0 h) and 2197 Pa (24 h) were determined and the wide range may be explained because of aging their different time. Yield stress values present an increases tendency with the increase of the aging time confirming that the gel strength increase with the increasing aging time.

The yield stress is a measurement of the gel strength, thus all the rheological experiments were performed with the objective to assess the structure of gel and its thixotropic behavior. The thixotropic behavior characterizes a waxy crude oil with rheological properties strongly dependent of the time and the aging time, these parameter play an important role in the formation of gel structure.

Dynamic yield stress was calculated from the flow curve data and corresponds to the shear stress needed to maintain the flow when the gel in the pipeline was broke. Dynamic stress is another engineering parameter that needs to be determined in order to plan a more efficient production and low cost transport operations in a waxy crude oil field.

6 SUGGESTIONS FOR FUTURE STUDIES

It is suggested to explore other geometries for the rotational rheometer, such as the vane, which has been widely recommended because it barely disturbs the sample at all upon insertion prior to testing and eliminates slippage.

Test frequency influences the measured yield stress because of the relaxation behavior of the fluid. Thus, G' usually decreases with decreasing frequency for complex fluids, then yield stress decrease too. Therefore, lower frequencies give a better description of the materials at rest. Frequencies of 0.1 and 0.05 Hz are suggested for future experiments with waxy crude oils.

The yield stress could be also determined using the creep/recovery technique, applying constant stress in steps. Thus, resulting strain needs to be measured as a function of time for each stress step. For shear stress below the yield stress, the gel behaves as an elastic solid and the strain response is constant but above the yield stress, the strain increases indefinitely with time achieving a steady state of shear indicating viscous flow. Therefore, the transition between these two stages corresponds to the yield stress value.

It is advised to develop experiments in the horizontal flow line, increasing the experimental matrix with the variables studied, (aging and pressure application time), in order to obtain a complete characterization of the viscoelastic and thixotropic behavior of the waxy crude oil at 5°C.

7 REFERENCES

- Ahmadpour, A.; Sadeghy, K.; Maddah-Sadatieh, S. The effect of a variable plastic viscosity on the restart problem of pipelines filled with gelled waxy crude oils. *Journal of Non-Newtonian Fluid Mechanics*, v. 205, p. 16-27, 2014.
- Andrade, D. *et al.* Influence of the initial cooling temperature on the gelation and yield stress of waxy crude oils. *RheologicaActa*, v. 54, n. 2, p. 149-157, 2014.
- Barnes, H.; Walters, K. The yield stress myth?. *Rheologica Acta*, v. 24, n. 4, p. 323-326, 1985.
- Betancourt, S. *et al.* Advancing fluid-property measurements. *Schlumberger Oilfield Review*, v. 19, n. 3, p. 56-70, 2015.
- Bird, R. Viscoelastic Hysteresis. Part I. Model Predictions. *Journal of Rheology*, v. 12, n. 4, p. 479, 1968.
- Chamkalani, A. Correlations between SARA Fractions, Density, and RI to Investigate the Stability of Asphaltene. *ISRN Analytical Chemistry*, v. 2012, p. 1-6, 2012.
- Cheng, C.; Boger, D.; Nguyen, Q. Influence of Thermal History on the Waxy Structure of Statically Cooled Waxy Crude Oil. *SPE Journal*, v. 5, n. 02, p. 148-157, 2000.
- Cheng, D. Yield stress: A time-dependent property and how to measure it. *RheologicaActa*, v. 25, n. 5, p. 542-554, 1986.
- Coussot, P. *et al.* Avalanche Behavior in Yield Stress Fluids. *Phys. Rev. Lett.*, v. 88, n. 17, 2002.
- Coussot, P. *et al.* Viscosity bifurcation in thixotropic, yielding fluids. *Journal of Rheology*, v. 46, n. 3, p. 573, 2002.
- Da Silva, J.; Coutinho, J. Dynamic rheological analysis of the gelation behaviour of waxy crude oils. *RheologicaActa*, v. 43, n. 5, p. 433-441, 2004.
- Davidson, M. *et al.* A model for restart of a pipeline with compressible gelled waxy crude oil. *Journal of Non-Newtonian Fluid Mechanics*, v. 123, n. 2-3, p. 269-280, 2004.
- De Souza Mendes, P. *et al.* Startup flow of gelled crudes in pipelines. *Journal of Non-Newtonian Fluid Mechanics*, v. 179-180, p. 23-31, 2012.
- Dimitriou, C.; McKinley, G. A comprehensive constitutive law for waxy crude oil: a thixotropic yield stress fluid. *Soft Matter*, v. 10, n. 35, p. 6619-6644, 2014.
- Dimitriou, C.; McKinley, G.; Venkatesan, R. Rheo-PIV Analysis of the Yielding and Flow of Model Waxy Crude Oils. *Energy & Fuels*, v. 25, n. 7, p. 3040-3052, 2011.
- Ekaputra, A. *et al.* Impacts of Viscosity, Density and Pour Point to the Wax Deposition. *Journal of Applied Sciences*, v. 14, n. 23, p. 3334-3338, 2014.

- El-Gamal, I. Combined effects of shear and flow improvers: the optimum solution for handling waxy crudes below pour point. *Colloids and Surfaces A: Physicochemical and Engineering Aspects*, v. 135, n. 1-3, p. 283-291, 1998.
- Fleming, F., Camargo, R. M. T., Montesanti, J. R., Goncalves, M. A., (2013). Lessons Learned on Wax Issues From Deep Offshore Brazil. *OTC Brasil*.
- Gao, P.; Zhang, J.; Ma, G. Direct image-based fractal characterization of morphologies and structures of wax crystals in waxy crude oils. *Journal of Physics: Condensed Matter*, v. 18, n. 50, p. 11487-11506, 2006.
- Garcia, M. *et al.* PARAFFIN DEPOSITION IN OIL PRODUCTION. OIL COMPOSITION AND PARAFFIN INHIBITORS ACTIVITY. *Petroleum Science and Technology*, v. 16, n. 9-10, p. 1001-1021, 1998.
- Geest, Charlie Van Der. EXPERIMENTAL STUDY AND MODELING OF THE STARTUP FLOW OF WAXY CRUDES IN PIPELINES AND THE RHEOLOGICAL BEHAVIOR OF GELLED WAXY CRUDES. Campinas: Faculdade de Engenharia Mecânica, Universidade Estadual de Campinas, 2015. Dissertação de Mestrado.
- Ghannam, M. *et al.* Rheological properties of heavy & light crude oil mixtures for improving flowability. *Journal of Petroleum Science and Engineering*, v. 81, p. 122-128, 2012.
- Guo, L. *et al.* Study on Thixotropic Properties of Waxy Crude Oil Based on Hysteresis Loop Area. *Engineering*, v. 07, n. 07, p. 469-476, 2015.
- Guo, L. *et al.* Evaluation of Thixotropic Models for Waxy Crudes Based on Stepwise Shearing Measurements. *Petroleum Science and Technology*, v. 31, n. 9, p. 895-901, 2013.
- Hasan, S.; Ghannam, M.; Esmail, N. Heavy crude oil viscosity reduction and rheology for pipeline transportation. *Fuel*, v. 89, n. 5, p. 1095-1100, 2010.
- Hénaut, I., Vincké O., Brucy F., Waxy Crude Oil Restart: Mechanical Properties of Gelled Oils. SPE Annual Technical Conference and Exhibition, SPE 56771, Houston, Texas, USA, 1999.
- Hou, L. Experimental study on yield behavior of Daqing crude oil. *Rheologica Acta*, v. 51, n. 7, p. 603-607, 2012.
- Hou, L.; Zhang, J. New method for rapid thixotropic measurement of waxy crude. *Journal of Central South University of Technology*, v. 14, n. S1, p. 471-473, 2007.
- Hou, L.; Zhang, J. Effects of Thermal and Shear History on the Viscoelasticity of Daqing Crude Oil. *Petroleum Science and Technology*, v. 25, n. 5, p. 601-614, 2007.
- Japper-Jaafar, A. *et al.* Yield stress measurement of gelled waxy crude oil: Gap size requirement. *Journal of Non-Newtonian Fluid Mechanics*, v. 218, p. 71-82, 2015.

- Kané, M. *et al.* Morphology of paraffin crystals in waxy crude oils cooled in quiescent conditions and under flow. *Fuel*, v. 82, n. 2, p. 127-135, 2003.
- Kané, M.; Djabourov, M.; Volle, J. Rheology and structure of waxy crude oils in quiescent and under shearing conditions. *Fuel*, v. 83, n. 11-12, p. 1591-1605, 2004.
- Karan, K.; Ratulowski, J.; German, P. Measurement of waxy crude properties using novel laboratory techniques, 2015.
- Kelechukwu, E. M., Prediction of wax deposition risk of malasyan crude from viscosity-temperature correlation for dead crude. *Int. J. Sci. Adv. Technol.*, 1, 89-100, 2011
- Kok, M. *et al.* Comparison of wax appearance temperatures of crude oils by differential scanning calorimetry, thermomicroscopy and viscometry. *Fuel*, v. 75, n. 7, p. 787-790, 1996.
- Kok, M.; Gundogar, A. DSC study on combustion and pyrolysis behaviors of Turkish crude oils. *Fuel Processing Technology*, v. 116, p. 110-115, 2013.
- Lee, H. *et al.* Waxy Oil Gel Breaking Mechanisms: Adhesive versus Cohesive Failure. *Energy & Fuels*, v. 22, n. 1, p. 480-487, 2008.
- K. J. Leontaritis and G. A. Mansoori, "Asphaltene flocculation during oil production and processing: a thermodynamic colloidal model," in *Proceedings of the SPE International Symposium on Oilfield Chemistry*, SPE 16258, San Antonio, Tex, USA, 1987.
- Liu, G. *et al.* Experimental Study on the Compressibility of Gelled Crude Oil. *SPE Journal*, v. 20, n. 02, p. 248-254, 2015.
- Lopes-da-Silva, J.; Coutinho, J. Analysis of the Isothermal Structure Development in Waxy Crude Oils under Quiescent Conditions. *Energy & Fuels*, v. 21, n. 6, p. 3612-3617, 2007.
- Magda, J. *et al.* Time-Dependent Rheology of a Model Waxy Crude Oil with Relevance to Gelled Pipeline Restart †. *Energy & Fuels*, v. 23, n. 3, p. 1311-1315, 2009.
- Malkin, A. *Rheology fundamentals*. Toronto-Scarborough, Ont.: ChemTec Pub., 1994.
- Marchesini, F. *et al.* Rheological Characterization of Waxy Crude Oils: Sample Preparation. *Energy & Fuels*, v. 26, n. 5, p. 2566-2577, 2012.
- Martins, A. *et al.* Experimental and Theoretical Simulation of Gravel-Pack Displacement in Extended Horizontal-Offshore Wells. *SPE Drilling & Completion*, v. 20, n. 02, p. 141-146, 2005.
- Mendes, R. *et al.* Modeling the rheological behavior of waxy crude oils as a function of flow and temperature history. *Journal of Rheology*, v. 59, n. 3, p. 703-732, 2015.

- Mewis, J.; Wagner, N. Thixotropy. *Advances in Colloid and Interface Science*, v. 147-148, p. 214-227, 2009.
- Møller, P.; Mewis, J.; Bonn, D. Yield stress and thixotropy: on the difficulty of measuring yield stresses in practice. *Soft Matter*, v. 2, n. 4, p. 274, 2006.
- Moristis, G. Flow Assurance Challenges Production from Deeper Water. *Oils and Gas Journal*, v. 99, n. 66, 2001.
- Oh, K. *et al.* Yield Stress of Wax Gel using Vane Method. *Petroleum Science and Technology*, v. 27, n. 17, p. 2063-2073, 2009.
- Oh, K.; Jemmett, M.; Deo, M. Yield Behavior of Gelled Waxy Oil: Effect of Stress Application in Creep Ranges. *Industrial & Engineering Chemistry Research*, v. 48, n. 19, p. 8950-8953, 2009.
- Oh, K.; Jemmett, M.; Deo, M. Yield Behavior of Gelled Waxy Oil: Effect of Stress Application in Creep Ranges. *Industrial & Engineering Chemistry Research*, v. 48, n. 19, p. 8950-8953, 2009.
- Paso, K. Comprehensive Treatise on Shut-in and Restart of Waxy Oil Pipelines. *Journal of Dispersion Science and Technology*, v. 35, n. 8, p. 1060-1085, 2014.
- Paso, K. *et al.* Rheological Degradation of Model Wax-Oil Gels. *Journal of Dispersion Science and Technology*, v. 30, n. 4, p. 472-480, 2009.
- Perkins, T.; Turner, J. Starting Behavior of Gathering Lines and Pipelines Filled with Gelled Prudhoe Bay Oil. *Journal of Petroleum Technology*, v. 23, n. 03, p. 301-308, 1971.
- Rao, M. *Rheology of fluid, semisolid, and solid foods*. 2014
- Remizov, S. Structural and rheological properties of microheterogeneous systems 'solid hydrocarbons–liquid hydrocarbons'. *Colloids and Surfaces A: Physicochemical and Engineering Aspects*, v. 175, n. 3, p. 271-275, 2000.
- Roenningsen, H. *et al.* Wax precipitation from North Sea crude oils: 1. Crystallization and dissolution temperatures, and Newtonian and non-Newtonian flow properties. *Energy & Fuels*, v. 5, n. 6, p. 895-908, 1991.
- Rønningsen, H. Rheological behaviour of gelled, waxy North Sea crude oils. *Journal of Petroleum Science and Engineering*, v. 7, n. 3-4, p. 177-213, 1992.
- Rønningsen, H. Production of Waxy Oils on the Norwegian Continental Shelf: Experiences, Challenges, and Practices. *Energy & Fuels*, v. 26, n. 7, p. 4124-4136, 2012.
- Singh, P. *et al.* Formation and aging of incipient thin film wax-oil gels. *AIChE Journal*, v. 46, n. 5, p. 1059-1074, 2000.

- Smith, P.; Ramsden, R. The prediction of oil gelation in submarine pipelines and the pressure required for restarting flow, 1978.
- Speight, J. The chemistry and technology of petroleum. Boca Raton: Taylor & Francis, 2007.
- Stokes, J.; Telford, J. Measuring the yield behaviour of structured fluids. *Journal of Non-Newtonian Fluid Mechanics*, v. 124, n. 1-3, p. 137-146, 2004.
- Tarcha, B. *et al.* Critical quantities on the yielding process of waxy crude oils. *Rheologica Acta*, v. 54, n. 6, p. 479-499, 2015.
- Teng, H.; Zhang, J. Modeling the Thixotropic Behavior of Waxy Crude. *Industrial & Engineering Chemistry Research*, v. 52, n. 23, p. 8079-8089, 2013.
- Thuc, P. *et al.* The Problem in Transportation of High Waxy Crude Oils Through Submarine Pipelines at JV Vietsovpetro Oil Fields, Offshore Vietnam. *JCPT*, v. 42, n. 6, 2003.
- Tinsley, J. *et al.* Waxy Gels with Asphaltenes 1: Characterization of Precipitation, Gelation, Yield Stress, and Morphology. *Energy & Fuels*, v. 23, n. 4, p. 2056-2064, 2009.
- Tropea, C.; Yarin, A.; Foss, J. Springer handbook of experimental fluid mechanics. Traducaao . Berlin: Springer Science+Business Media, 2007.
- Venkatesan, R. *et al.* The strength of paraffin gels formed under static and flow conditions. *Chemical Engineering Science*, v. 60, n. 13, p. 3587-3598, 2005.
- Venkatesan, R. *et al.* The Effect of Asphaltenes on the Gelation of Waxy Oils. *Energy & Fuels*, v. 17, n. 6, p. 1630-1640, 2003.
- Venkatesan, R.; Singh, P.; Fogler, H. Delineating the Pour Point and Gelation Temperature of Waxy Crude Oils. *SPE Journal*, v. 7, n. 04, p. 349-352, 2002.
- Vinay, G.; Wachs, A.; Frigaard, I. Start-up transients and efficient computation of isothermal waxy crude oil flows. *Journal of Non-Newtonian Fluid Mechanics*, v. 143, n. 2-3, p. 141-156, 2007.
- Visintin, R. *et al.* Rheological Behavior and Structural Interpretation of Waxy Crude Oil Gels. *Langmuir*, v. 21, n. 14, p. 6240-6249, 2005.
- Wardhaugh, L. The measurement and description of the yielding behavior of waxy crude oil. *Journal of Rheology*, v. 35, n. 6, p. 1121, 1991.
- Webber, R. Yield Properties of Wax Crystal Structures Formed in Lubricant Mineral Oils. *Industrial & Engineering Chemistry Research*, v. 40, n. 1, p. 195-203, 2001.
- Webber, R. Low temperature rheology of lubricating mineral oils: Effects of cooling rate and wax crystallization on flow properties of base oils. *Journal of Rheology*, v. 43, n. 4, p. 911, 1999.

- Yi, S.; Zhang, J. Relationship between Waxy Crude Oil Composition and Change in the Morphology and Structure of Wax Crystals Induced by Pour-Point-Depressant Beneficiation. *Energy & Fuels*, v. 25, n. 4, p. 1686-1696, 2011.
- Zhang, J.; Liu, X. Some advances in crude oil rheology and its application. *Journal of Central South University of Technology*, v. 15, n. S1, p. 288-292, 2008.
- Zhao, Y. *et al.* Controlled Shear Stress and Controlled Shear Rate Nonoscillatory Rheological Methodologies for Gelation Point Determination. *Energy & Fuels*, v. 27, n. 4, p. 2025-2032, 2013.
- Zhao, Y. *et al.* Gelation Behavior of Model Wax–Oil and Crude Oil Systems and Yield Stress Model Development. *Energy & Fuels*, v. 26, n. 10, p. 6323-6331, 2012.